Electronic Supporting Information

Solvent-Free Synthesis and Reactivity of Nickel(II) Borohydride and Ni(II) Hydride

Sakthi Raje* and Raja Angamuthu*

Laboratory of Inorganic Synthesis and Bioinspired Catalysis, Department of Chemistry, Indian Institute of Technology Kanpur, Kanpur 208016, INDIA.

Email: sakthir@iitk.ac.in; raja@iitk.ac.in

Homepage: http://www.lisbic.com/

Table of contents (figures and tables):

Experimental Section

Materials: $NiCl_2 \cdot 6H_2O$ (Rankem), $NiBr_2$ (Alfa aesar), NiI_2 (Alfa aesar), $NaBPh_4$ (Alfa aesar), $NaBH_4$ (SDFCL), $NaBD_4$ (Alfa aesar), and AgOTs (Alfa aesar), Benzenethiol (SDFCL), 1,2-diphenyl disulfane (SDFCL) and 1,3-diphenylpropane-1,3-dione (or) dibenzoylmethane (Alfa aesar) were used as received from commercial sources. 2,11-diaza[3,3](2,6)-pyridinophane (L^H)[1] was synthesised according to reported procedures. Solvents were distilled under a dry nitrogen atmosphere using conventional methods.

Elemental Analyses: Analyses were carried out on a Perkin-Elmer CHNS/O analyser.

NMR Spectroscopy: NMR spectra were recorded on JEOL 500 MHz and JEOL 400 MHz spectrometers. The temperature was kept constant using a variable temperature unit within the error limit of ±1 K. The software MestReNova was used for the processing of the NMR spectra.[2] Tetramethylsilane (TMS) or the deuterated solvent residual peaks were used for calibration.

Mass Spectrometry: Mass spectrometry experiments were performed on a Waters-Q-ToF-Premier-HAB213 equipped with an electrospray interface. Spectra were collected by a constant infusion of the sample dissolved in methanol or acetonitrile or dichloromethane with 0.1% formic acid. Mass spectral envelopes were simulated for comparison using freely available software "mMass" an open source mass spectrometry tool.[3]

TGA analysis: Thermogravimetric analyses (TGA) were performed on a Mettler Toledo Star System (heating rate of 5 °C min^{-1}).

Powder X-ray diffraction: Powder X-ray diffraction (PXRD) patterns were recorded with a two circle diffractometer (Rigaku MiniFlex 600) equipped with Kβ foil filtered Cu (λ = 1.54056 Å) radiation. The tube voltage and current were 40 kV and 15 mA, respectively.

UV-visible Spectroscopy: UV-Visible spectra were recorded in JASCO V-670 spectrophotometer.

FT-IR Spectroscopy: Infrared spectra were recorded in the range 4000−400 cm^{-1} on a PerkinElmer spectrophotometer.

X-ray crystallography: Single-crystal X-ray data were collected on a Bruker SMART APEX CCD diffractometer using graphite-monochromated Mo Kα radiation (λ = 0.71069 Å). The linear absorption coefficients, the scattering factors for the atoms, and the anomalous dispersion corrections were taken from International Tables for X-ray Crystallography. Data integration and reduction were conducted with SAINT. Empirical absorption correction was applied to the collected reflections with SADABS using XPREP. Structures were determined by a direct method using SHELXTL and refined

on F^2 by a full-matrix least-squares technique using the SHELXL-97 program package. The lattice parameters and structural data are provided as tables at the end of this Supporting Information. All the structures are deposited in Cambridge Crystallographic Data Centre, and the CCDC deposition numbers are provided then and there.

Mechanochemical synthesis of $[(L^H)Ni(\mu\text{-}Cl)]_2(Cl)_2$.

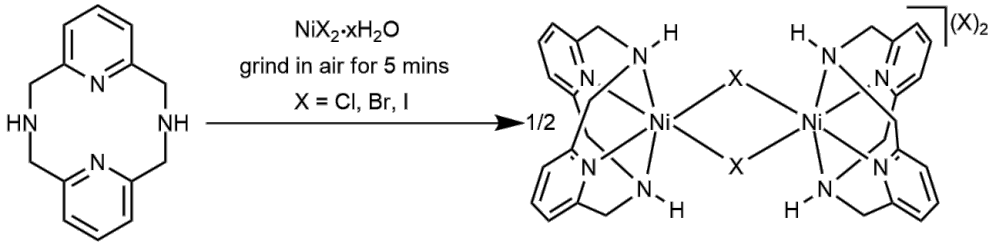

In a mortar 2,11-diaza[3,3](2,6)-pyridinophane (49 mg, 0.2 mmol) and $NiCl_2{\cdot}6H_2O$ (48 mg, 0.2 mmol) were manually ground with pestle for 5 minutes in open air. During the grinding process colour of the mixture turned to light violet and the mixture was analysed by PXRD. The light violet mixture was dissolved with 3 ml methanol and kept at room temperature for a day formed violet crystals.

Elemental anal. calcd. (%) for $C_{28}H_{32}Cl_4N_8Ni_2$ $3H_2O$: C, 42.36; H, 4.82; N, 14.12.

Found: C, 42.18; H, 4.44; N, 14.28

Mechanochemical synthesis of $[(L^H)Ni(\mu\text{-}Br)]_2(Br)_2$ and $[(L^H)Ni(\mu\text{-}I)]_2(I)_2$.

In a mortar 2,11-diaza[3,3](2,6)-pyridinophane (0.15 mmol) and anhydrous $NiBr_2$ or NiI_2 (0.15 mmol) were manually ground with a pestle for 2 minutes in open air. The mixture was further ground for an additional 3 minutes with 100 µl water while grinding colour has changed to light violet for $[Ni(L^H)(\mu\text{-}Br)]_2(Br)_2$ and teal green for $[Ni(L^H)(\mu\text{-}I)]_2(I)_2$. The obtained mixture was analysed by PXRD. The ground mixtures were dissolved with 3 ml methanol and kept at room temperature for a day formed crystals.

Elemental anal. calcd. (%) for $C_{28}H_{32}Br_4N_8Ni_2{\cdot}2.8H_2O$: C, 34.74; H, 3.91; N, 11.58.

Found: C, 34.83; H, 3.96; N, 11.47.

Elemental anal. calcd. (%) for $C_{28}H_{32}I_4N_8Ni_2{\cdot}4.2H_2O$: C, 28.74; H, 3.45; N, 9.49.

Found: C, 28.71; H, 3.51; N, 9.39.

Mechanochemical synthesis of $[(L^H)Ni(CH_3CN)_2](BPh_4)_2$.

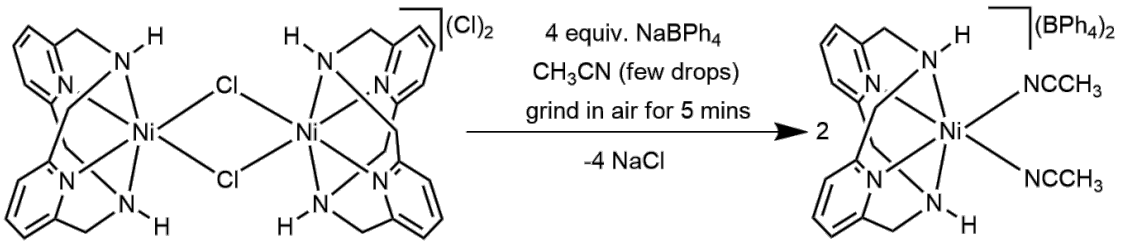

In a mortar $[(L^H)Ni(\mu\text{-}Cl)]_2(Cl)_2$ (74 mg, 0.1 mmol) and $NaBPh_4$ (144 mg, 0.42 mmol) were manually ground with a pestle for 2 minutes in open air. The light violet mixture was further ground for an additional 3 minutes with 100 µl CH_3CN as an assistive solvent, and the colour has changed to light purple. The mixture was analysed by PXRD, and washed with 1 ml water to remove the by-product NaCl. The light purple solid was dissolved with 3 ml acetonitrile and kept at room temperature for a day formed purple crystals. Yield: 0.194 g (95%)

Elemental anal. calcd. (%) for $C_{66}H_{62}B_2N_6Ni\cdot 1.1CH_3CN\cdot 0.7H_2O$: C, 76.03; H, 6.24; N, 9.23.

Found: C, 76.08; H, 6.31; N, 9.17.

Synthesis of $[(L^H)Ni(\mu\text{-}Cl)]_2(Cl)_2$.

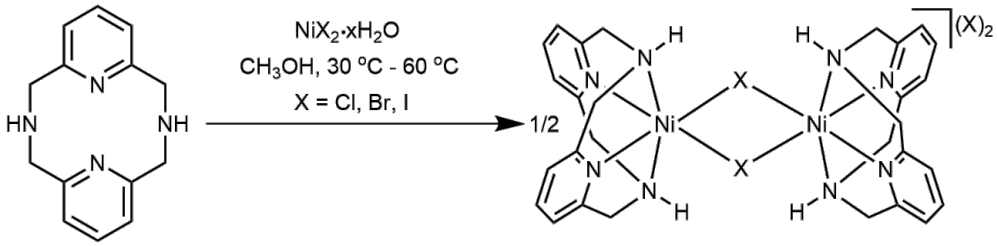

In a 100 ml round-bottom flask $NiCl_2{\cdot}6H_2O$ (0.238 g, 1 mmol) was dissolved in 5 ml methanol and 2,11-diaza[3,3](2,6)-pyridinophane (0.240 g, 1 mmol) dissolved in 10 ml methanol was added at room temperature. The reaction mixture was stirred at room temperature for 12 h, and then the resulting violet solution volume was reduced to half under reduced pressure. The violet solution was slowly diffused with diethyl ether and left at 0 ºC for a day to afford violet crystals of SCXRD-quality. Yield: 0.311 g (84%).

ESI-MS: *m/z* for $[(L^H)NiCl]^+ = C_{14}H_{16}ClN_4Ni$ = 333.0449 (calcd. 333.0417) and *m/z* for $[(L^H)Ni]^{2+} = C_{14}H_{16}N_4Ni$ = 149.0357 (calcd.149.0364).

Elemental anal. calcd. (%) for $C_{28}H_{32}Cl_4N_8Ni_2{\cdot}H_2O{\cdot}0.2CH_3OH$: C, 43.25; H, 4.81; N, 14.21.

Found: C, 43.18; H, 4.64; N, 14.16.

Synthesis of $[(L^H)Ni(\mu\text{-}Br)]_2(Br)_2$.

In a 100 ml round-bottom flask anhydrous $NiBr_2$ (0.219 g, 1 mmol) was suspended in 20 ml methanol and 2,11-diaza[3,3](2,6)-pyridinophane (0.242 g, 1 mmol) dissolved in 10 ml methanol was added at room temperature. The green-yellow suspension was stirred at room temperature for 12 h and then stirred at 60 ºC for an additional 2 h. The resulting violet solution volume was reduced to half under reduced pressure. The concentrated violet solution was slowly diffused with diethyl ether and left at 0 ºC for a day to afford violet crystals of SCXRD-quality. Yield: 0.348 g (76%).

ESI-MS: *m/z* for $[(L^H)NiBr]^+ = C_{14}H_{16}BrN_4Ni$ = 376.9924 (calcd. 376.9912) and *m/z* for $[(L^H)Ni]^{2+} = C_{14}H_{16}N_4Ni$ = 149.0335 (calcd.149.0364).

Elemental anal. calcd. (%) for $C_{28}H_{32}Br_4N_8Ni_2{\cdot}1.2H_2O{\cdot}0.2CH_3OH$: C, 35.03; H, 3.98; N, 11.51. Found: C, 34.93; H, 3.85; N, 11.31.

Synthesis of $[(L^H)Ni(\mu\text{-}I)]_2(I)_2$.

In a 100 ml round-bottom flask anhydrous NiI_2 (0.315 g, 1 mmol) was suspended in 30 ml methanol and 2,11-diaza[3,3](2,6)-pyridinophane (0.241 g, 1 mmol) dissolved in 10 ml methanol was added at room temperature. The green suspension was stirred at room temperature for 12 h and then stirred at

60 ^{o}C for an additional 2 h. The resulting green solution volume was reduced to half under reduced pressure. The concentrated green solution was slowly diffused with diethyl ether and left at 0 ^{o}C for two days to afford teal green crystals of SCXRD-quality. Yield: 0.387 g (70%).

ESI-MS: *m/z* for $[(L^{H})NiI]^{+}$= $C_{14}H_{16}IN_4Ni$ = 424.9773 (calcd. 424.9773) and *m/z* for $[(L^{H})Ni]^{2+}$ = $C_{14}H_{16}N_4Ni$ = 149.0312 (calcd.149.0364).

Elemental anal. calcd. (%) for $C_{28}H_{32}I_4N_8Ni_2 \cdot CH_3OH \cdot 0.1H_2O$: C, 30.71; H, 3.47; N, 9.55. Found: C, 30.71; H, 3.40; N, 9.39.

Synthesis of $[(L^H)Ni(CH_3CN)_2](BPh_4)_2$.

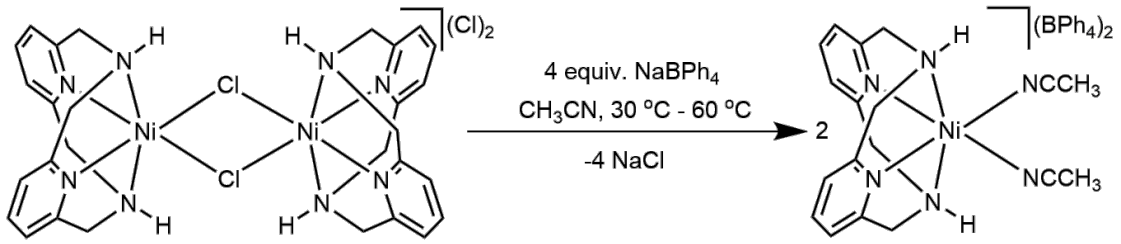

In a 100 ml round-bottom flask $[(L^H)Ni(\mu\text{-}Cl)]_2(Cl)_2$ (0.370 g, 0.5 mmol) was suspended in 10 ml acetonitrile, and $NaBPh_4$ (1.028 g, 3 mmol) was added as solid at room temperature. The resulting suspension was stirred at 60 ºC for 2 h and then cooled to room temperature. It was filtered thru Celite pad to remove the precipitated NaCl. The purple filtrate was evaporated under reduced pressure to yield purple solid, which was washed with methanol (10 ml) to remove excess $NaBPh_4$. The purple solid was dissolved in acetonitrile and slowly diffused with diethyl ether at room temperature to afford purple crystals of SCXRD-quality in a day. Yield: 0.918 g (90%).

ESI-MS: *m/z* for $[(L^H)Ni]^{2+} = C_{14}H_{16}N_4Ni$ = 149.0356 (calcd. 149.0364).

Elemental anal. calcd. (%) for $C_{66}H_{62}B_2N_6Ni\cdot 0.2CH_3CN$: C, 77.60; H, 6.14; N, 8.45.

Found: C, 77.71; H, 6.08; N, 8.31.

Synthesis of $[(L^H)Ni(H_2O)_2](OTs)_2$.

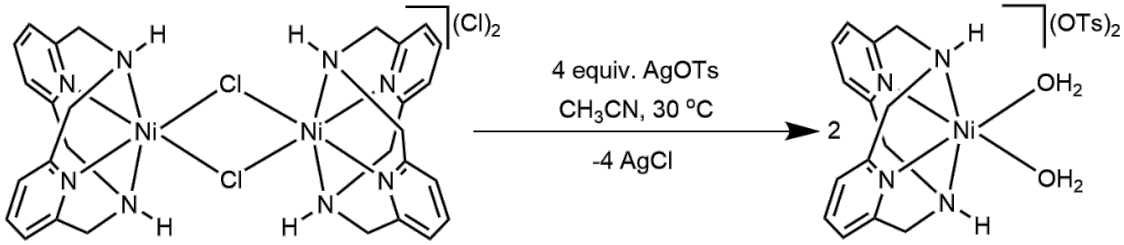

In a 15 ml screw capped vial covered with aluminium foil, $[(L^H)Ni(\mu\text{-}Cl)]_2(Cl)_2$ (90 mg, 0.12 mmol) was suspended in 10 ml acetonitrile, and AgOTs (0.140 g, 0.5 mmol) was added at room temperature. The resulting suspension was stirred at room temperature for 2 h and then filtered thru Celite pad to remove precipitated AgCl. The purple filtrate was concentrated and slowly diffused with diethyl ether at 0 ºC to afford purple crystals of SCXRD-quality in a day. Yield: 0.195 g (78%).

ESI-MS: *m/z* for $[(L^H)NiOTs]^+$ = 469.0846 (calcd. 469.0844) and *m/z* for $[(L^H)Ni]^{2+} = C_{14}H_{16}N_4Ni$ = 149.0349 (calcd. 149.0364).

Mechanochemical synthesis of $[(L^H)Ni(\eta^2\text{-}BH_4)](BPh_4)$.

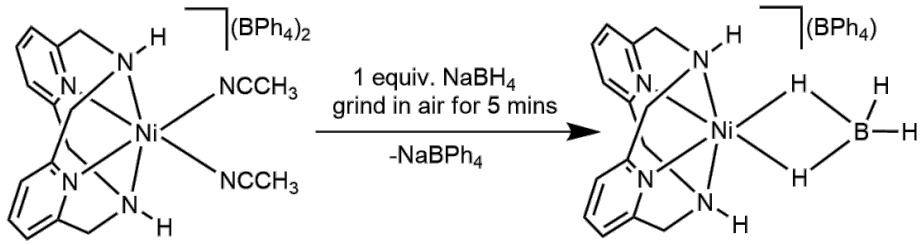

$[(L^H)Ni(CH_3CN)_2](BPh_4)_2$ (80 mg, 0.08 mmol) and $NaBH_4$ (3 mg, 0.08 mmol) were placed in a mortar and manually ground with a pestle for 3 minutes in open air. The violet solid was collected and analysed by IR spectroscopy and PXRD. After the analysis the violet powder was washed with acetonitrile (1 ml) and diethyl ether (2 ml), then dried under vacuum for an hour. Yield: 40 mg (79%). IR: $\nu(B\text{-}H)_{terminal}$ 2411 and 2370 cm^{-1}; $\nu(B\text{-}H)_{bridging}$ 2035 and 1970 cm^{-1}.

IR spectroscopy data were consistent with the solution phase synthesised $[(L^H)Ni(\eta^2\text{-}BH_4)](BPh_4)$ complex.

Synthesis of $[(L^H)Ni(\eta^2\text{-}BH_4)](BPh_4)$.

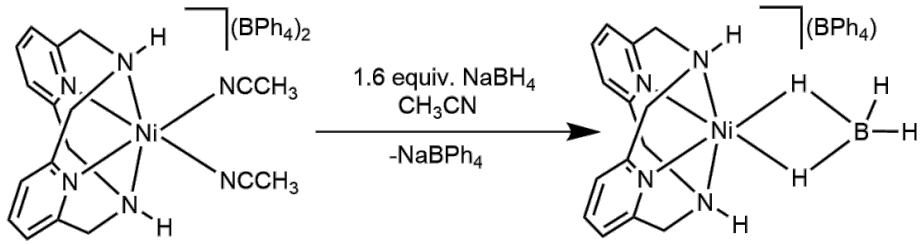

In an oven dried 50 ml Schlenk flask $[(L^H)Ni(CH_3CN)_2](BPh_4)_2$ (50 mg, 0.05 mmol) was dissolved in 2 ml acetonitrile and stirred for 5 minutes to become the purple solution. In another Schlenk flask $NaBH_4$ (3 mg, 0.08 mmol) was suspended in 3 ml acetonitrile and stirred for 30 minutes at room temperature, and the turbid solution was layered via cannula filter into the purple solution at room temperature under N_2 atmosphere. Immediately the colour of the solution was turned to violet from purple, and the deep violet crystals began to form immediately. The obtained crystals were filtered and washed with 5 ml acetonitrile. Yield: 22 mg (71 %).

IR: $\nu(B\text{-}H)_{terminal}$ 2411 and 2370 cm^{-1}; $\nu(B\text{-}H)_{bridging}$ 2035 and 1970 cm^{-1}.

Elemental anal. calcd. (%) for $C_{38}H_{40}B_2N_4Ni\cdot 0.3CH_3CN\cdot 0.7H_2O$: C, 70.47; H, 6.48; N, 9.15.

Found: C, 70.47; H, 6.36; N, 9.17.

Synthesis of $[(L^H)Ni(\eta^2\text{-}BD_4)](BPh_4)$ complex.

It was synthesised by following $[(L^H)Ni(\eta^2\text{-}BH_4)](BPh_4)$ synthesis procedure, and $NaBD_4$ (0.08 mmol) was used instead of $NaBH_4$ (0.08 mmol).

IR: $\nu(B\text{-}D)_{terminal}$ 1819 and 1746 cm^{-1}

Synthesis of $[(L^H)Ni(\mu\text{-}H)]_2(BPh_4)_2$.

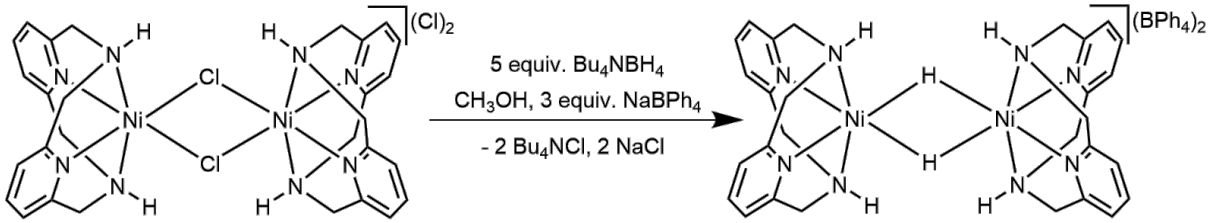

In an oven dried 50 ml Schlenk flask $[(L^H)Ni(\mu\text{-}Cl)]_2(Cl)_2$ (75 mg, 0.1 mmol) was dissolved in 5 ml methanol and Bu_4NBH_4 (130 mg, 0.5 mmol) was added as solid all at once. The colour of the solution immediately turned to deep yellow-brown from violet, and 5 ml methanolic solution of $NaBPh_4$ (105 mg, 0.3 mmol) was added through a cannula. The deep yellow microcrystalline solid was started to form within 5 minutes, and the flask was left at -20 ^oC for an hour. It was filtered through the cannula and washed with 5 ml methanol; the deep yellow solid was dried under vacuum. Yield: 77 mg (61%).

^1H NMR (400 MHz, CD_3CN) δ_H = 8.16 (t, J = 7.2 Hz, 4H, Py), 7.78 (d, J = 7.1 Hz, 8H, Py), 7.25 (bs, 16H, Ph), 6.97 (bs, 16H, Ph), 6.83 (bs, 8H, Ph), 2.70 (s, 16H, -CH_2), -7.37 (s, 2H, Ni-H).

Elemental anal. calcd. (%) for $C_{76}H_{74}B_2N_8Ni_2 \cdot 1.6CH_3OH$: C, 72.27; H, 6.28; N, 8.69. Found: C, 72.34; H, 6.38; N, 8.61.

The yellow solid was attempted to crystallise in multiple solvents but crystallisation of $[(L^H)Ni(\mu\text{-}H)]_2(BPh_4)_2$ were not fruitful. The light green crystals of SCXRD-quality were formed at -20 ^oC from (2:1) mixture of acetonitrile and methanol, which was confirmed as $[(L^H)Ni(\mu\text{-}OCH_3)]_2(BPh_4)_2$.

Synthesis of $[(L^H)Ni(\mu\text{-}H)]_2(I)_2$.

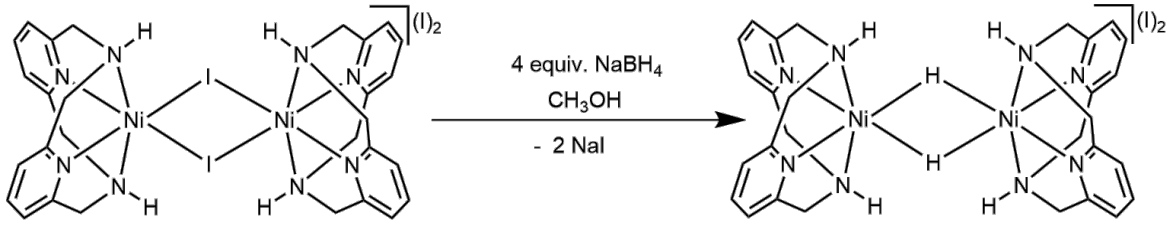

In an oven dried 50 ml Schlenk flask $[(L^H)Ni(\mu\text{-}I)]_2(I)_2$ (110 mg, 0.1 mmol) was dissolved in 2 ml methanol and $NaBH_4$ (15 mg, 0.4 mmol) was added as solid at room temperature. The brown mixture was left at -25 ^oC for a day formed brown crystals of SCXRD-quality. Yield: 56 mg (65%) (little white precipitate were present which could be NaI).

Synthesis of $[(L^H)Ni(\mu\text{-}SPh)]_2(BPh_4)_2$.

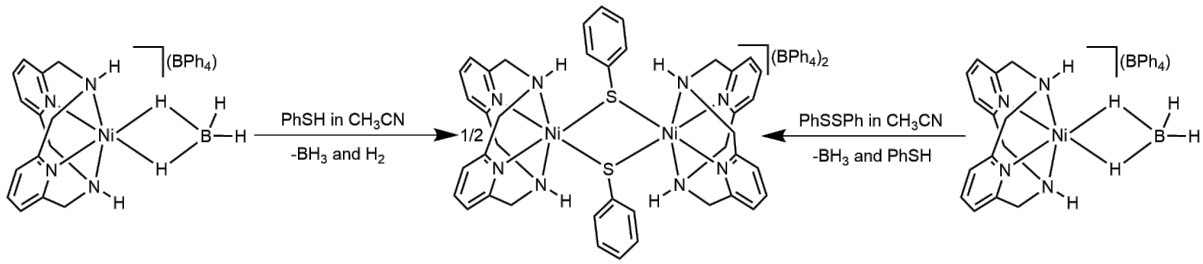

In a Schlenk flask $[(L^H)Ni(\eta^2\text{-}BH_4)](BPh_4)$ (25 mg, 0.04 mmol) was suspended in 3 ml acetonitrile and benzenethiol (5 mg, 0.04 mmol) was added. It was stirred for 3 h at room temperature; slowly the purple suspension turned into a clear lime green solution and concentrated to 1 ml under reduced pressure. The deep lime green solution was layered by diethyl ether 10 ml and left at -20 ^oC for a day formed lime green crystals of SCXRD-quality. Yield: 24 mg (82%). ESI-MS: *m/z* for $[(L^H)Ni(SPh)(O_2)]^+ = C_{20}H_{22}N_5NiO_2S = 439.0752$ (calcd. 439.0840).

Elemental anal. calcd. (%) for $C_{88}H_{82}B_2N_8Ni_2S_2 \cdot 2.1CH_3CN \cdot 0.7H_2O$: C, 71.28; H, 5.82; N, 9.11. Found: C, 71.34; H, 5.93; N, 9.21.

Similar result was generated when 1,2-diphenyldisulfane (0.04 mmol) was used instead of benzenethiol (0.04 mmol).

Synthesis of [(L^H)Ni(dbm)](BPh_4).

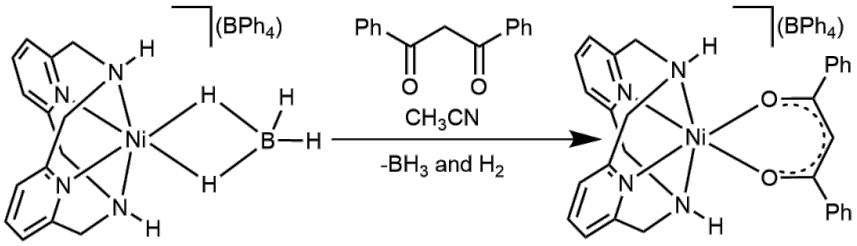

In a Schlenk flask [(L^H)Ni(η^2-BH_4)](BPh_4) (25 mg, 0.04 mmol) was suspended in 4 ml acetonitrile and dibenzoylmethane (9 mg, 0.04 mmol) was added. The purple suspension was slowly turned to yellow upon stirring for 2 h at room temperature and concentrated to dryness under reduced pressure. The obtained yellow solid was dissolved in dichloromethane and diffused with diethyl ether at 0 ^oC for a day formed yellow crystals of SCXRD-quality. Yield: 31 mg (92%).

ESI-MS: *m/z* for [(L^H)Ni(dbm)]$^+$ = $C_{29}H_{27}N_5NiO_2$ = 521.1489 (calcd. 521.1487).

Elemental anal. calcd. (%) for $C_{78}H_{78}B_2N_8Ni_2O_2$: C, 60.48; H, 5.08; N, 5.06.

Found: C, 60.43; H, 5.17; N, 5.15.

Synthesis of $[(L^H)Ni(\mu\text{-}OCH_3)]_2(BPh_4)_2$.

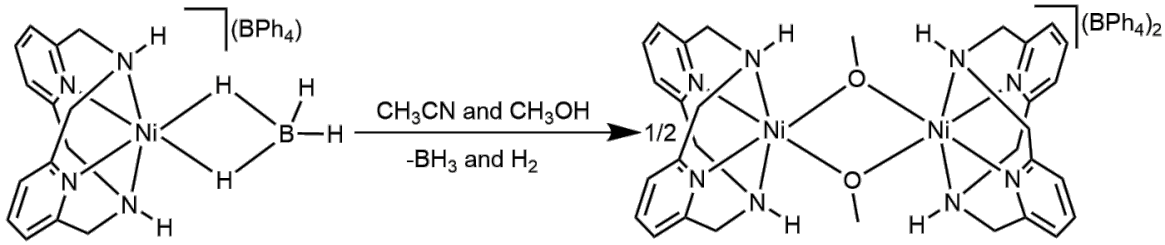

In a Schlenk flask $[(L^H)Ni(\eta^2\text{-}BH_4)](BPh_4)$ (25 mg, 0.04 mmol) was suspended in 3 ml acetonitrile and 0.5 ml methanol. It was stirred for 2 h at room temperature; the violet suspension turned into a light green solution and concentrated to 1 ml. It was left at -20 ^oC for a day formed light green crystals of SCXRD-quality. Yield: 24 mg (92%).

Elemental anal. calcd. (%) for $C_{78}H_{78}B_2N_8Ni_2O_2 \cdot 2.1CH_3CN \cdot 1.2CH_3OH$: C, 70.38; H, 6.31; N, 9.94. Found: C, 70.29; H, 6.40; N, 10.02.

The reaction of $[(L^H)Ni(\eta^2\text{-}BH_4)](BPh_4)$ and CH_3I.

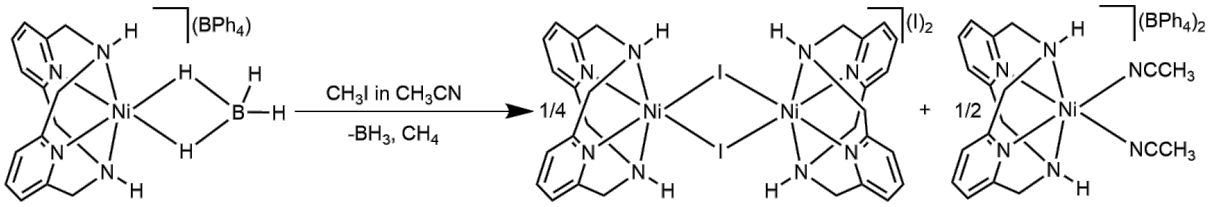

In a Schlenk flask $[(L^H)Ni(\eta^2\text{-}BH_4)](BPh_4)$ (20 mg, 0.03 mmol) was suspended in 3 ml acetonitrile and CH_3I (10 mg, 0.07 mmol) was added. The violet suspension was stirred at room temperature for an hour; slowly becomes a deep yellow solution then turned to purple, and the volume was concentrated to 1 ml. It was kept at room temperature for a day formed teal green crystals, which was filtered and the purple filtrate was diffused with diethyl ether at 0 ^oC formed purple crystals of SCXRD-quality. Yield of teal green crystals 13 mg (40%) with respect to $[(L^H)Ni(\eta^2\text{-}BH_4)](BPh_4)$ and purple crystals 14 mg (46%) with respect to $[(L^H)Ni(\eta^2\text{-}BH_4)](BPh_4)$. ESI-MS: *m/z* for $[(L^H)NiI]^+$= $C_{14}H_{16}IN_4Ni$ = 424.9774 (calcd. 424.9773) and *m/z* for $[(L^H)Ni]^{2+}$ = $C_{14}H_{16}N_4Ni$ = 149.0356 (calcd. 149.0364).

The ESI-MS and SCXRD analysis confirmed that the teal green crystals were $[(L^H)Ni(\mu\text{-}I)]_2(I)_2$ and the purple crystals were $[(L^H)Ni(CH_3CN)_2](BPh_4)_2$.

The reaction of $[(L^H)Ni(\eta^2\text{-}BH_4)](BPh_4)$ and (bromomethyl)benzene.

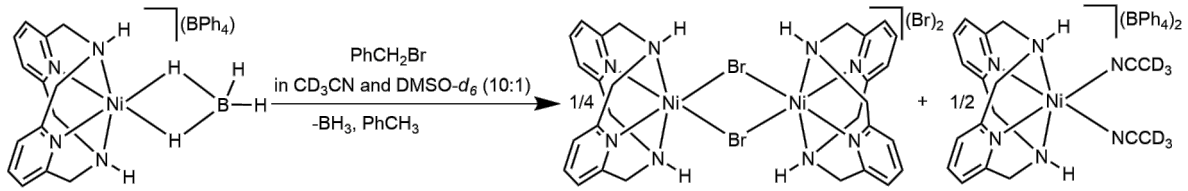

A Teflon screw-capped NMR tube was flushed with N_2 three times. $[(L^H)Ni(\eta^2\text{-}BH_4)](BPh_4)$ (7 mg, 0.01 mmol) was transferred into the tube and CD_3CN (0.5 ml) was added. The violet suspension was not dissolved at room temperature then DMSO-d_6 (50 µl) was added to make a homogeneous solution, immediately the purple suspension turned to the deep yellow solution along with bubble formation. The solution was degassed for three freeze-thaw-pump cycles then (bromomethyl)benzene (1 µl, 0.008 mmol) was added. The deep green-yellow solution was degassed for three freeze-thaw-pump cycles, and the tube was sealed with N_2. The conversion was monitored by ^1H NMR spectroscopy at room temperature and the formed paramagnetic complex was analysed by ESI-MS (Figure S12 and S27).

The reaction of $[(L^H)Ni(\eta^2\text{-}BH_4)](BPh_4)$ with Air.

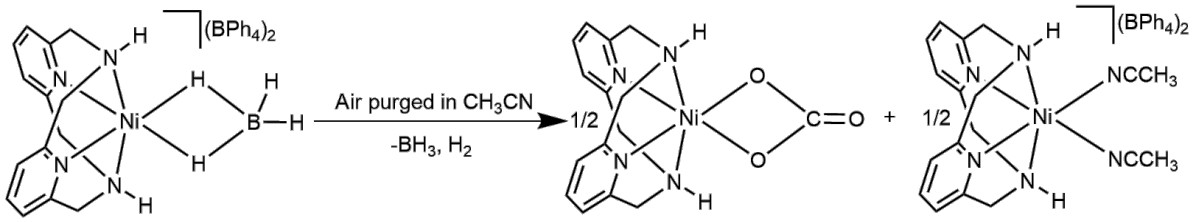

In an oven dried Schlenk flask $[(L^H)Ni(\eta^2\text{-}BH_4)](BPh_4)$ (23 mg, 0.036 mmol) was suspended in 4 ml acetonitrile under a nitrogen atmosphere. Air was purged for 30 minutes, while stirring the violet suspension turned into a clear light yellow solution within 5 min then turned to a purple solution with little turbidity. It was filtered, and the clear purple solution volume was reduced to 1 ml, which was left at 0 ^oC for a week formed purple and violet crystals of SCXRD-quality.

ESI-MS: *m/z* for $[(L^H)Ni(HCOO)]^+ = C_{15}H_{17}N_4NiO_2 = 343.0715$ (calcd.343.0705) and *m/z* for $[(L^H)Ni]^{2+} = C_{14}H_{16}N_4Ni = 149.0329$ (calcd. 149.0364).

The SCXRD analysis confirmed that the violet crystals were $[(L^H)Ni(CO_3)]$ and the purple crystals were $[(L^H)Ni(CH_3CN)_2](BPh_4)_2$.

The reaction of $[(L^H)Ni(\eta^2\text{-}BH_4)](BPh_4)$ with SO_2.

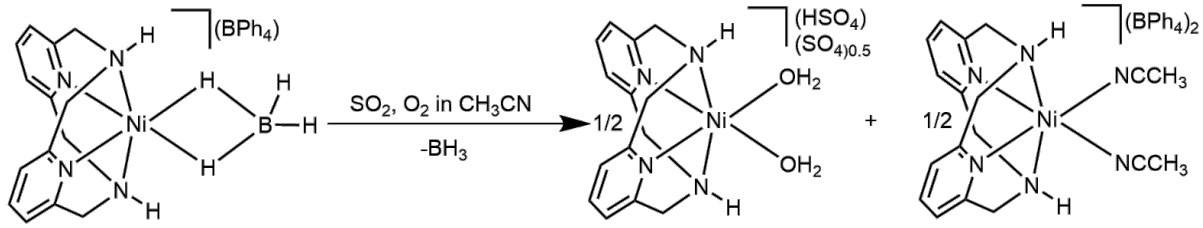

In an oven dried Schlenk flask $[(L^H)Ni(\eta^2\text{-}BH_4)](BPh_4)$ (23 mg, 0.036 mmol) was suspended in 4 ml acetonitrile under a nitrogen atmosphere. The flask was sealed with SO_2 atmosphere; immediately colour changed to deep yellow along with little turbidity. It was stirred for 30 minutes at room temperature, and the solvent evaporated to dryness. The obtained light purple solid was suspended in 5 ml acetonitrile and filtered off the precipitate. The filtrate was diffused with diethylether and left at 0 ^oC for two days formed purple crystals. The filtered precipitate was dissolved with 1 ml methanol and diffused with diethylether at 0 ^oC were formed violet crystals of SCXRD-quality. The yield of purple crystals 13 mg (35%) with respect to $[(L^H)Ni(\eta^2\text{-}BH_4)](BPh_4)$ and the light violet crystals 7 mg (40%) with respect to $[(L^H)Ni(\eta^2\text{-}BH_4)](BPh_4)$. ESI-MS (cation mode): *m/z* for $[(L^H)Ni(HSO_4)]^+$ = $C_{14}H_{17}N_4NiO_4S$ = 395.0277 (calcd. 395.0324) and *m/z* for $[(L^H)Ni(HCOO)]^+$ = $C_{15}H_{17}N_4NiO_2$ = 395.0716 (calcd. 343.0705). ESI-MS (anion mode): *m/z* for HSO_4 anion = 96.9597 (calcd. 96.9597).

The SCXRD analysis confirmed that the violet crystals were $[(L^H)Ni(H_2O)_2](HSO_4)(SO_4)_{0.5}$ and the purple crystals were $[(L^H)Ni(CH_3CN)_2](BPh_4)_2$.

The reaction of $[(L^H)Ni(\eta^2\text{-}BH_4)](BPh_4)$ with $[Ph_3C]PF_6$.

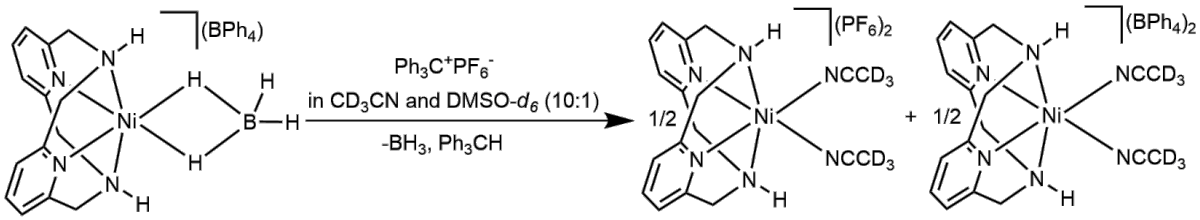

A Teflon screw-capped NMR tube was flushed with N_2 three times. $[(L^H)Ni(\eta^2\text{-}BH_4)](BPh_4)$ (7 mg, 0.011 mmol) was transferred into the tube and CD_3CN (0.5 ml) was added. The violet suspension was not dissolved at room temperature then DMSO-d_6 (50 μl) was added to make a homogeneous solution, immediately the purple suspension turned to the deep yellow solution along with bubble formation. The solution was degassed for three freeze-thaw-pump cycles, and the tube was sealed with N_2. ^1H NMR spectroscopy was recorded at room temperature, which confirmed the formation of $[(L^H)Ni(\mu\text{-}H)]_2(BPh_4)_2$ then trityl hexafluorophosphate (4 mg, 0.01 mmol) was added. The deep green-black solution was degassed for three freeze-thaw-pump cycles, and the tube was sealed with N_2. The conversion was monitored by ^1H NMR spectroscopy at room temperature (Figure S26).

Figure S 1. ESI-MS of $[(L^H)Ni(\mu\text{-}Cl)]_2(Cl)_2$.

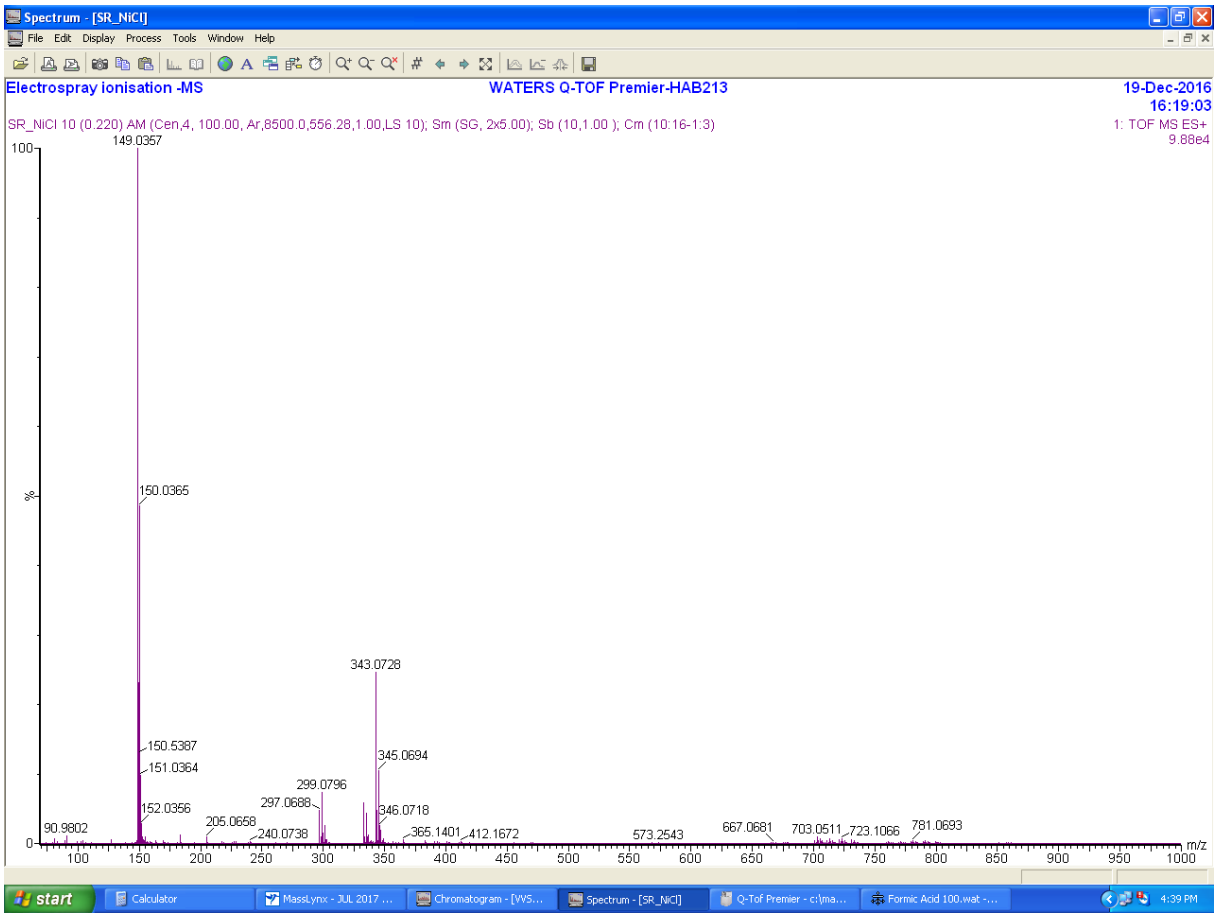

Calculated *m/z* for $[(L^H)NiCl]^+ = C_{14}H_{16}ClN_4Ni = 333.0417$; observed *m/z* = 333.0449. Calculated *m/z* for $[(L^H)Ni(HCOO)]^+$ = 343.0705; observed *m/z* = 343.0728 and calculated *m/z* for $[(L^H)Ni]^{2+}$ = 149.0359; observed *m/z* = 149.0357.

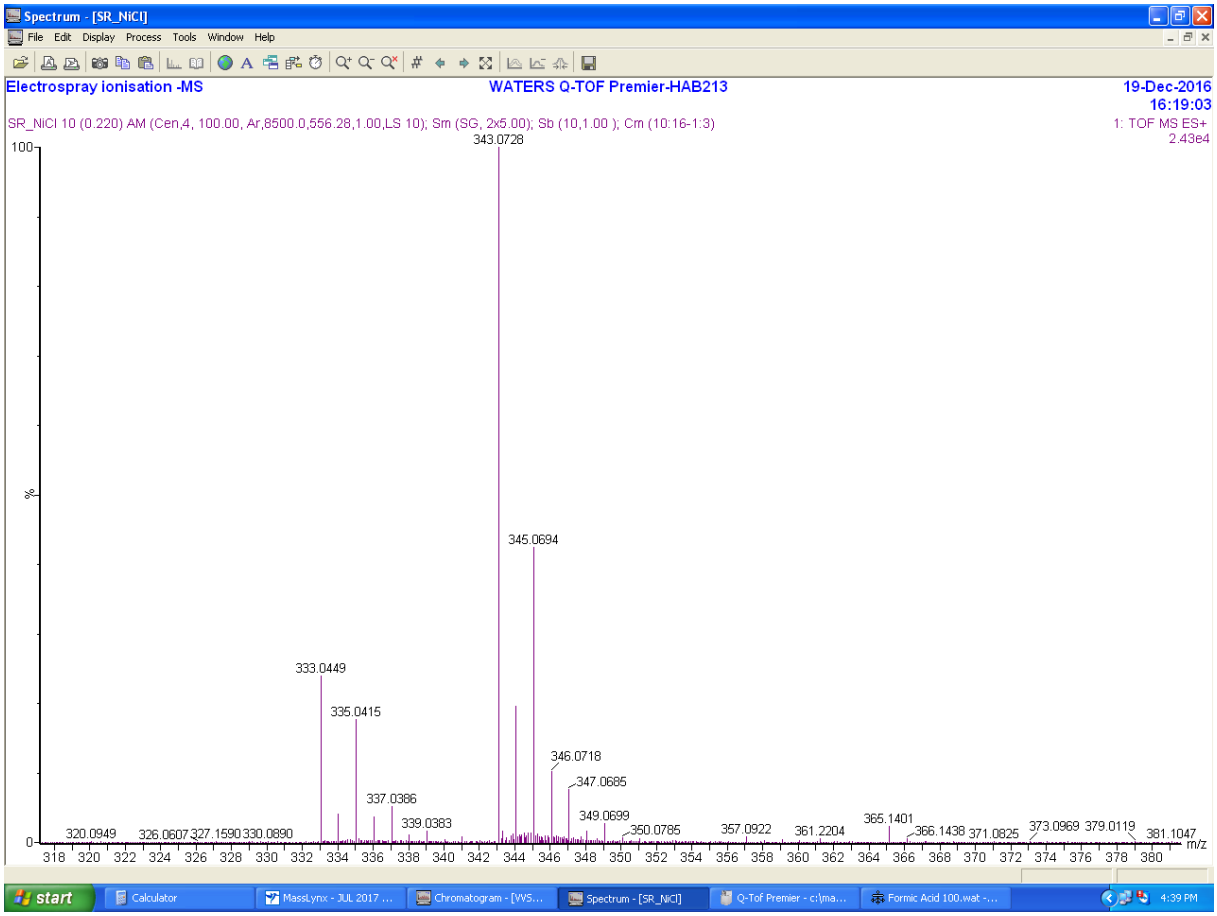

Calculated *m/z* for $[(L^H)NiCl]^+ = C_{14}H_{16}ClN_4Ni$ = 333.0417; observed *m/z* = 333.0449. Calculated *m/z* for $[(L^H)Ni(HCOO)]^+$ = 343.0705; observed *m/z* = 343.0728.

Simulated ESI-MS of $[(L^H)NiCl]^+$

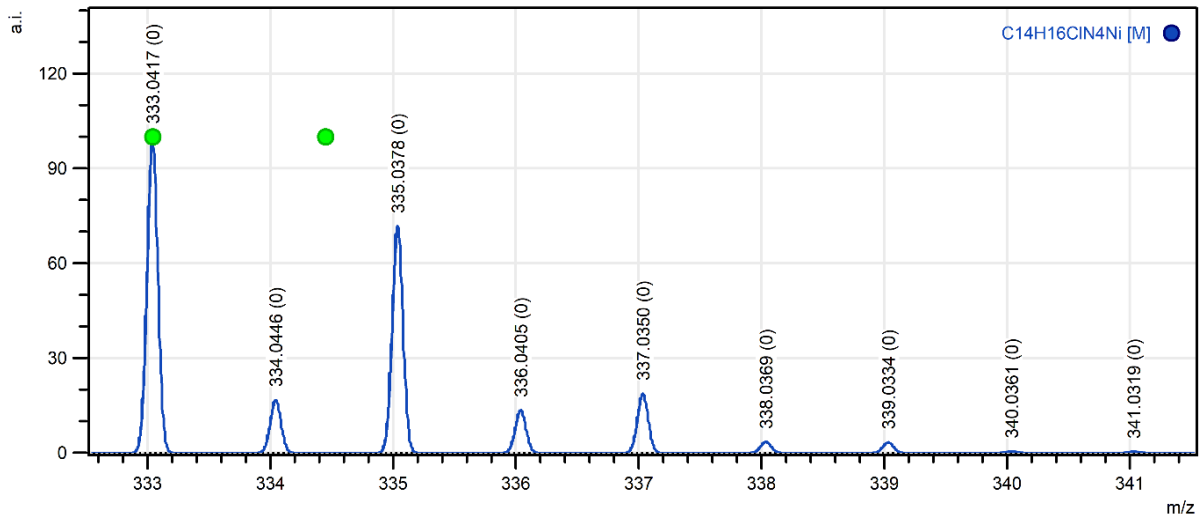

Figure S 2. ESI-MS of $[(L^H)Ni(\mu\text{-}Br)]_2(Br)_2$.

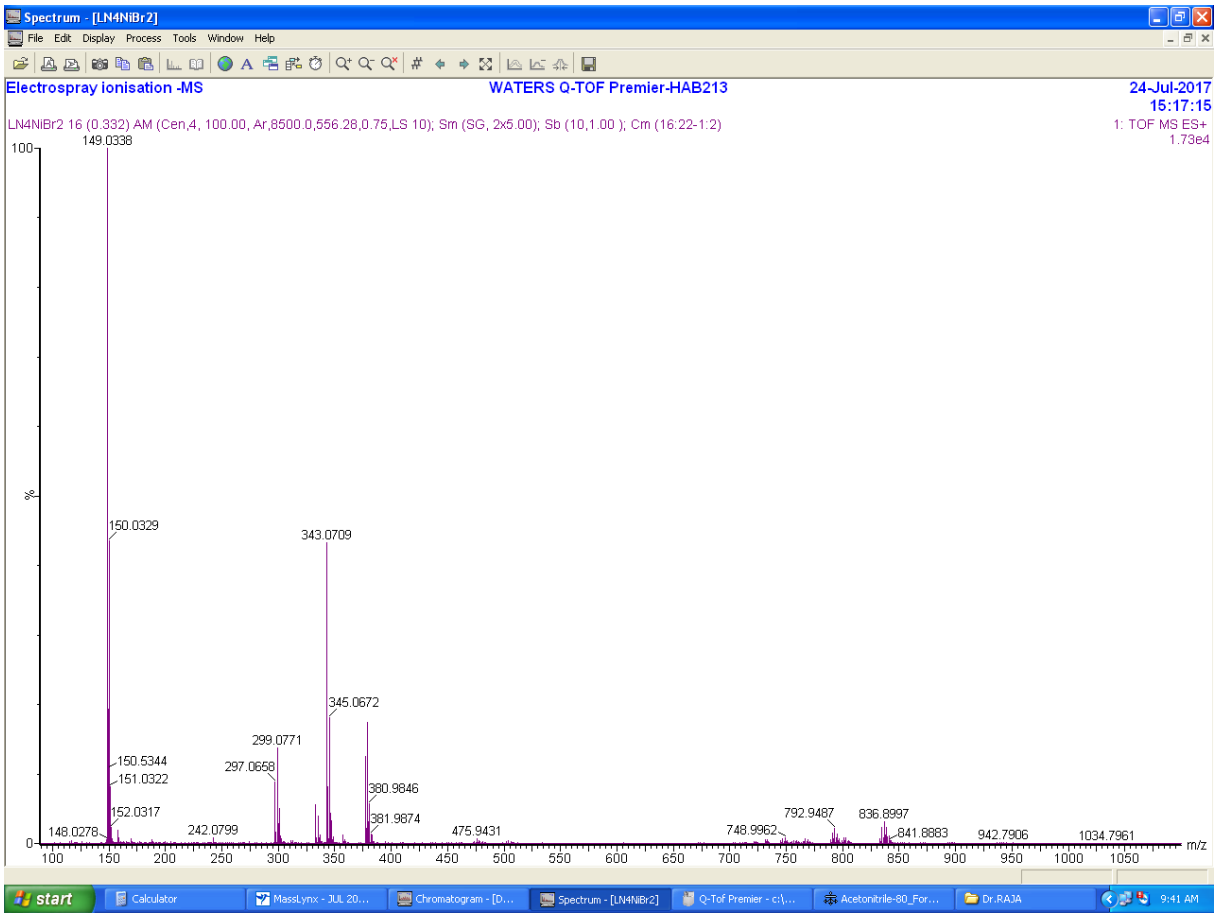

Calculated *m/z* for $[(L^H)NiBr]^+ = C_{14}H_{16}BrN_4Ni = 376.9912$; observed *m/z* = 376.9913. Calculated *m/z* for $[(L^H)Ni(HCOO)]^+$ = 343.0705; observed *m/z* = 343.0709 and calculated *m/z* for $[(L^H)Ni]^{2+}$ = 149.0359; observed *m/z* = 149.0338.

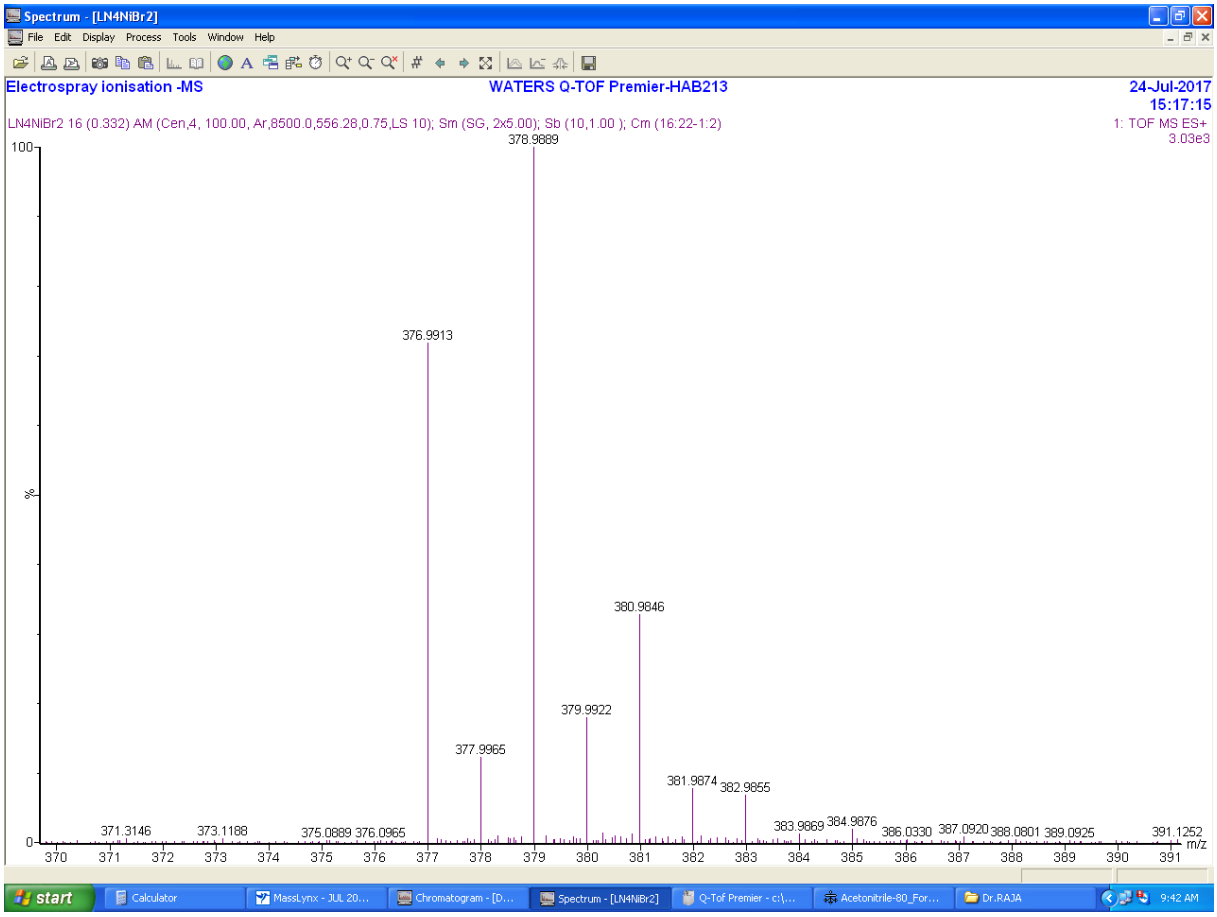

Calculated *m/z* for $[(L^{H})NiBr]^{+}$ = $C_{14}H_{16}BrN_4Ni$ = 376.9912; observed *m/z* = 376.9913.

Simulated ESI-MS of $[(L^{H})NiBr]^{+}$

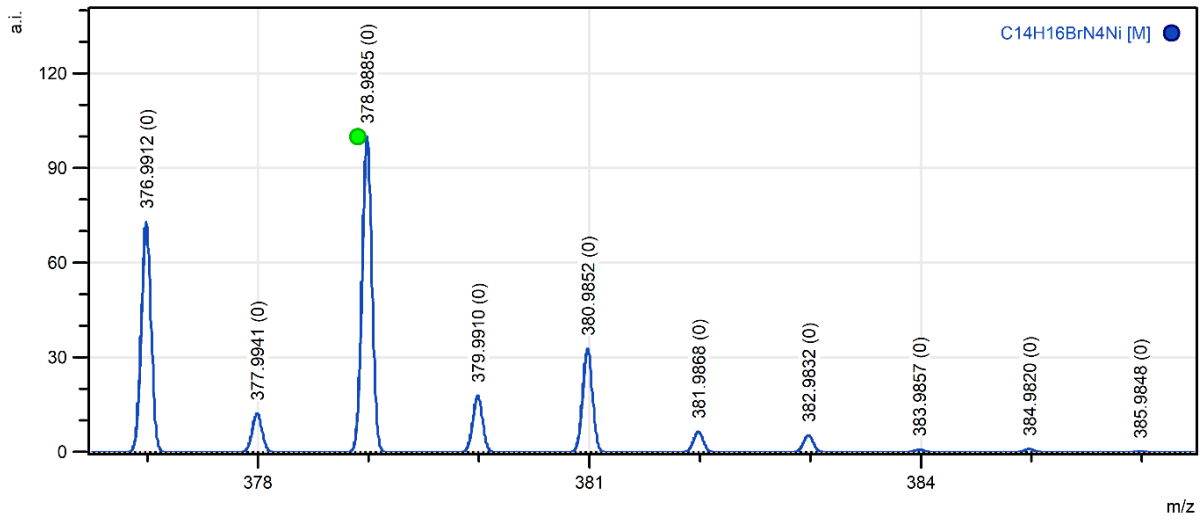

Figure S 3. ESI-MS of $[(L^H)Ni(\mu\text{-}I)]_2(I)_2$.

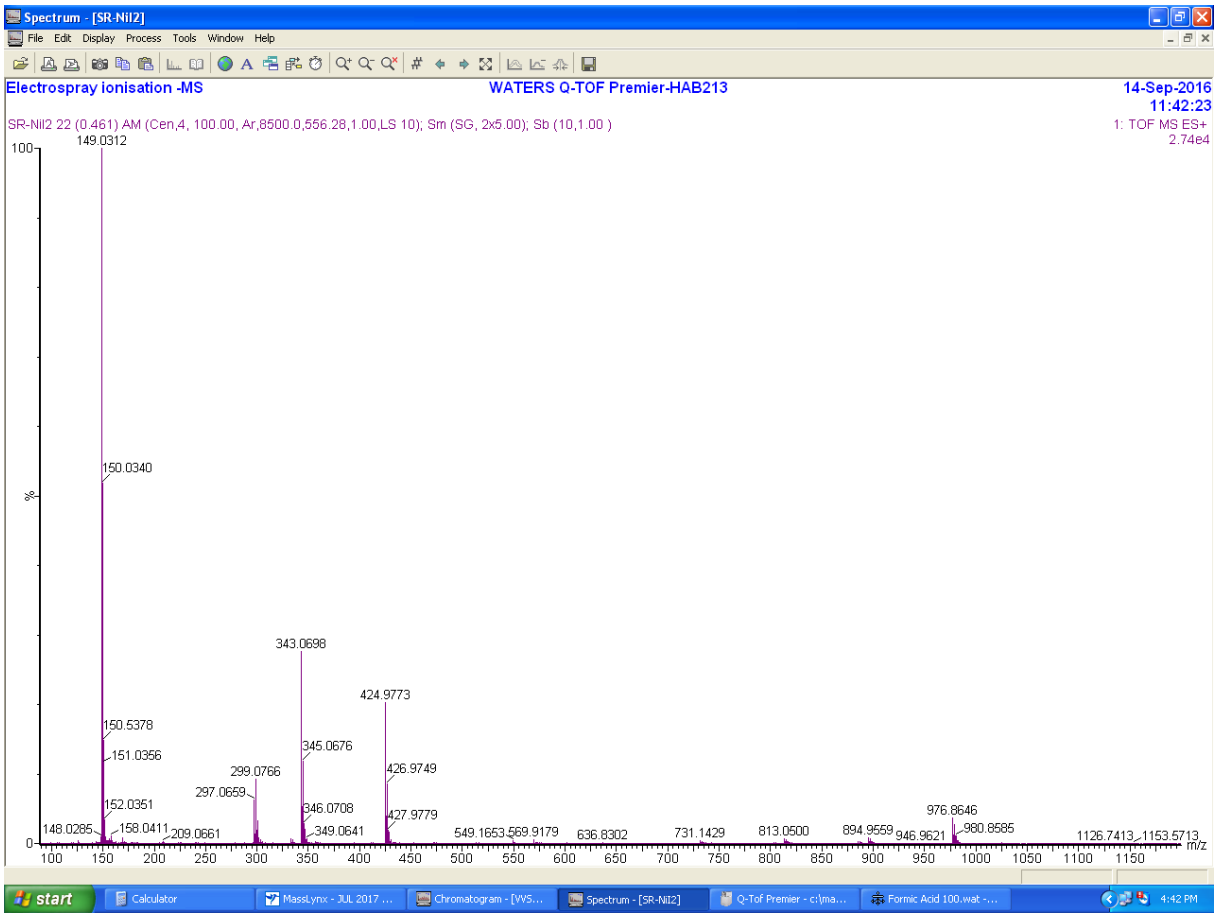

Calculated *m/z* for $[(L^H)NiI]^+ = C_{14}H_{16}IN_4Ni = 424.9773$; observed *m/z* = 424.9773. Calculated *m/z* for $[(L^H)Ni(HCOO)]^+$ = 343.0705; observed *m/z* = 343.0698 and calculated *m/z* for $[(L^H)Ni]^{2+}$ = 149.0359; observed *m/z* = 149.0312.

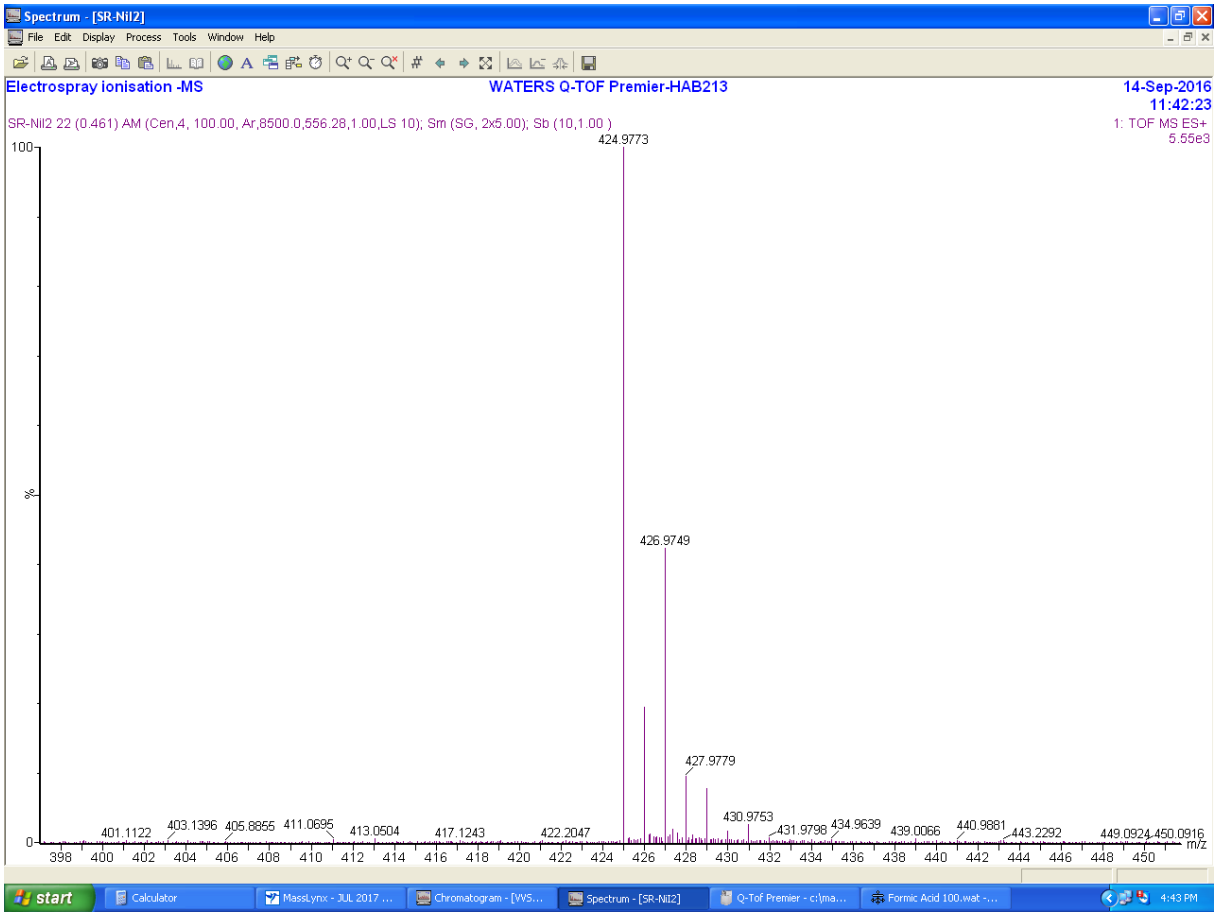

Calculated *m/z* for $[(L^{H})NiI]^{+}$ = $C_{14}H_{16}IN_4Ni$ = 424.9773; observed *m/z* = 424.9773.

Simulated ESI-MS of $[(L^{H})NiI]^{+}$

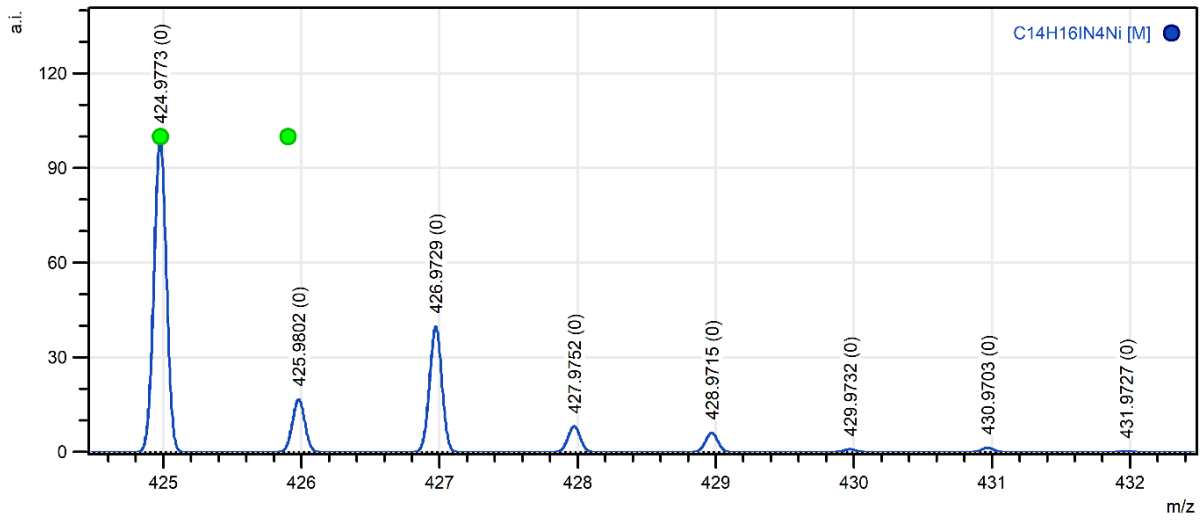

Figure S 4. ESI-MS of $[(L^H)Ni(CH_3CN)_2](BPh_4)_2$.

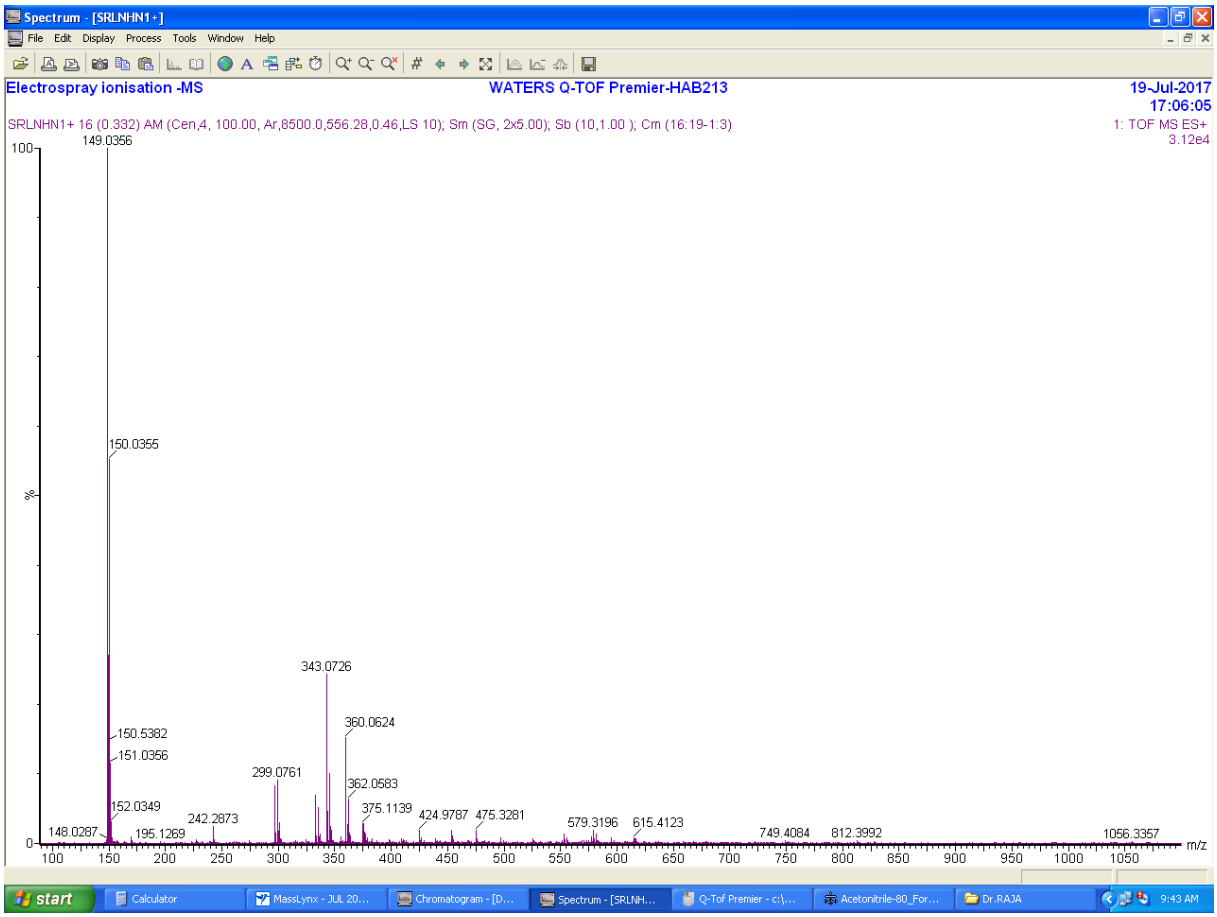

Calculated *m/z* for $[(L^H)Ni]^{2+}$ = 149.0359; observed *m/z* = 149.0356. Calculated *m/z* for $[(L^H)Ni(HCOO)]^+$ = 343.0705; observed *m/z* = 343.0726.

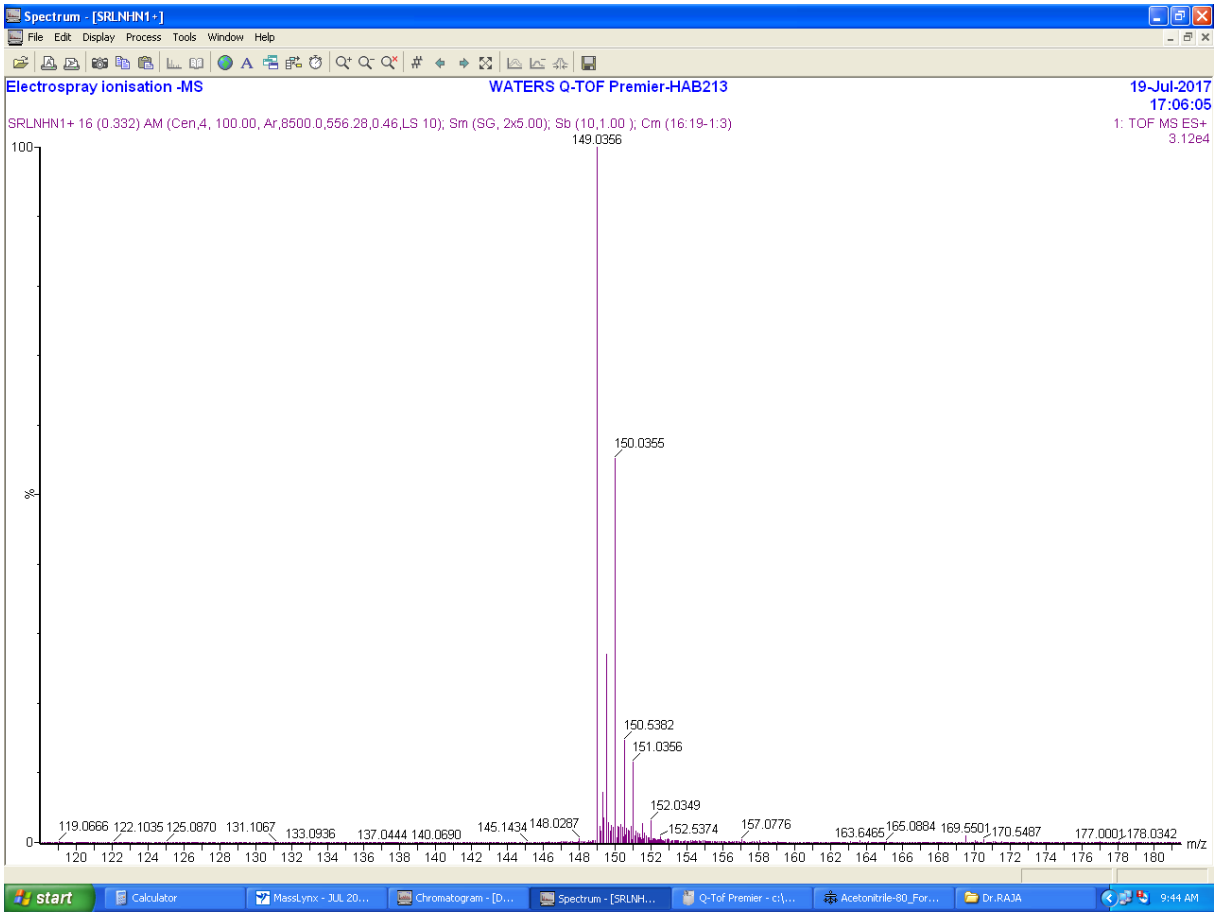

Calculated *m/z* for $[(L^{H})Ni]^{2+}$ = $C_{14}H_{16}N_4Ni$ = 149.0359; observed *m/z* = 149.0356.

Figure S 5. ESI-MS of $[(L^H)Ni(H_2O)_2](OTs)_2$.

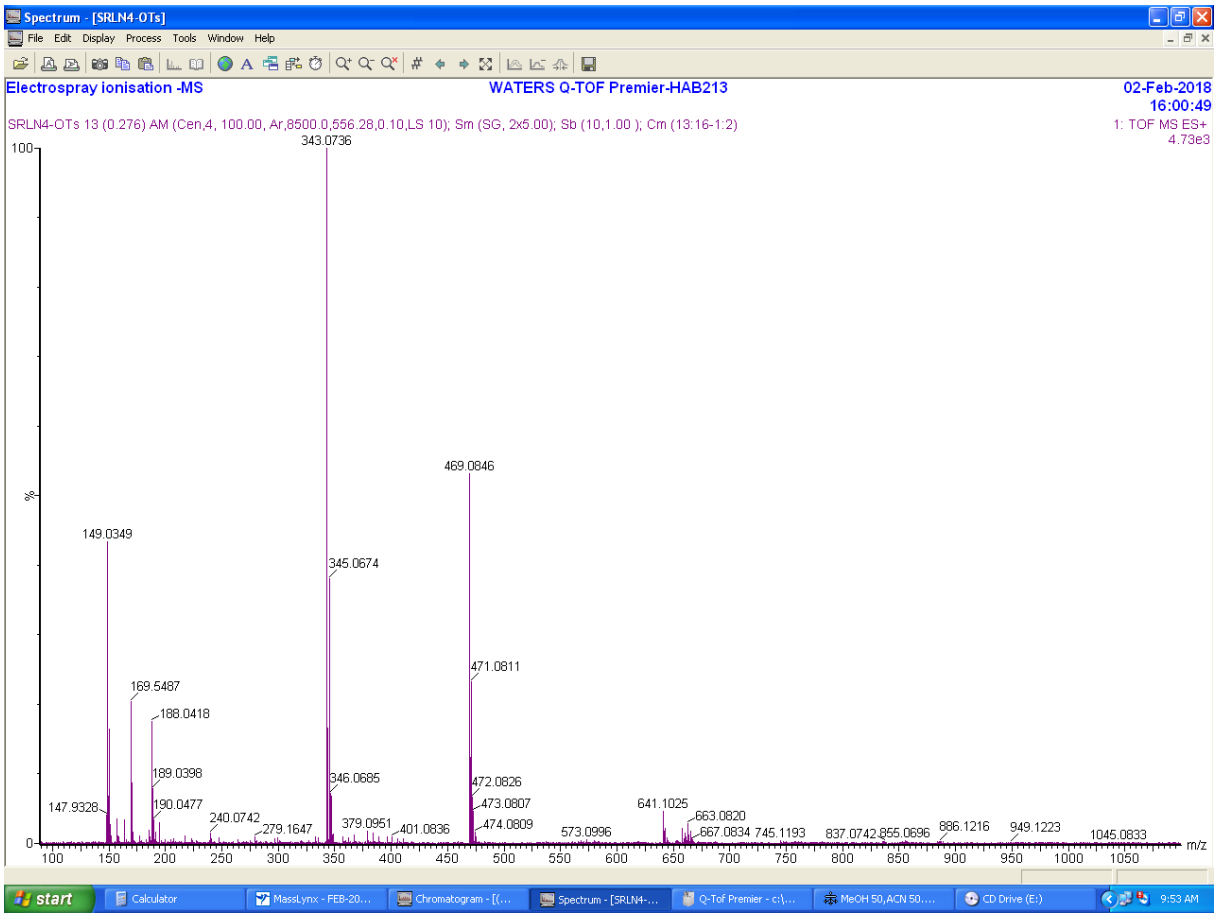

Calculated *m/z* for $[(L^H)Ni]^{2+}$ = 149.0359; observed *m/z* = 149.0349. Calculated *m/z* for $[(L^H)NiOTs]^+$ = $C_{21}H_{23}N_4NiO_3S$ = 469.0844; observed *m/z* = 469.0846 and calculated *m/z* for $[(L^H)Ni(HCOO)]^+$ = 343.0705; observed *m/z* = 343.0736.

Simulated ESI-MS of $[(L^H)NiOTs]^+$

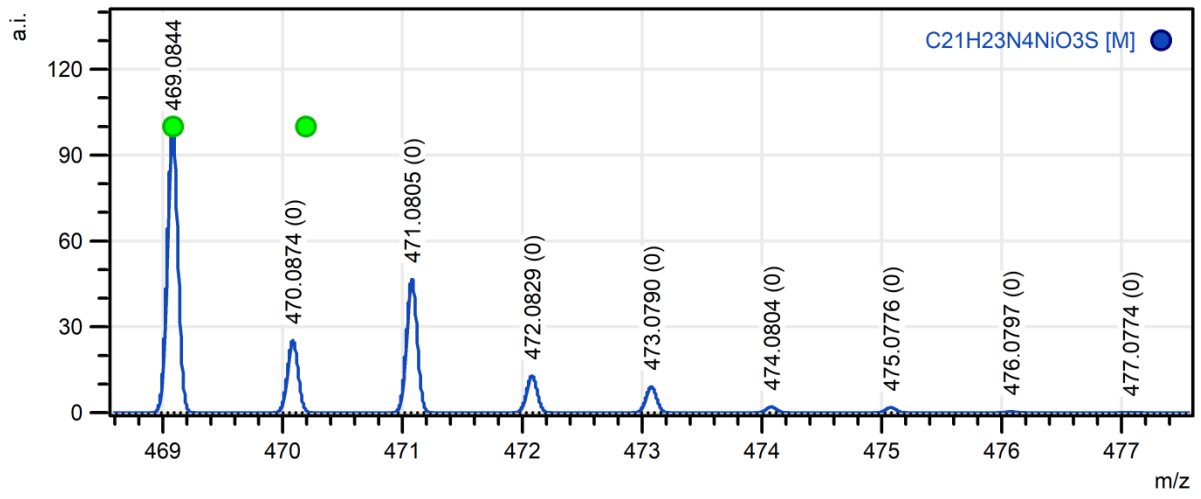

Figure S 6. ESI-MS of $[(L^H)Ni(\mu\text{-SPh})]_2(BPh_4)_2$.

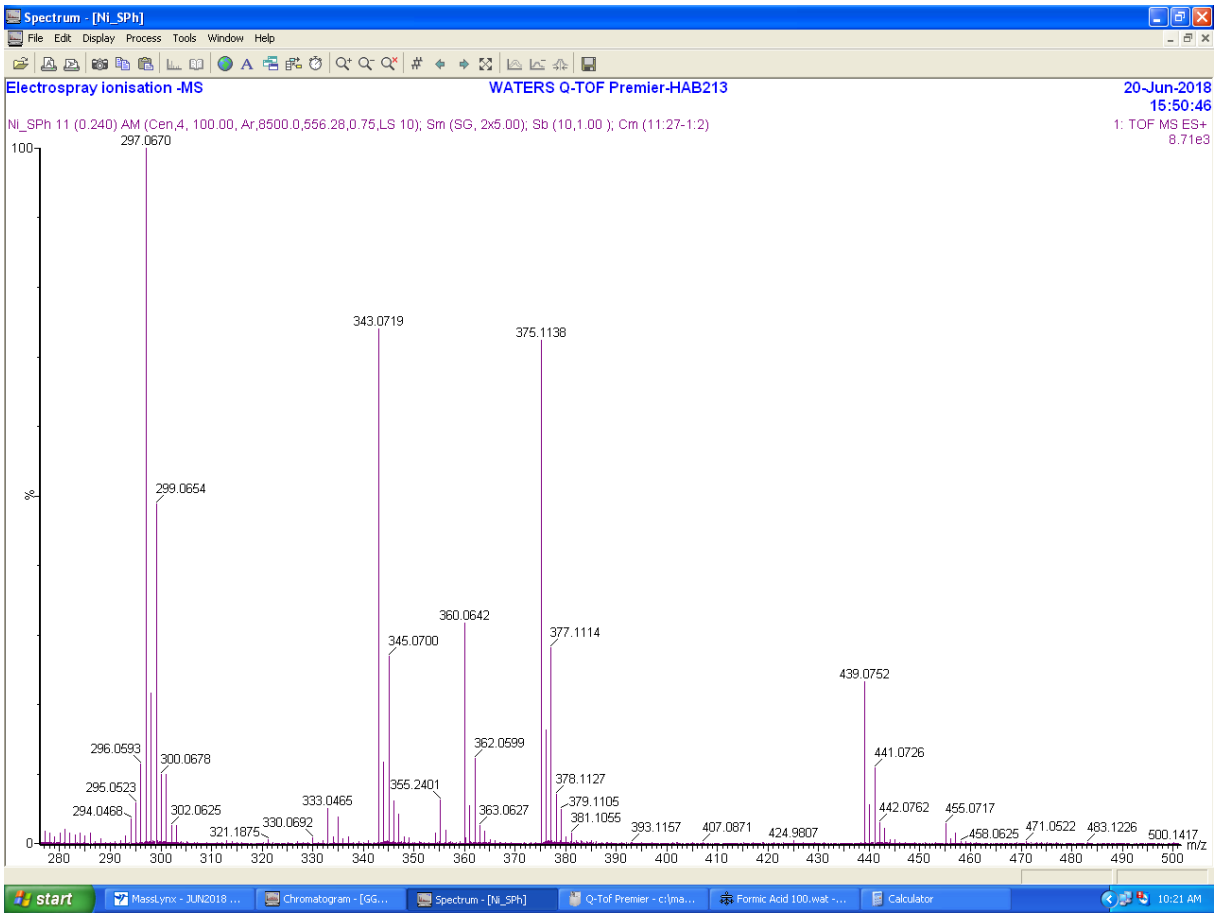

Calculated *m/z* for $[(L^H)Ni(SPh)(O_2)]^+ = C_{20}H_{21}N_4NiO_2S = 439.0739$; observed *m/z* = 439.0752.

Simulated ESI-MS of $[(L^H)Ni(SPh)(O_2)]^+$

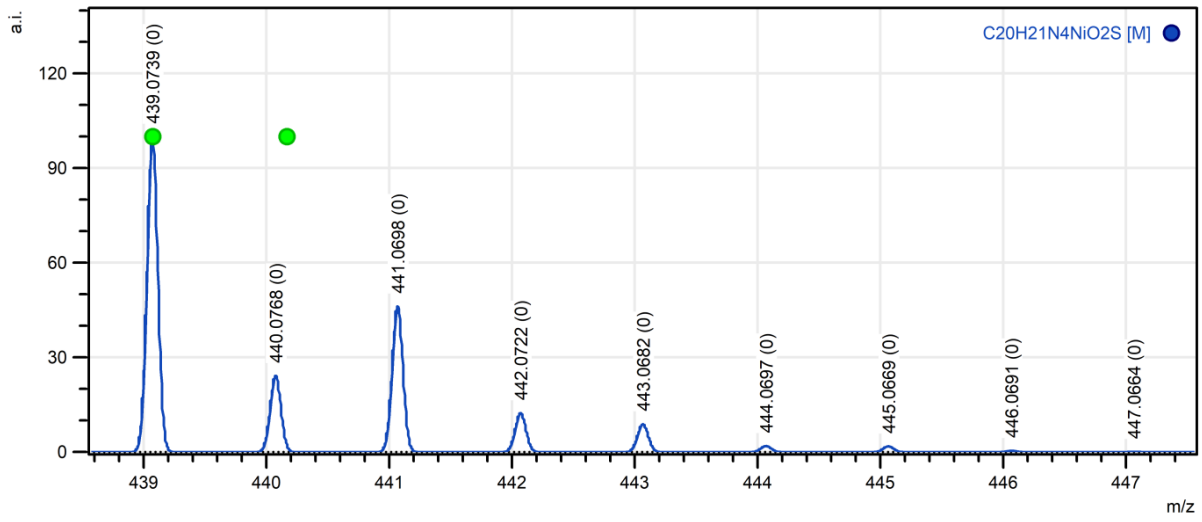

Figure S 7. ESI-MS of [(L^H)Ni(dbm)](BPh_4).

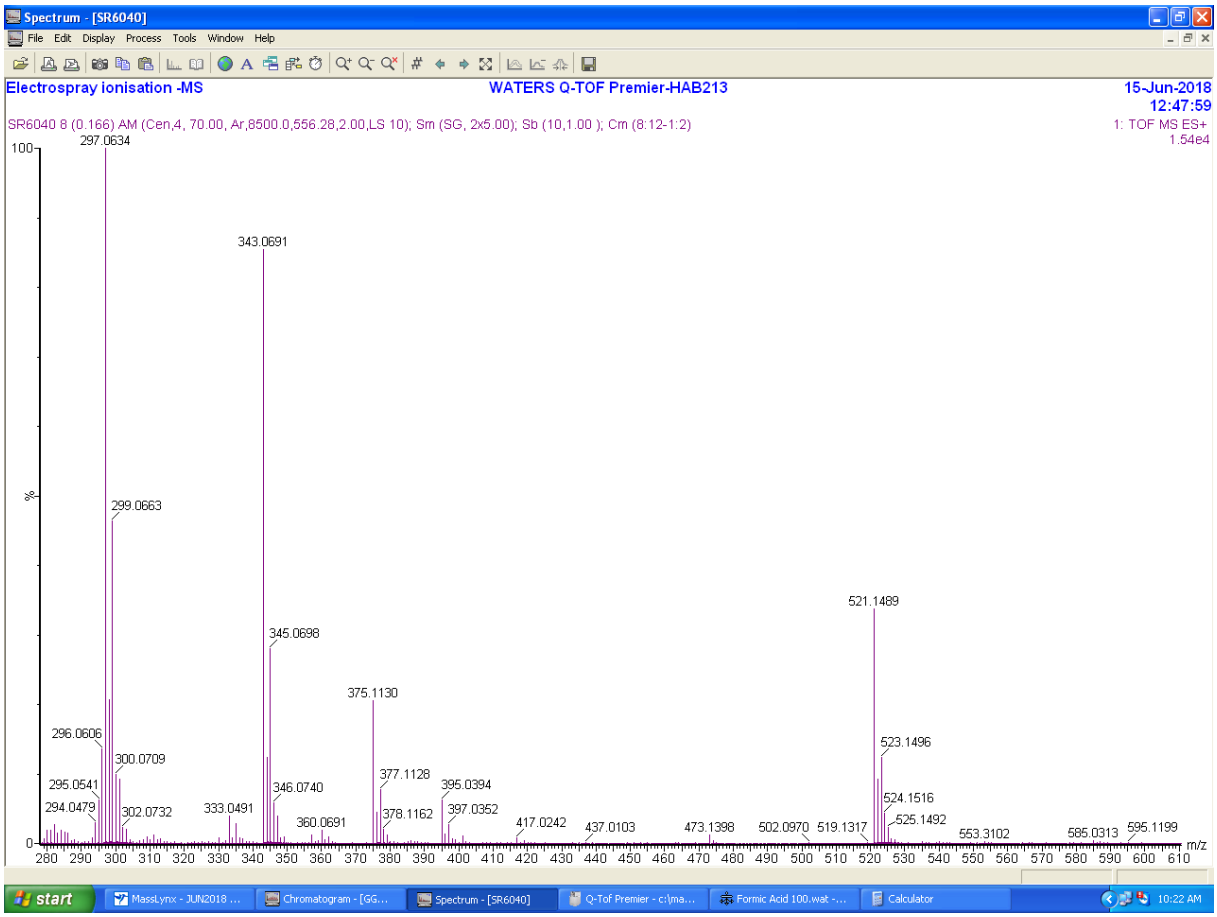

Calculated *m/z* for $[(L^H)Ni(PhCOCHCOPh)]^+ = C_{29}H_{27}N_4NiO_2 = 521.1487$; observed *m/z* = 521.1489.

Simulated ESI-MS of $[(L^H)Ni(PhCOCHCOPh)]^+$

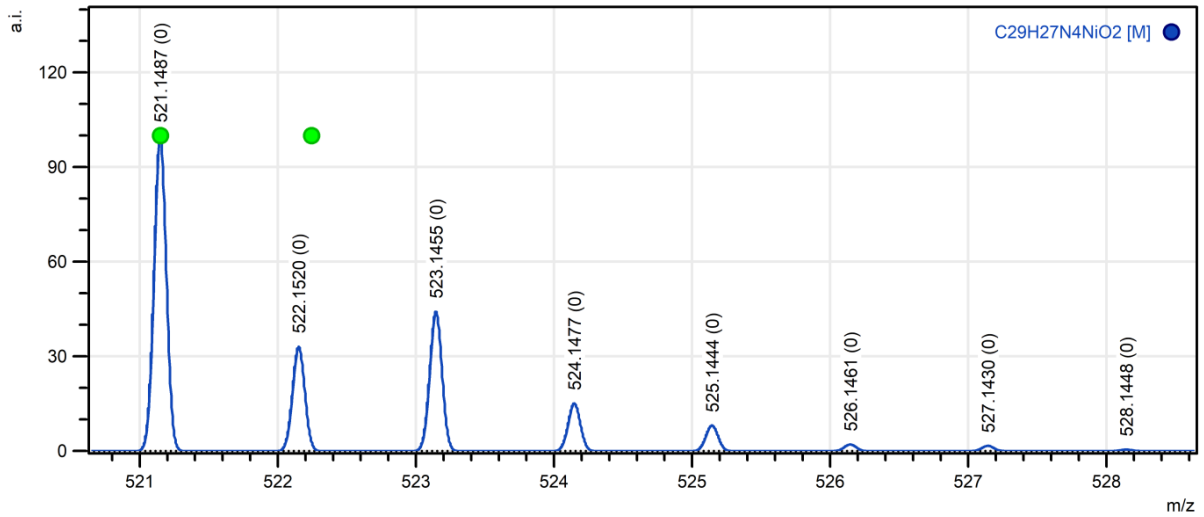

Figure S 8. ESI-MS of $[(L^H)Ni(\eta^2\text{-}BH_4)](BPh_4)$ and benzyl bromide reaction mixture in CH_3CN.

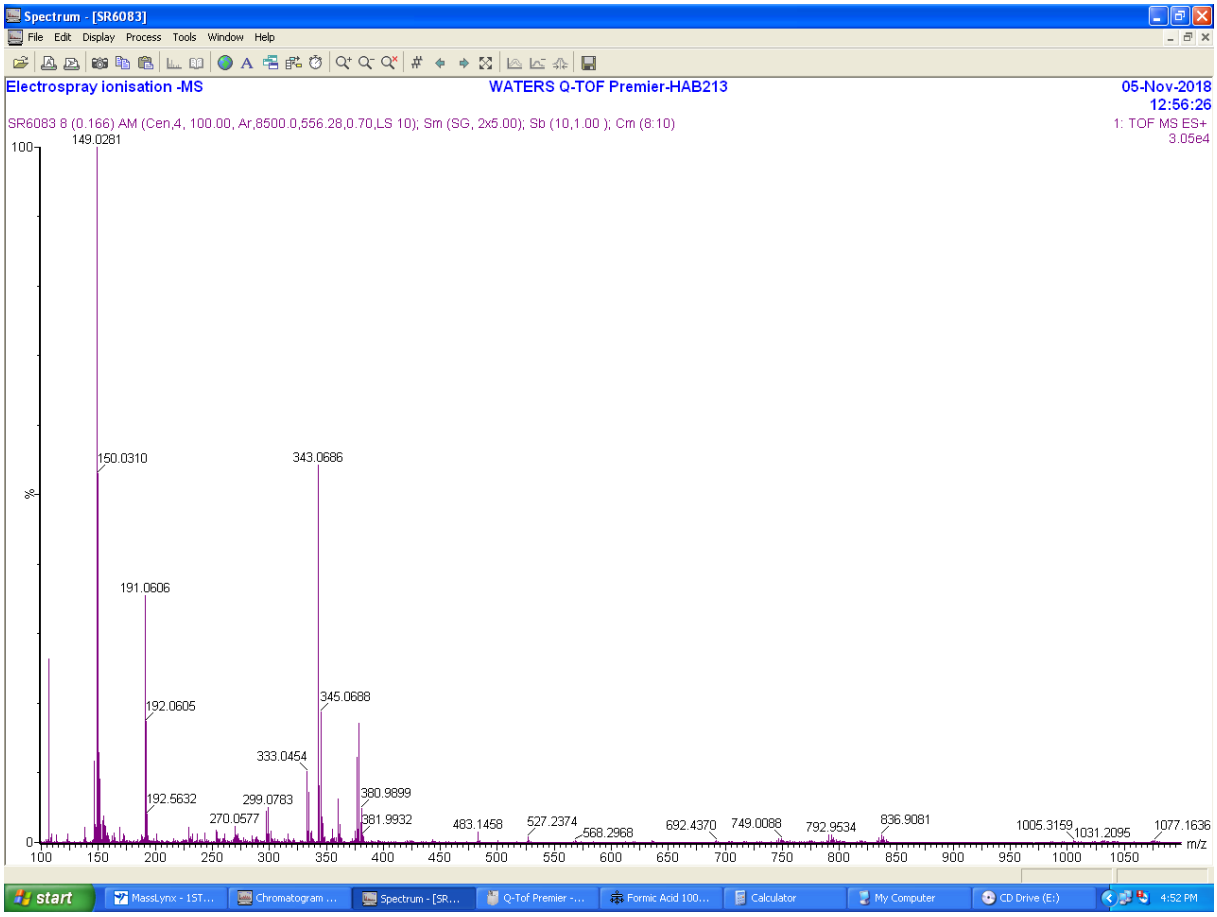

Calculated *m/z* for $[(L^H)NiBr]^+ = C_{14}H_{16}BrN_4Ni = 376.9912$; observed *m/z* = 376.9926. Calculated *m/z* for $[(L^H)Ni(HCOO)]^+ = 343.0705$; observed *m/z* = 343.0686 and calculated *m/z* for $[(L^H)Ni]^{2+} = 149.0359$; observed *m/z* = 149.0281.

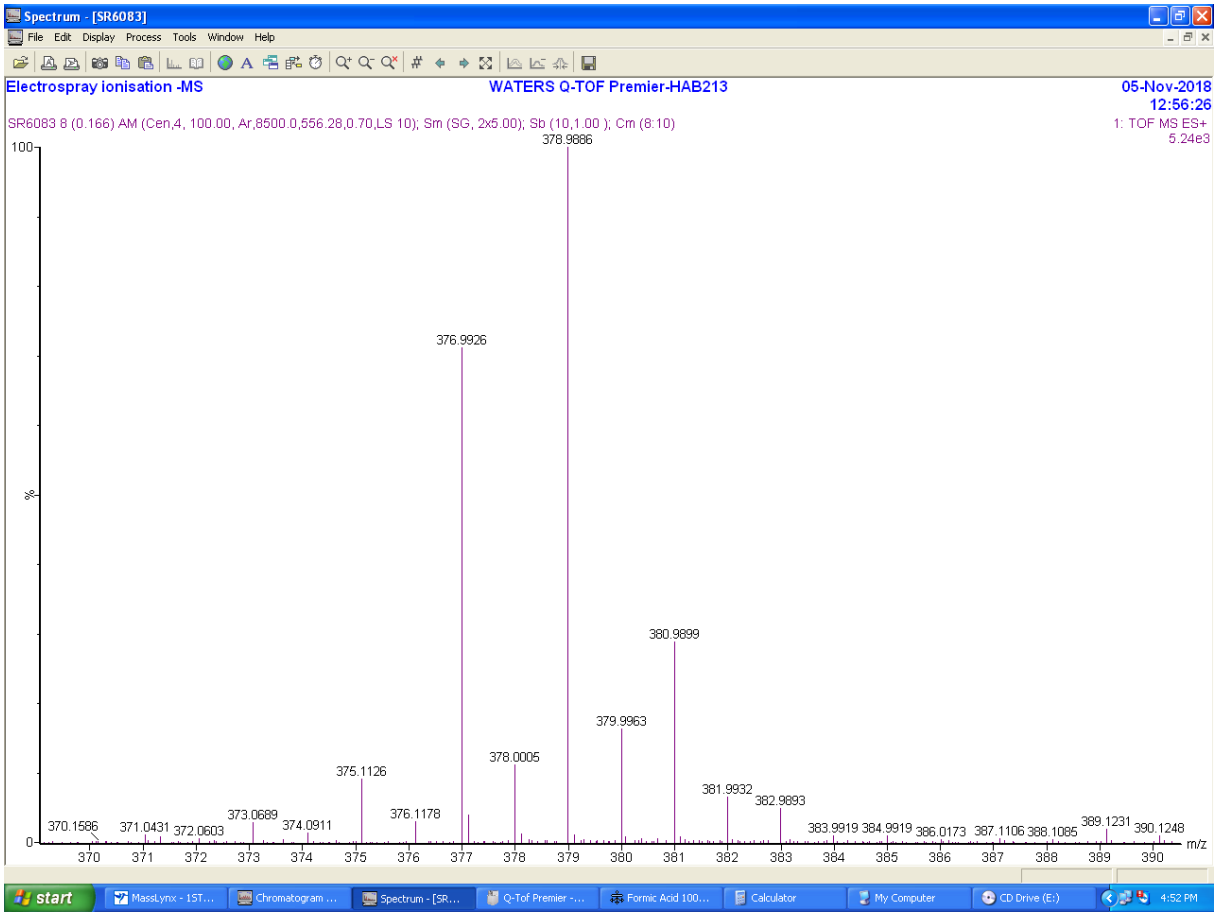

Calculated *m/z* for $[(L^{H})NiBr]^{+}$ = $C_{14}H_{16}BrN_4Ni$ = 376.9912; observed *m/z* = 376.9926.

Simulated ESI-MS of $[(L^{H})NiBr]^{+}$

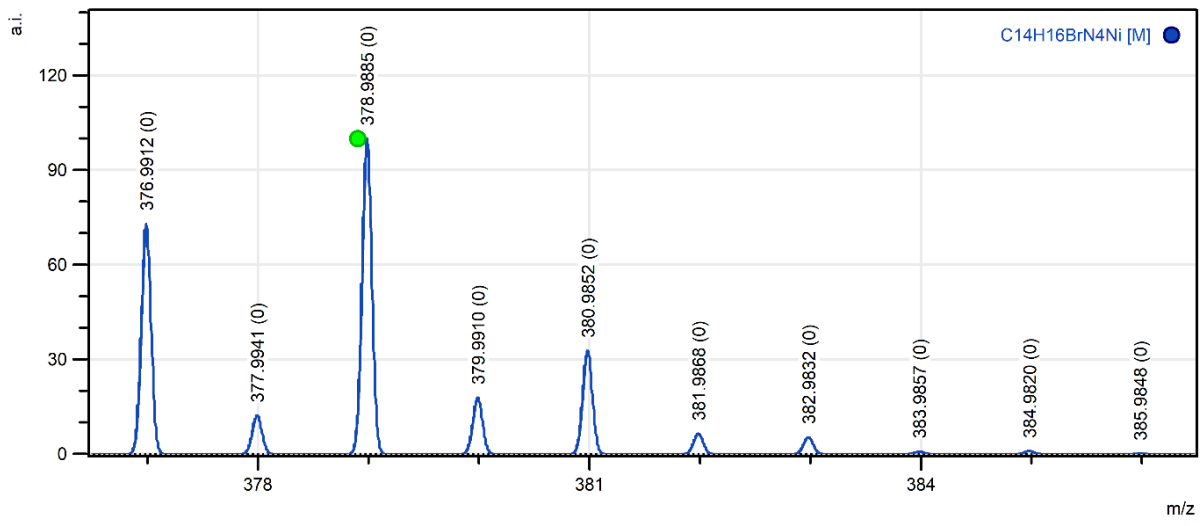

Figure S 9. ESI-MS of $[(L^H)Ni(\eta^2\text{-}BH_4)](BPh_4)$ and CH_3I reaction mixture in CH_3CN.

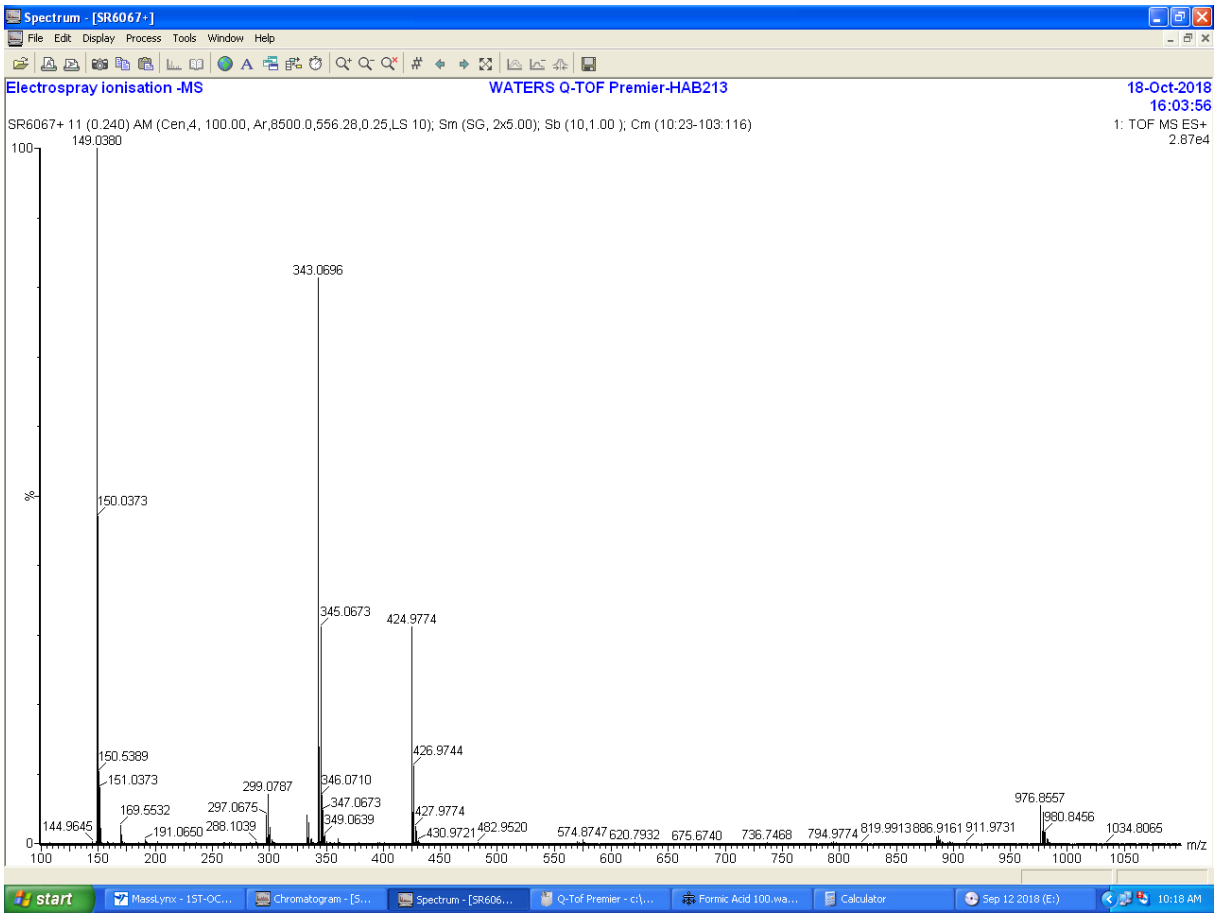

Calculated *m/z* for $[(L^H)NiI]^+ = C_{14}H_{16}IN_4Ni = 424.9773$; observed *m/z* = 424.9774. Calculated *m/z* for $[(L^H)Ni(HCOO)]^+$ = 343.0705; observed *m/z* = 343.0696 and calculated *m/z* for $[(L^H)Ni]^{2+}$ = 149.0359; observed *m/z* = 149.0380.

Simulated ESI-MS of $[(L^H)NiI]^+$

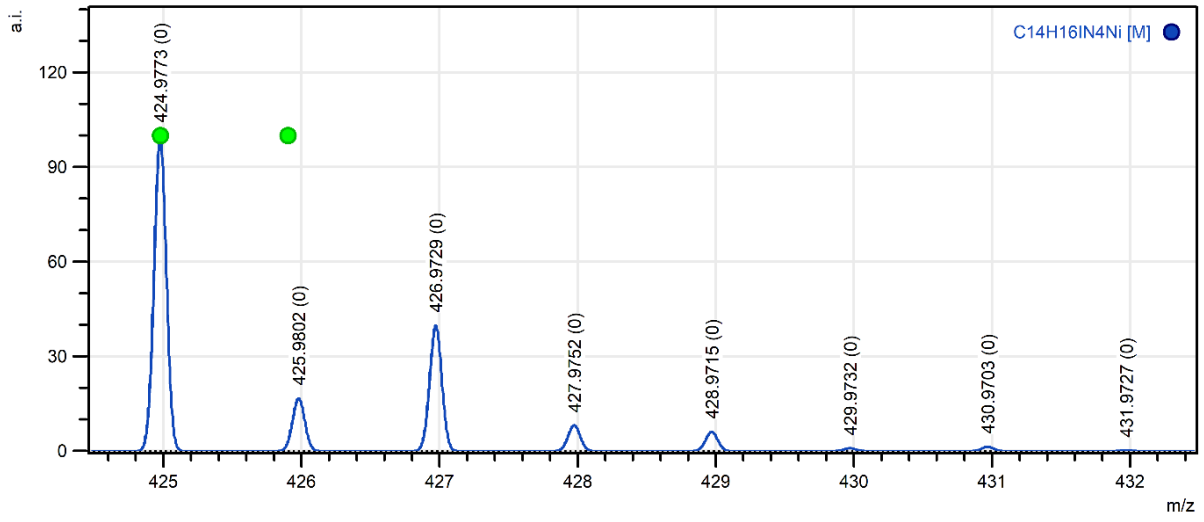

Figure S 10. ESI-MS of $[(L^H)Ni(HCOO)](BPh_4)$.

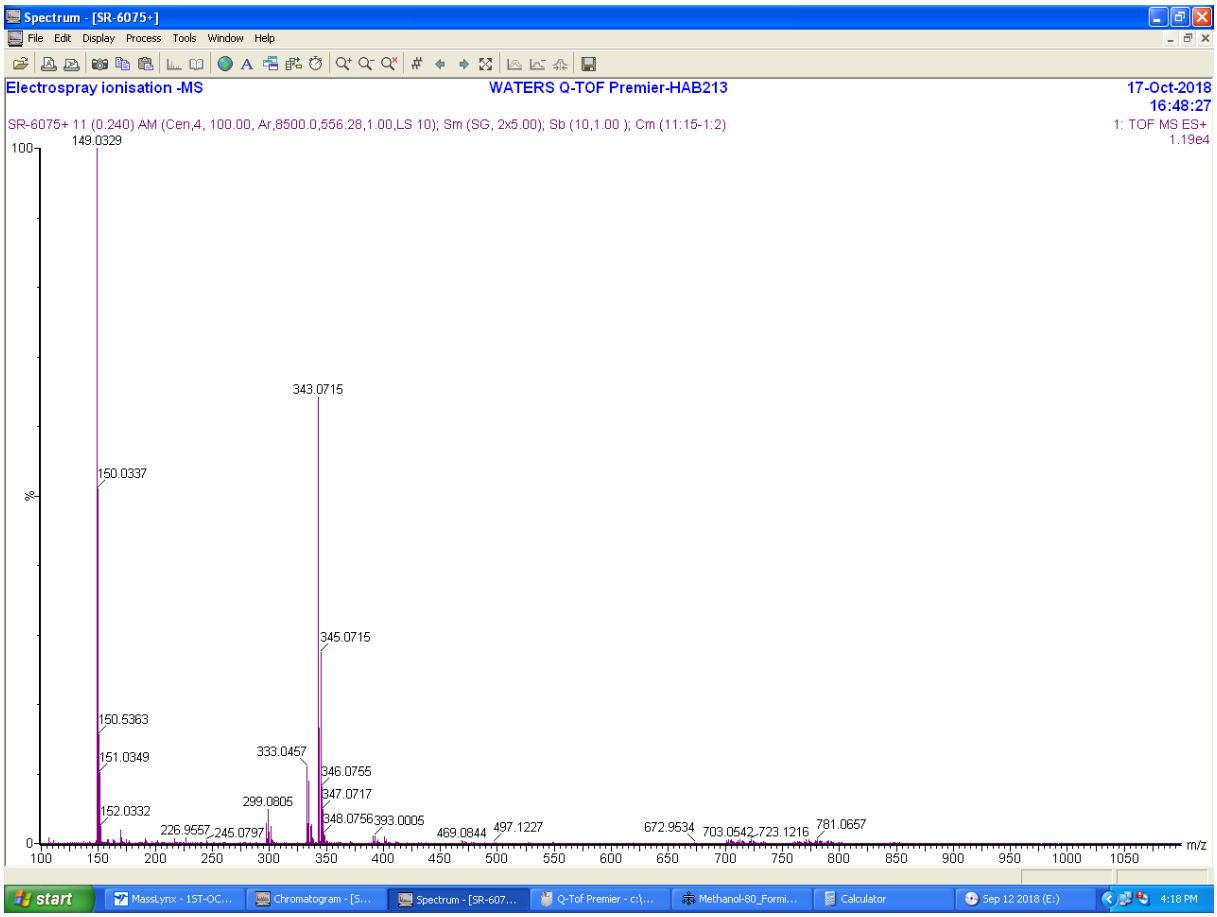

Calculated *m/z* for $[(L^H)Ni(HCOO)]^+$ = 343.0705; observed *m/z* = 343.0715 and calculated *m/z* for $[(L^H)Ni]^{2+}$ = 149.0359; observed *m/z* = 149.0329.

Simulated ESI-MS of $[(L^H)Ni(HCOO)]^+$

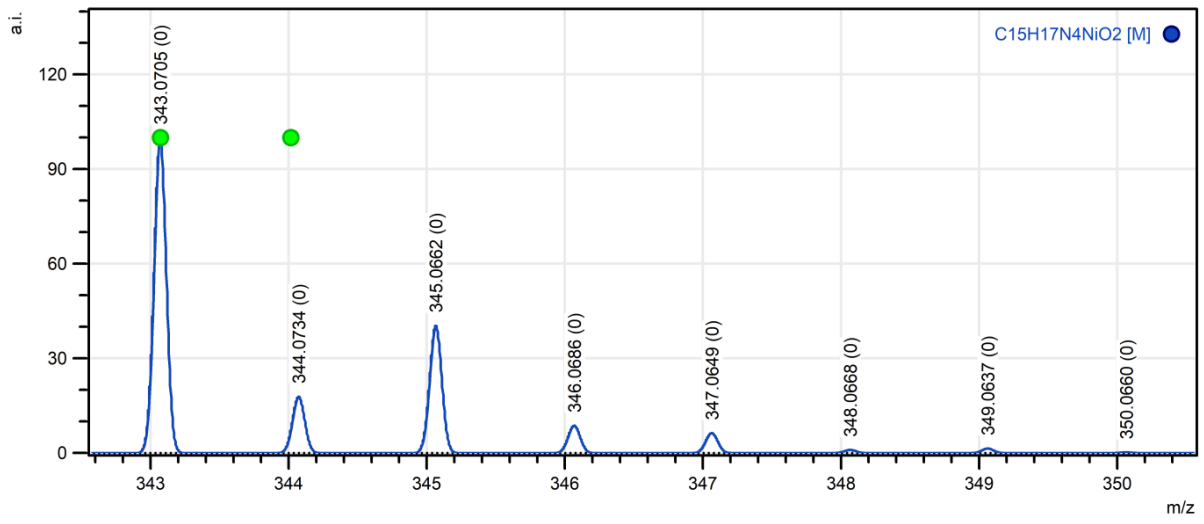

Figure S 11. ESI-MS of $[(L^H)Ni(HSO_4)](BPh_4)$(cation mode).

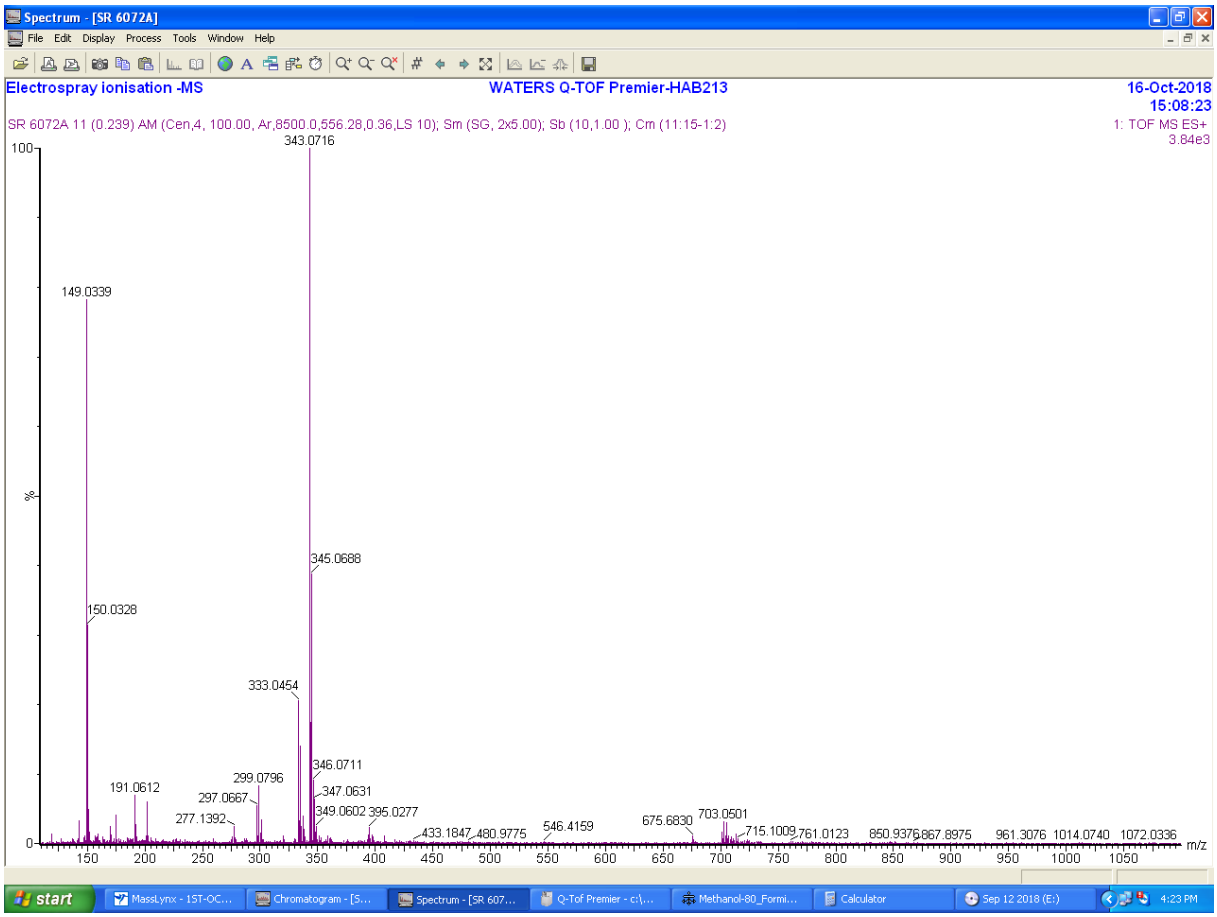

Calculated *m/z* for $[(L^H)Ni(HSO_4)]^+$ = $C_{14}H_{17}N_4NiO_4S$ = 395.0324; observed *m/z* = 395.0277 and calculated *m/z* for $[(L^H)Ni(HCOO)]^+$ = 343.0705; observed *m/z* = 395.0716.

Simulated ESI-MS of $[(L^H)Ni(HSO_4)]^+$

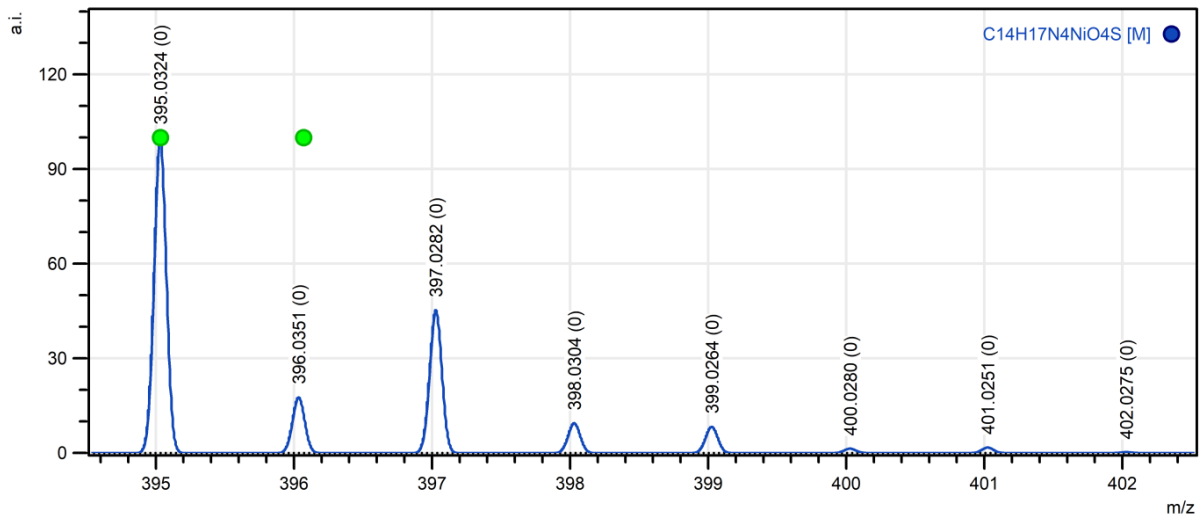

Figure S 12. ESI-MS of [(L^H)Ni(HSO_4)](BPh_4)(anion mode).

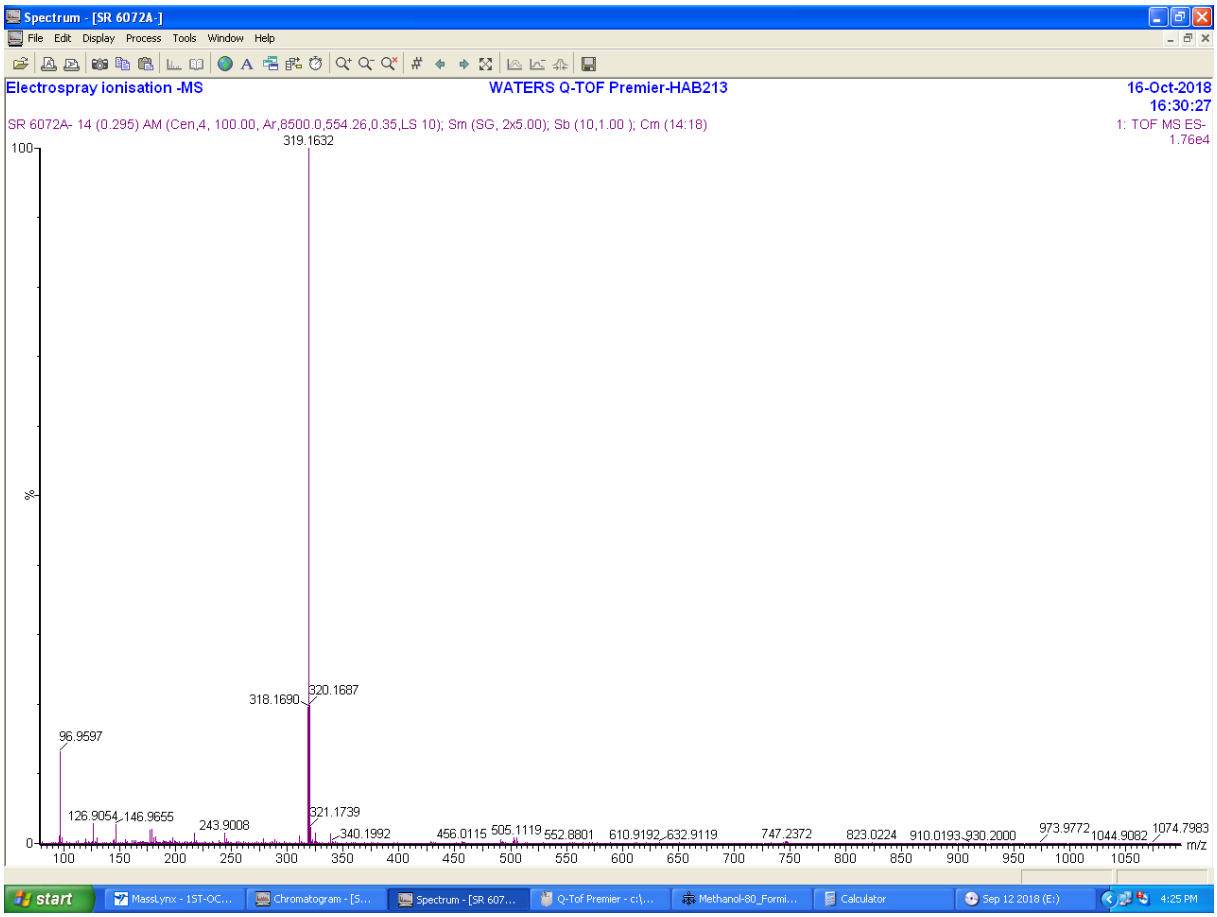

Calculated *m/z* for HSO_4 anion = 96.9596; observed *m/z* = 96.9597.

Simulated ESI-MS of HSO_4 anion

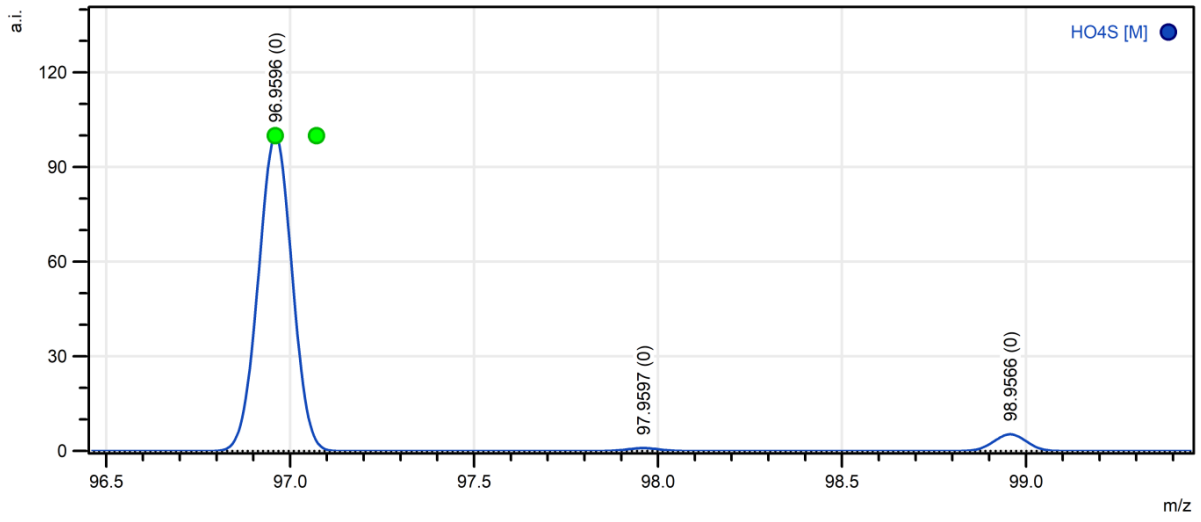

Figure S 13. PXRD patterns for mechanochemically synthesised $[(L^H)Ni(\mu\text{-}X)]_2(X)_2$ (X = Cl, Br, I)

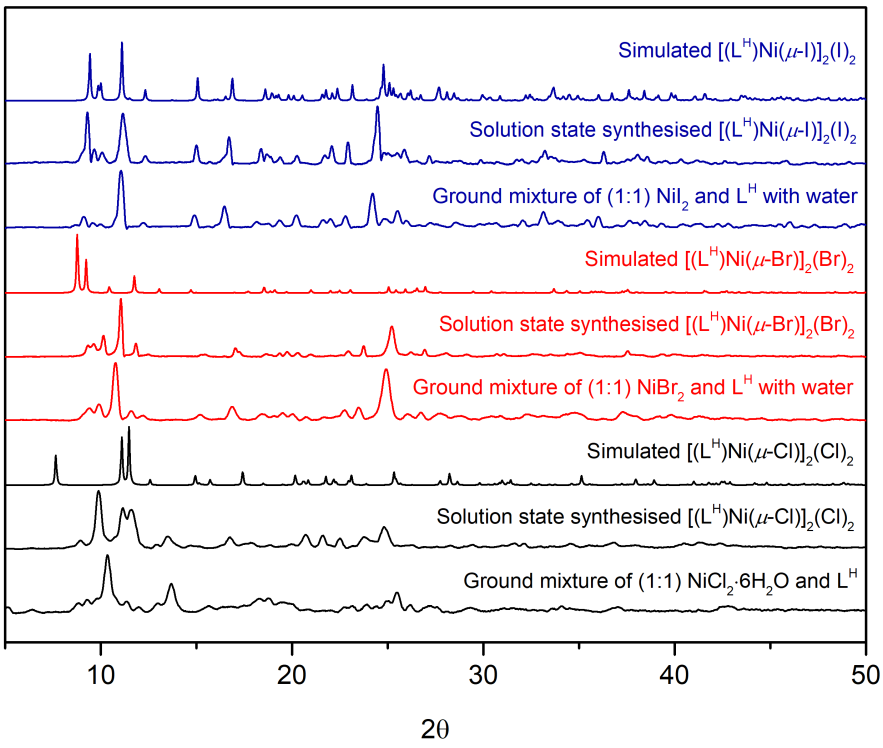

Figure S 14. Variation of PXRD patterns during mechanochemical syntheses of $[(L^H)Ni(\mu\text{-}Cl)]_2(Cl)_2$ and $[(L^H)Ni(CH_3CN)_2](BPh_4)_2$.

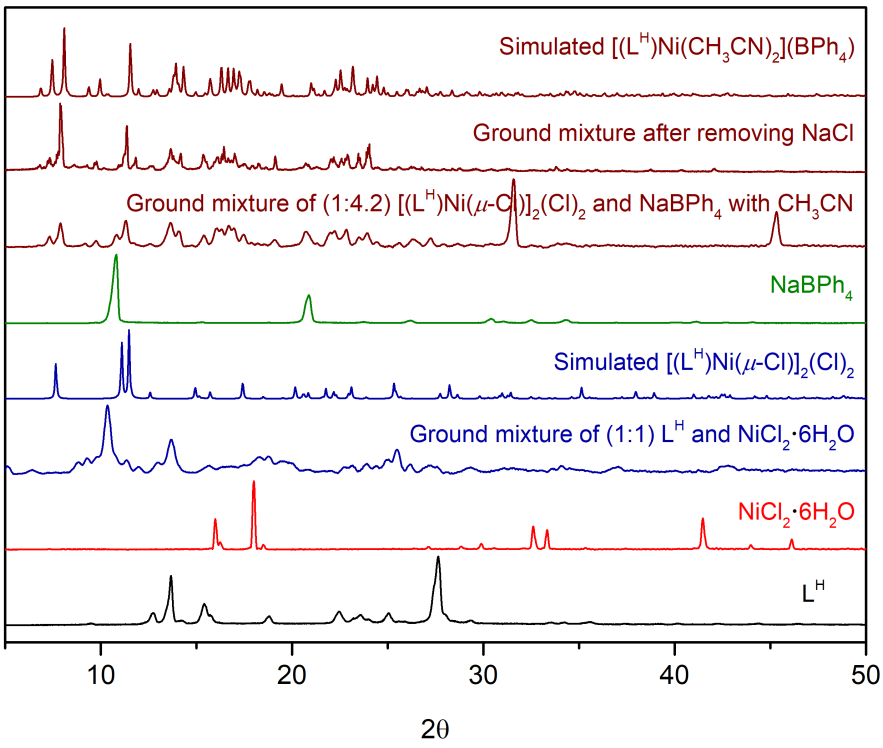

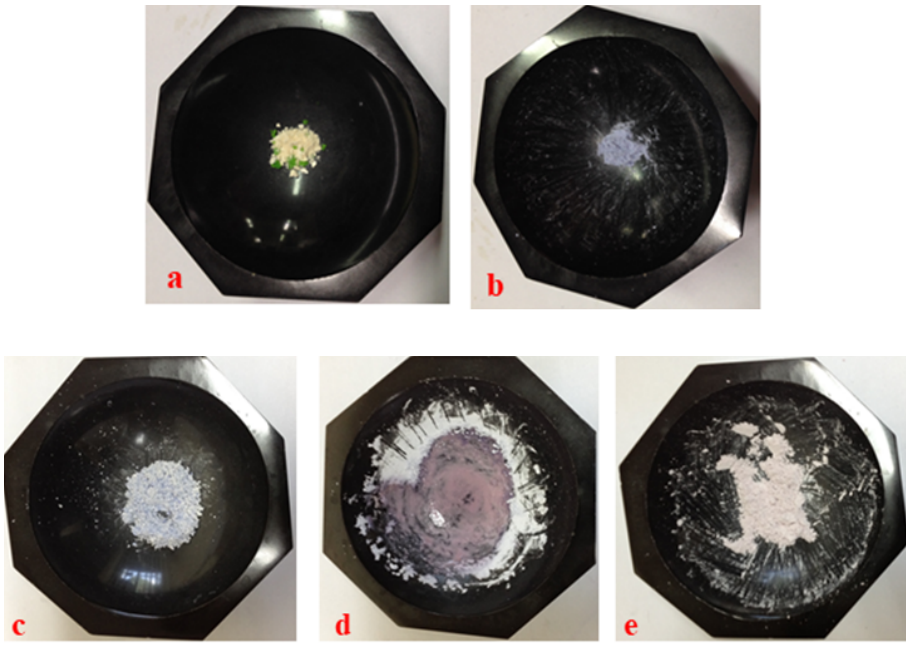

(a) L^H and $NiCl_2{\cdot}6H_2O$ (b) After grinding (c) $[(L^H)Ni(\mu\text{-}Cl)]_2(Cl)_2$ and $NaBPh_4$ (d) with 0.1 ml CH_3CN (e) After grinding.

Figure S 15. UV-vis spectrum of $[(L^H)Ni(CH_3CN)_2](BPh_4)_2$.

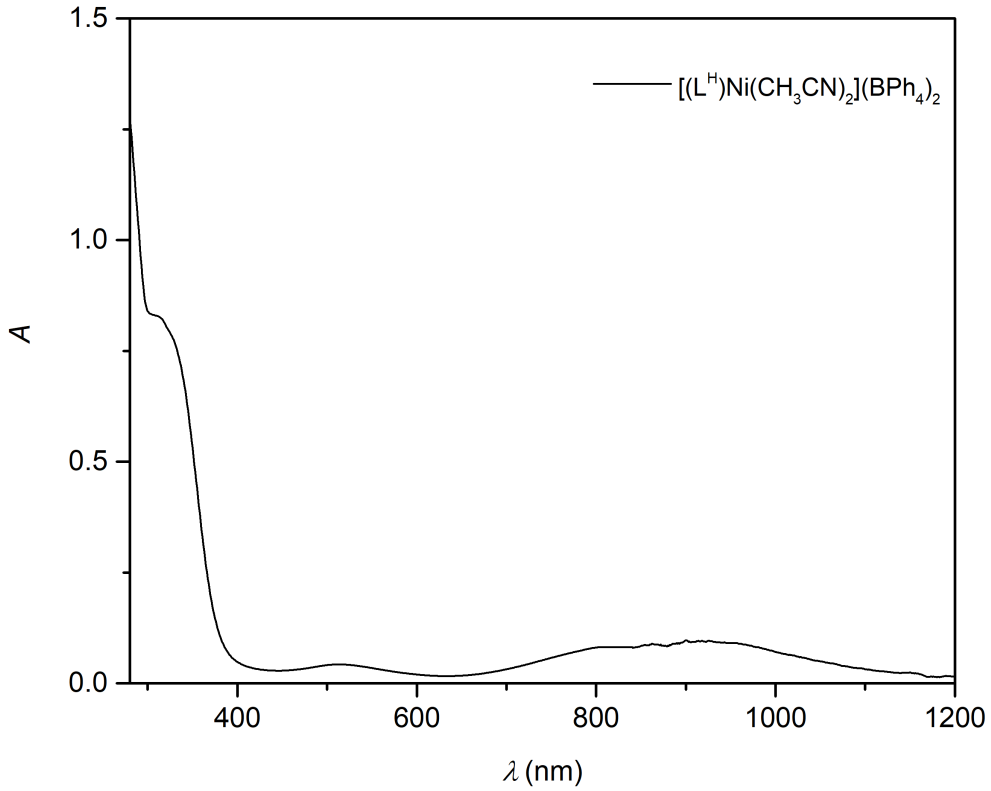

2 mM of $[(L^H)Ni(CH_3CN)_2](BPh_4)_2$ in acetonitrile.

Figure S 16. FT-IR for the ground mixture of (1:1) $[(L^H)Ni(CH_3CN)_2](BPh_4)_2$ and $NaBH_4$.

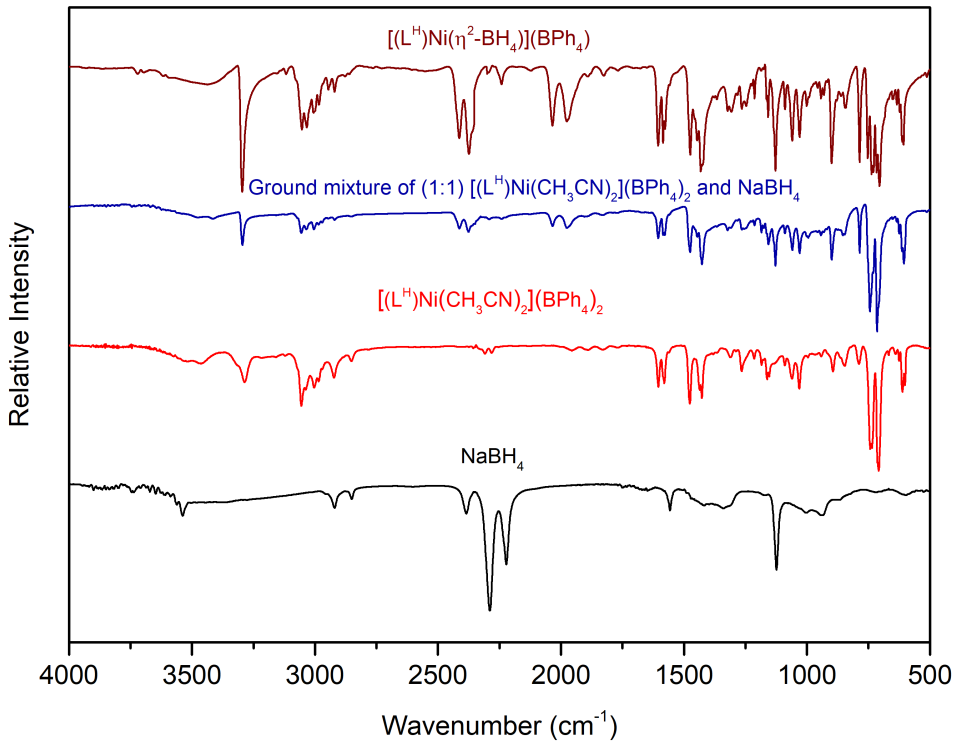

Figure S 17. FT-IR of $[(L^H)Ni(\eta^2\text{-}BH_4)](BPh_4)$ and $[(L^H)Ni(\eta^2\text{-}BD_4)](BPh_4)$.

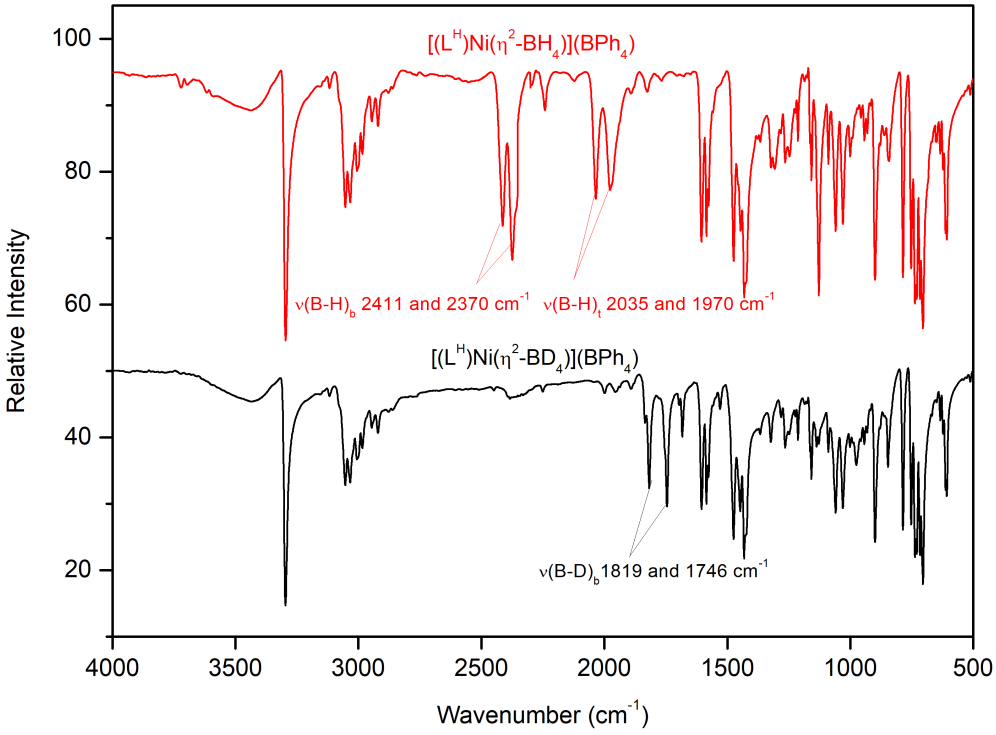

Figure S 18. PXRD patterns for the ground mixture of (1:1) $[(L^H)Ni(CH_3CN)_2](BPh_4)_2$ and $NaBH_4$.

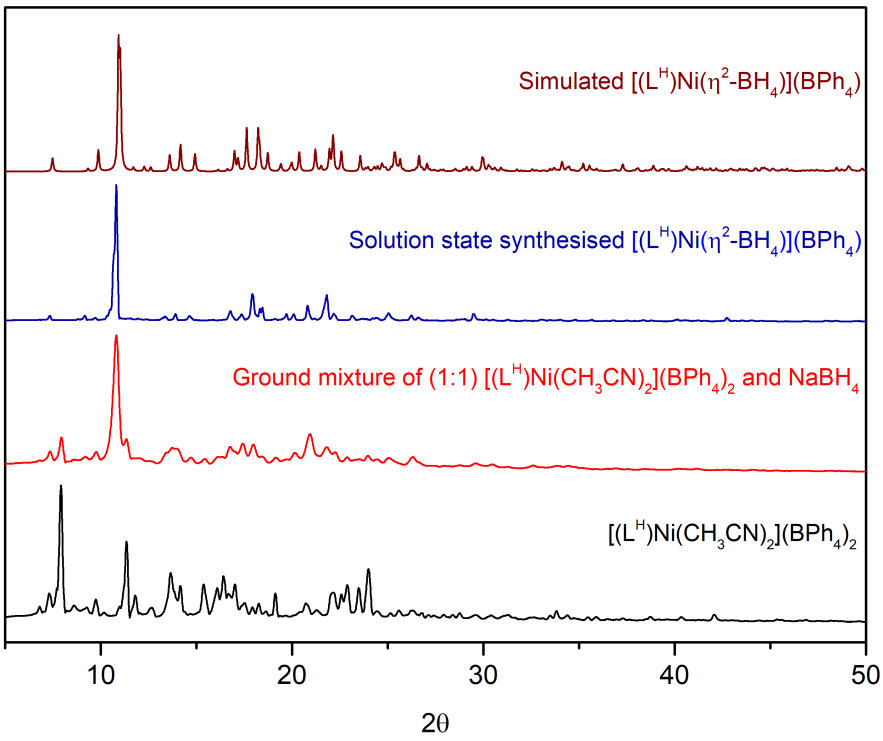

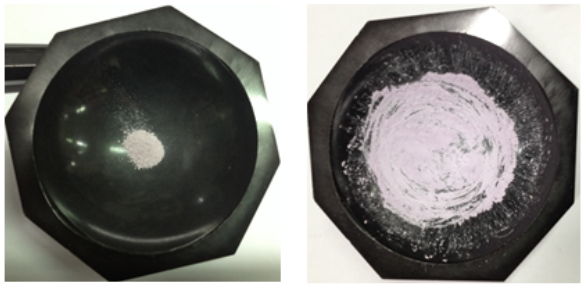

$[Ni(L^H)(CH_3CN)_2](BPh_4)_2$ and NaBH4 after grinding

Figure S 19. TGA of $[(L^H)Ni(\eta^2\text{-}BH_4)](BPh_4)$ and $[(L^H)Ni(\eta^2\text{-}BD_4)](BPh_4)$.

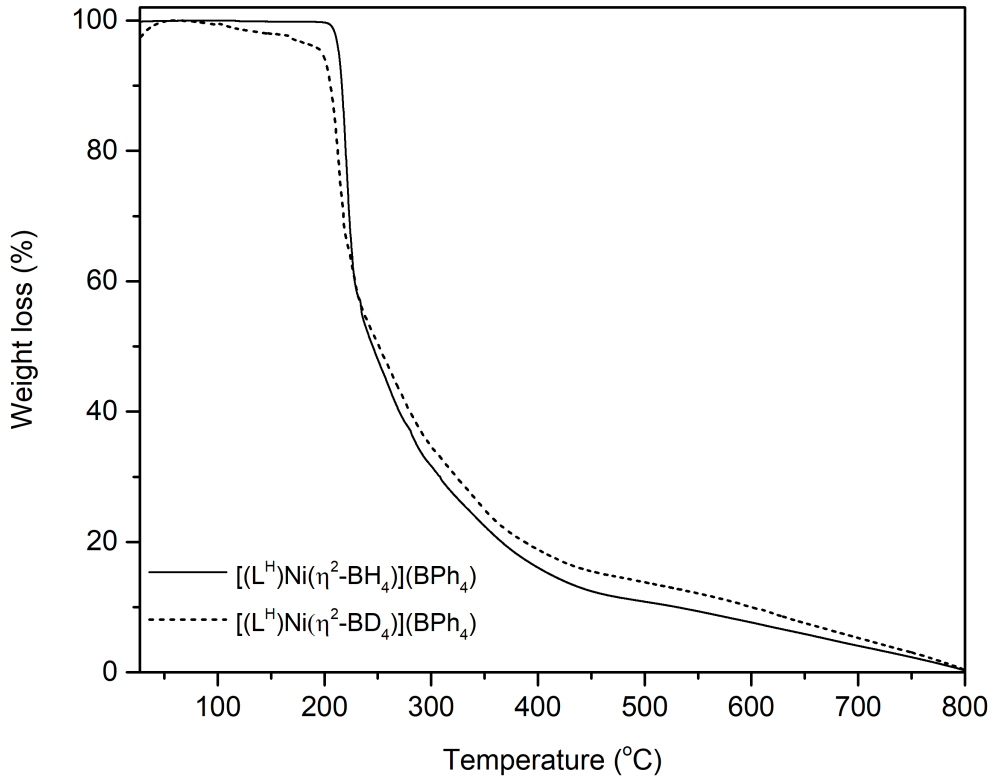

Figure S 20. UV-vis spectrum of [(L^H)Ni(η^2-BH_4)](BPh_4).

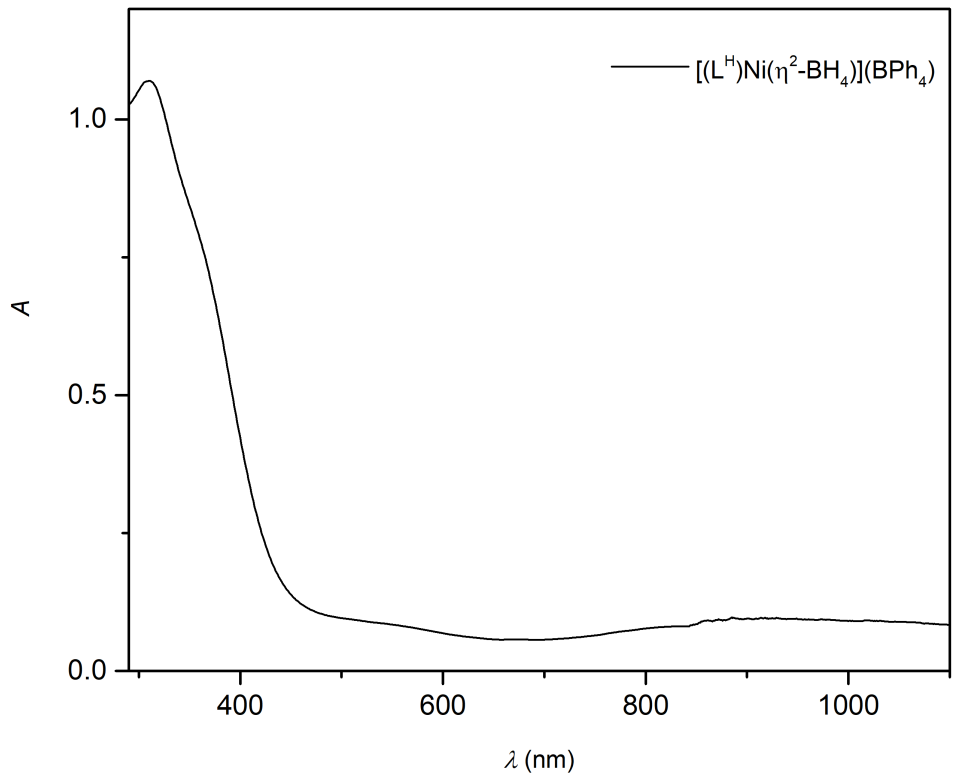

[(L^H)Ni(η^2-BH_4)](BPh_4) (2 mM) solubility was modest in acetonitrile. The violet suspension was stirred for 20 minutes at room temperature to make a homogeneous solution, and the colour was changed to yellow.

Figure S 21. ^{1}H NMR of [(L^{H})Ni(η^{2}-BH$_4$)](BPh$_4$) at 298 K.

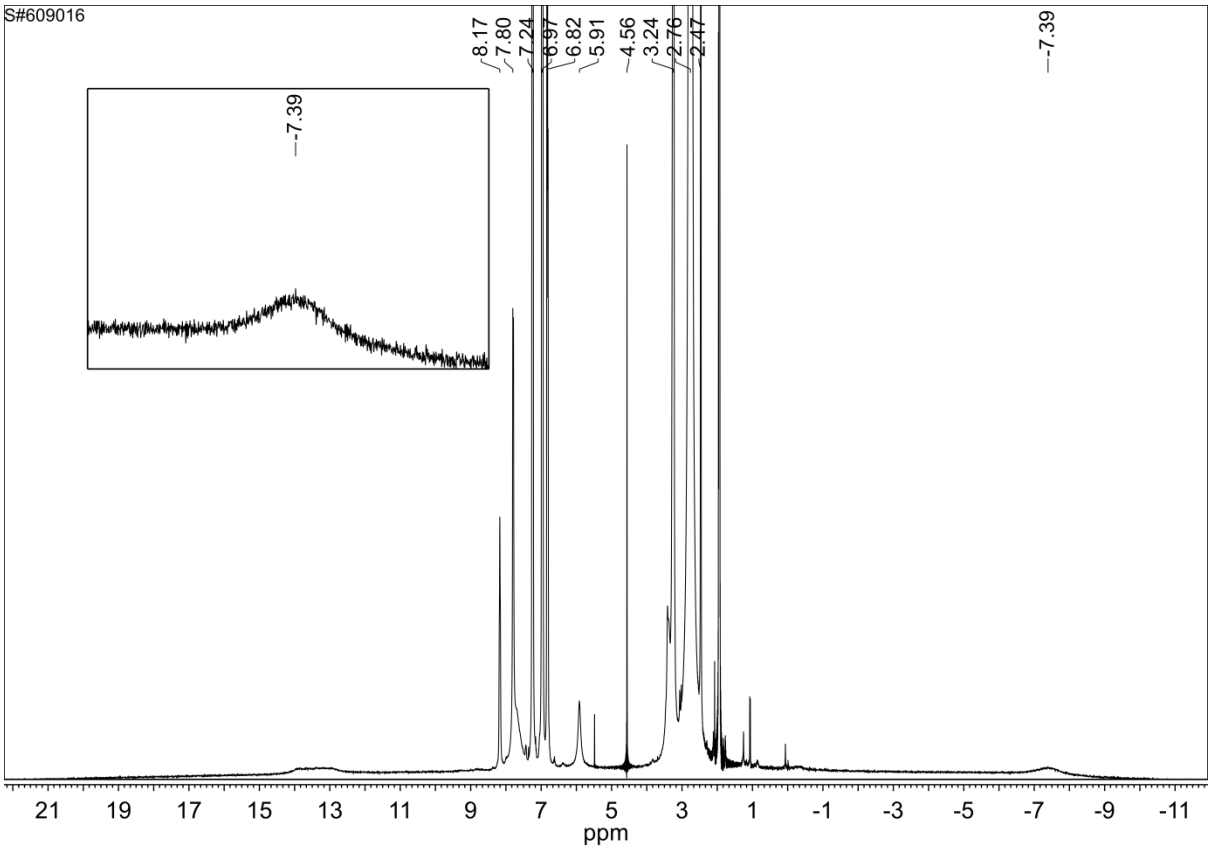

[(L^{H})Ni(η^{2}-BH$_4$)](BPh$_4$) solubility was modest in CD_3CN (0.6 ml), and DMSO-*d*$_6$ (0.05 ml) was added to make this as a homogeneous solution in air. After the addition of DMSO-*d*$_6$ colour of the solution turned to deep yellow along with bubble formation at room temperature (298 K), immediately ^{1}H NMR spectroscopy was recorded at a variable temperature (293 K to 233 K).

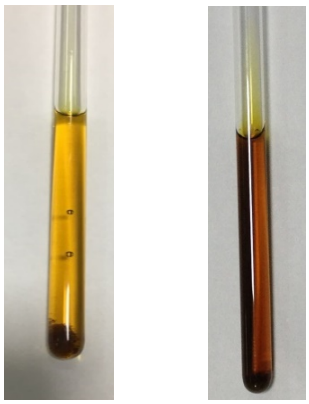

Figure S 22. ^{1}H NMR of [(L^{H})Ni(η^{2}-BH_4)](BPh_4) at a variable temperature (293 K to 233 K).

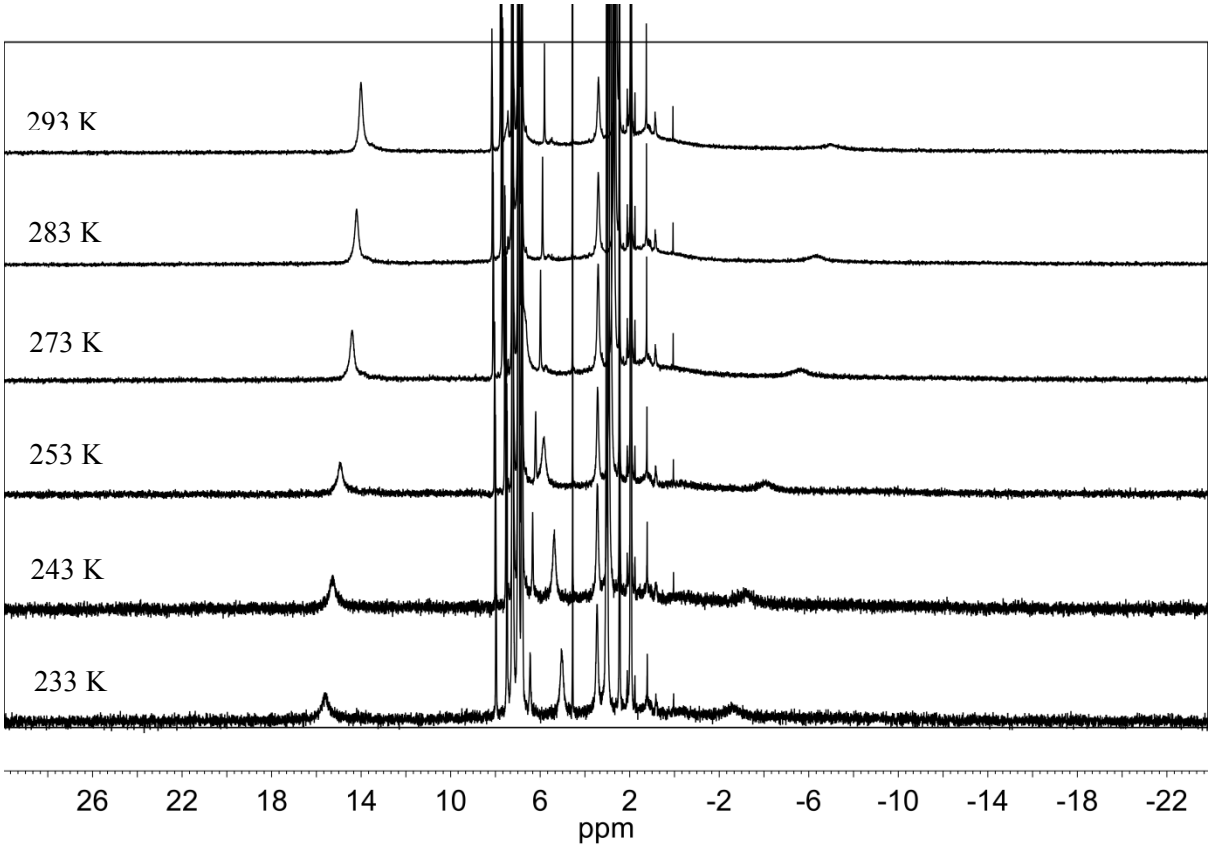

Figure S 23. ^{1}H NMR of $[(L^{H})Ni(\mu\text{-}H)]_2(BPh_4)_2$ at 298 K in CD_3CN and DMSO-d_6 (10:1).

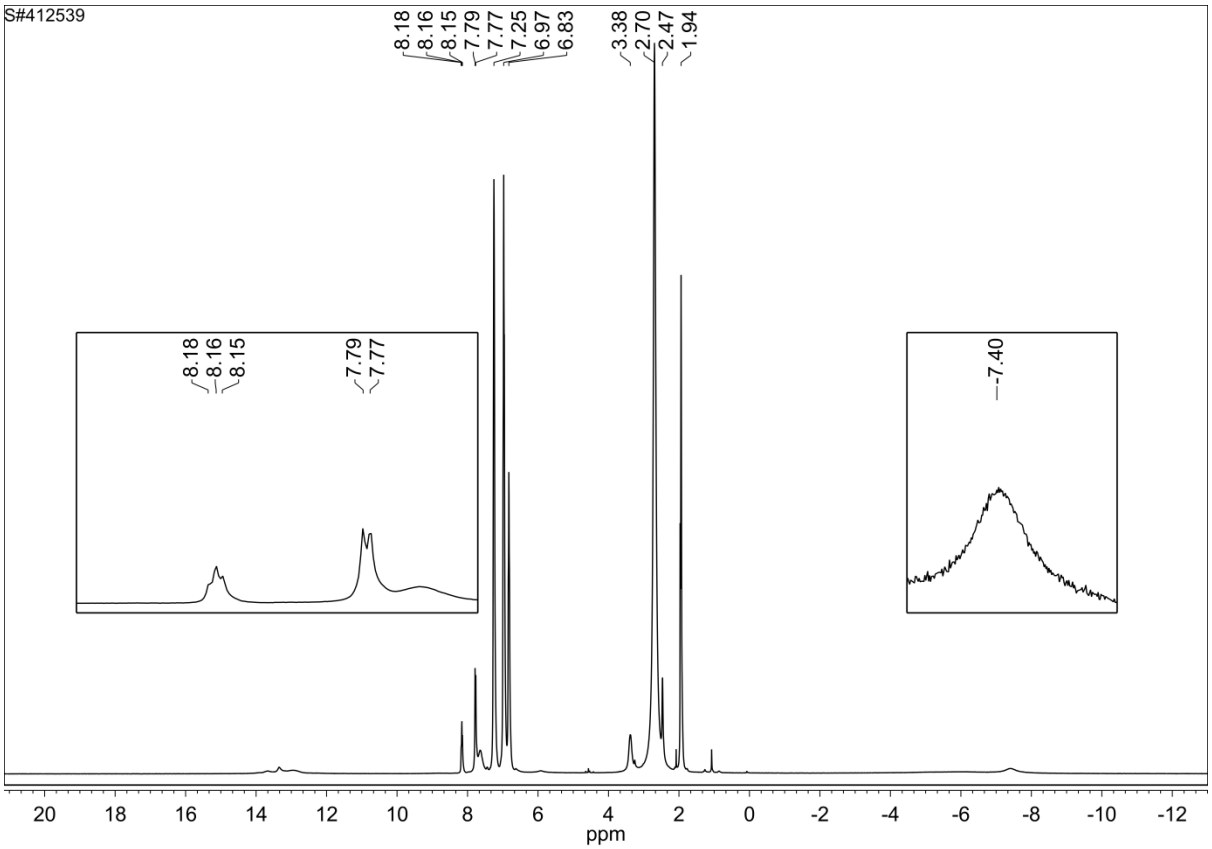

In a J. Young NMR tube $[(L^{H})Ni(\mu\text{-}H)]_2(BPh_4)_2$ was dissolved with CD_3CN (0.5 ml) and DMSO-d_6 (0.05 ml) at room temperature. The deep yellow-brown solution was degassed for three freeze-thaw-pump cycles and the tube was sealed under N_2.

Figure S 24. ^{1}H NMR of $[(L^{H})Ni(CH_3CN)_2](BF_4)_2$ at 298 K in CD_3CN.

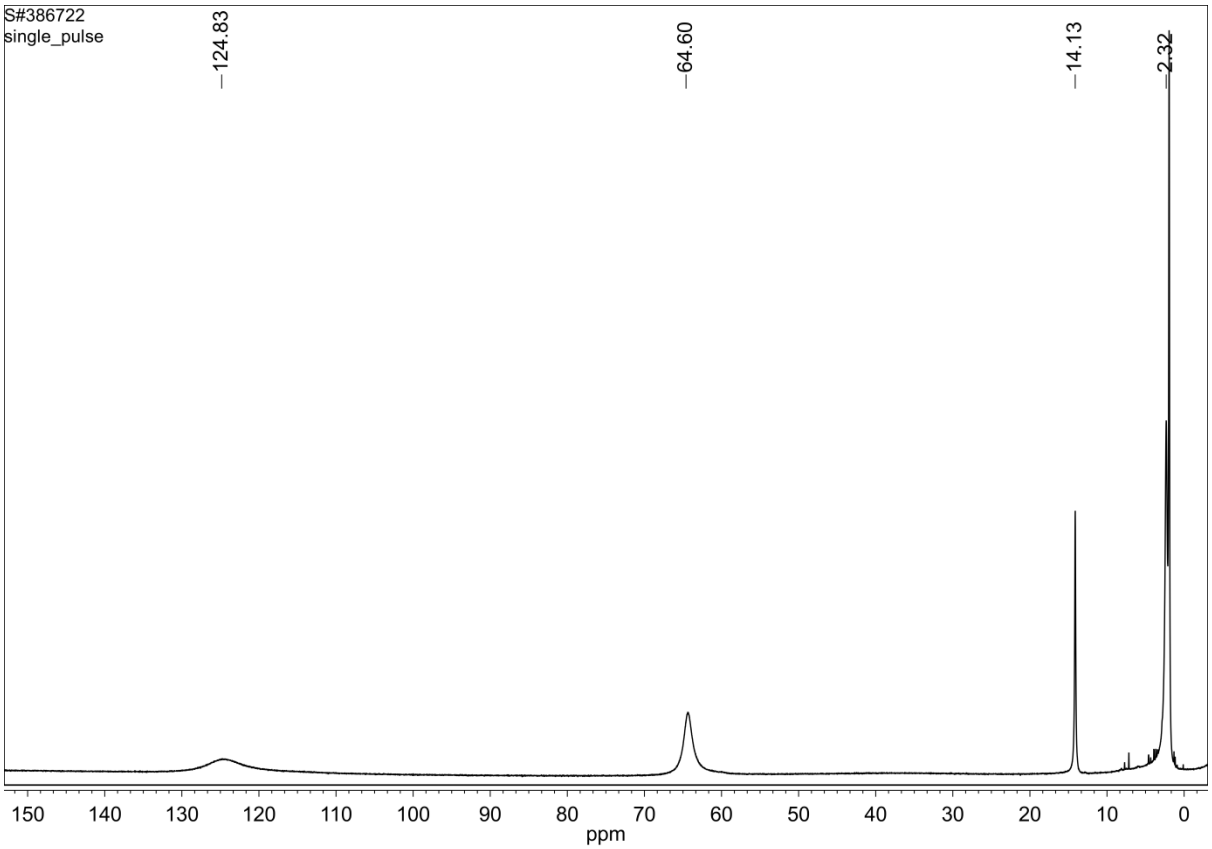

Figure S 25. ^{1}H NMR of $[(L^{H})Ni(\mu\text{-}SPh)]_2(BPh_4)_2$ in $CDCl_3$ and DMSO-d_6 (10:1) at 298 K.

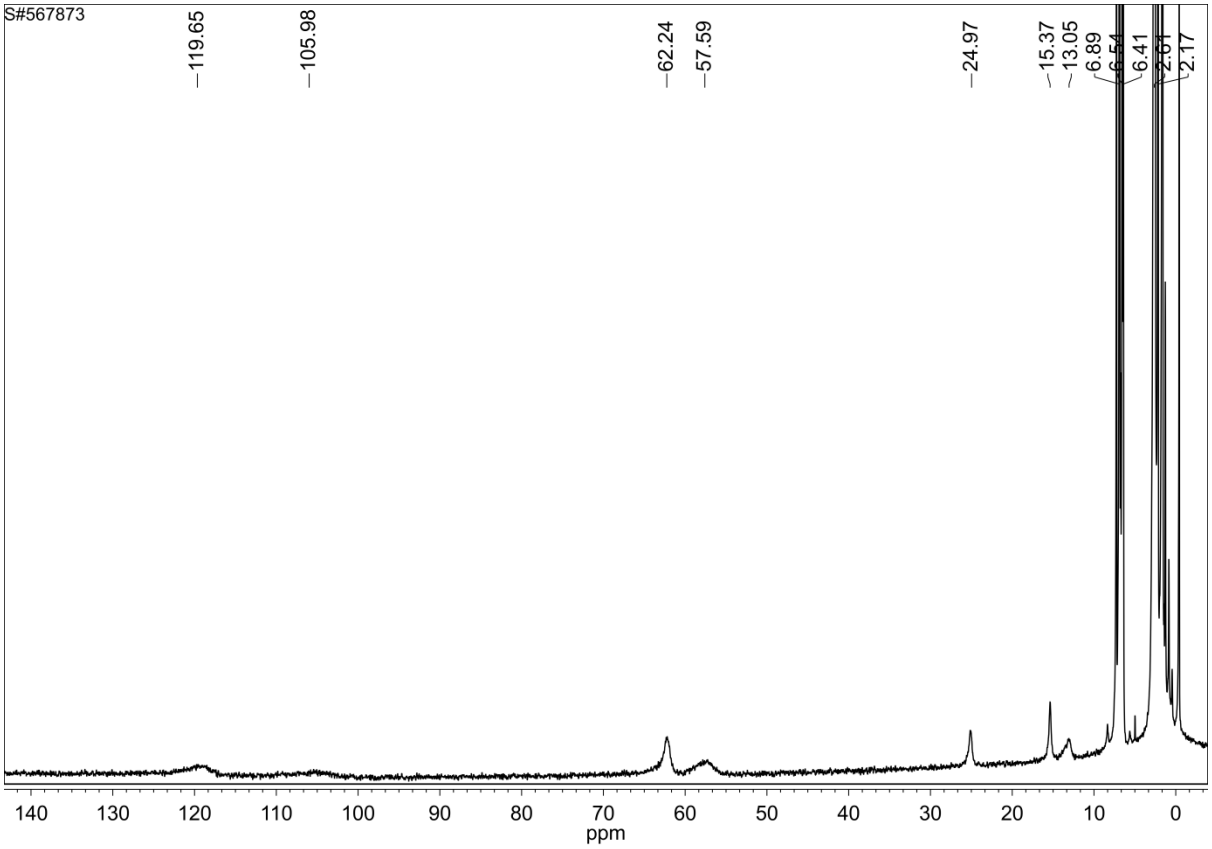

Figure S 26. Hydride transfer to trityl hexafluorophosphate.

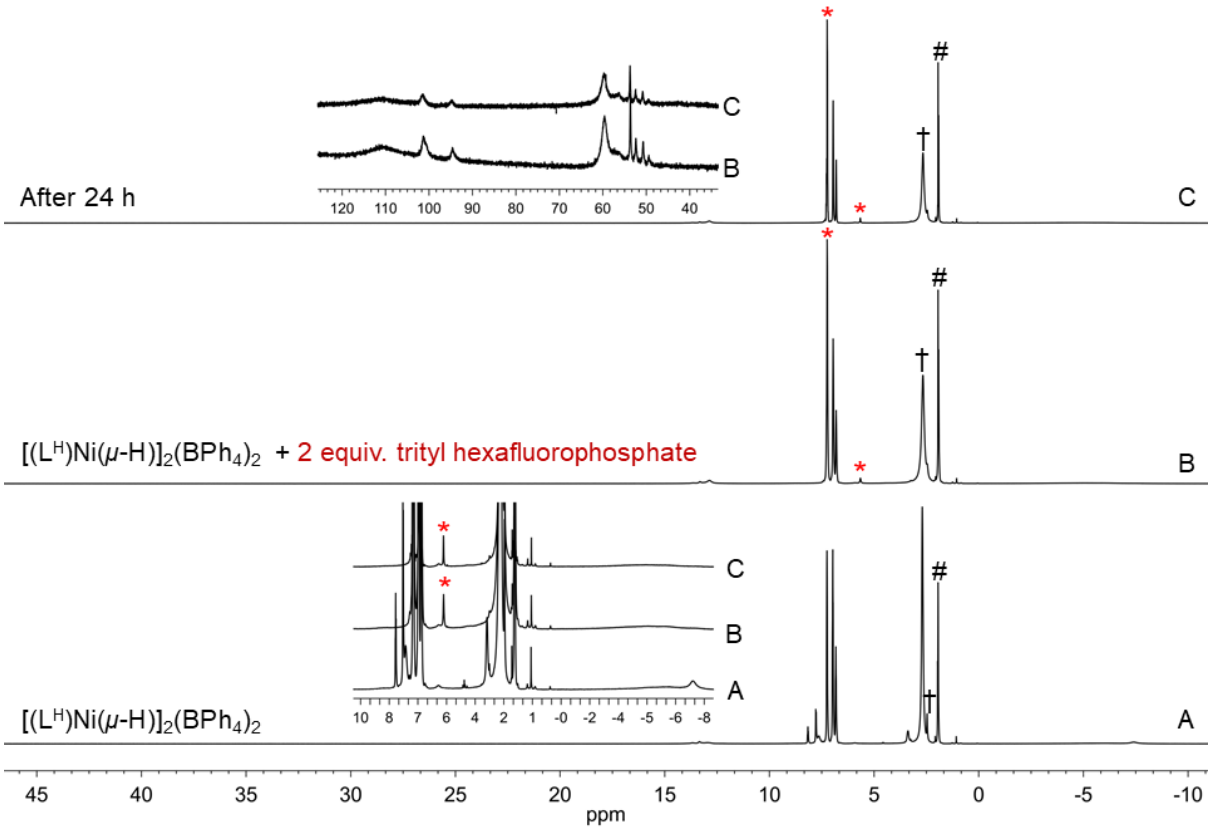

A. $[(L^H)Ni(\eta^2\text{-}BH_4)](BPh_4)$ dissolved with CD_3CN (0.5 ml) and DMSO-d_6 (0.05 ml) at room temperature. ^1H NMR spectroscopy was recorded at room temperature, which has confirmed the formation of $[(L^H)Ni(\mu\text{-}H)]_2(BPh_4)_2$ (# CD_3CN and † DMSO-d_6).

B. Two equivalent of trityl hexafluorophosphate was added, and ^1H NMR spectroscopy was recorded at room temperature. Triphenylmethane signal indicated by red asterisks and the inset have shown the formed paramagnetic complex.

C. ^1H NMR spectroscopy recorded after 24 h at room temperature. Triphenylmethane signal indicated by red asterisks and the paramagnetic complex shown in the inset.

Figure S 27. Hydride transfer to benzyl bromide.

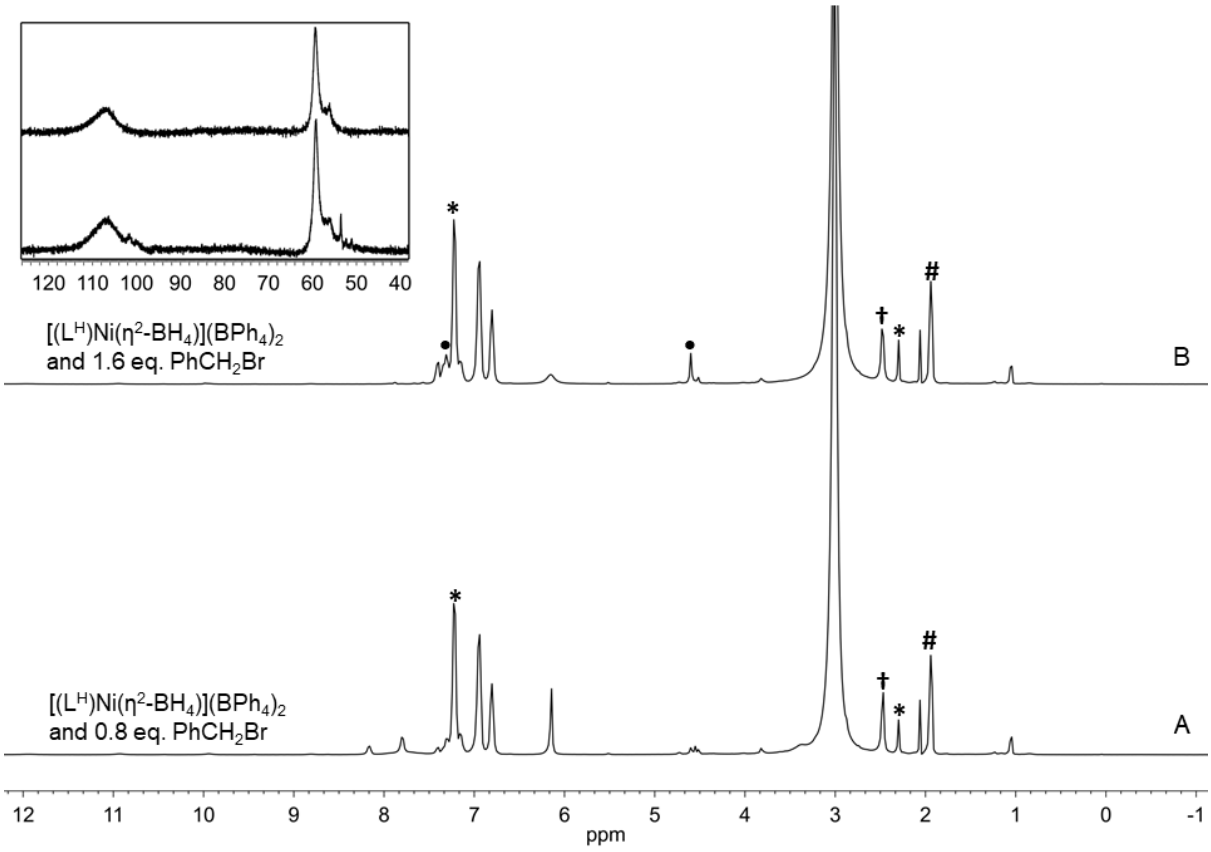

A. $[(L^H)Ni(\eta^2\text{-}BH_4)](BPh_4)$ and 0.8 equivalent benzyl bromide dissolved with CD_3CN (0.5 ml) and DMSO-d_6 (0.05 ml) at room temperature. ^1H NMR spectroscopy was recorded at room temperature and the formed methylbenzene signal indicated by asterisks (*). (# CD_3CN and † DMSO-d_6)

B. ^1H NMR spectroscopy was recorded at room temperature after adding 1.6 equivalent benzyl bromide. The excess benzyl bromide signal indicated by the black dot (•) and the inset have shown the formed paramagnetic complex.

Figure S 28. ORTEP of $[(L^{H})Ni(\mu\text{-}Cl)]_2(Cl)_2$.

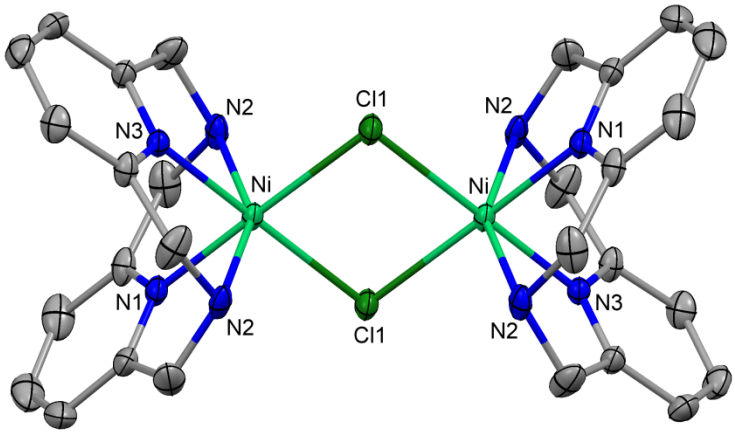

ORTEP of $[(L^{H})Ni(\mu\text{-}Cl)]_2^{2+}$ dication at 50% probability level. Solvent molecule, chloride anions and hydrogen atoms are omitted for clarity. Selected bond distances [Å] and angles [deg]: Ni-N(3), 1.996(2); Ni-N(1), 2.002(3); Ni-N(2)#1, 2.1458(19); Ni-N(2), 2.1458(19); Ni-Cl(1), 2.3990(8); Ni-Cl(1)#2, 2.4076(9); Cl(1)-Ni#2, 2.4076(9); N(3)-Ni-N(1), 88.89(10); N(3)-Ni-N(2)#1, 80.29(5); N(1)-Ni-N(2)#1, 80.17(6); N(3)-Ni-N(2), 80.29(5); N(1)-Ni-N(2), 80.17(6); N(2)#1-Ni-N(2), 152.50(10); N(3)-Ni-Cl(1), 179.75(8); N(1)-Ni-Cl(1), 91.36(7); N(2)#1-Ni-Cl(1), 99.75(5); N(2)-Ni-Cl(1), 99.75(5); N(3)-Ni-Cl(1)#2, 92.25(8); N(1)-Ni-Cl(1)#2, 178.86(7); N(2)#1-Ni-Cl(1)#2, 100.02(6); N(2)-Ni-Cl(1)#2, 100.02(6); Cl(1)-Ni-Cl(1)#2, 87.51(3); Ni-Cl(1)-Ni#2, 92.49(3).

Table S 1. Crystallographic data for $[(L^{H})Ni(\mu\text{-}Cl)]_2(Cl)_2$.

Identification code	CCDC-1878190	
Empirical formula	C30 H40 Cl4 N8 Ni2 O2	
Formula weight	803.92	
Temperature	100(2) K	
Wavelength	0.71073 Å	
Crystal system	Monoclinic	
Space group	C 2/m	
Unit cell dimensions	a = 17.2098(11) Å	α = 90°.
	b = 8.7962(5) Å	β = 112.273(2)°
	c = 12.4668(7) Å	γ = 90°.
Volume	1746.42(18) $Å^3$	
Z	2	
Density (calculated)	152.9 mg/m^3	
Absorption coefficient	1.425 mm^{-1}	
F(000)	832	
Crystal size	0.29 x 0.21 x 0.12 mm^3	
Theta range for data collection	2.558 to 28.347°.	
Index ranges	-22<=h<=21, -11<=k<=11, -16<=l<=16	
Reflections collected	8942	
Independent reflections	2313 [$R_{(int)}$ = 0.0460]	
Completeness to theta = 25.500°	99.7 %	
Absorption correction	Semi-empirical from equivalents	
Max. and min. transmission	0.7457 and 0.5688	
Refinement method	Full-matrix least-squares on F^2	
Data / restraints / parameters	2313 / 4 / 132	
Goodness-of-fit on F^2	1.069	
Final R indices [I>2sigma(I)]	R1 = 0.0416, wR2 = 0.0825	
R indices (all data)	R1 = 0.0636, wR2 = 0.0896	
Largest diff. peak and hole	0.946 and -0.592 e.$Å^{-3}$	

Figure S 29. ORTEP of $[(L^{H})Ni(\mu\text{-}Br)]_2(Br)_2$.

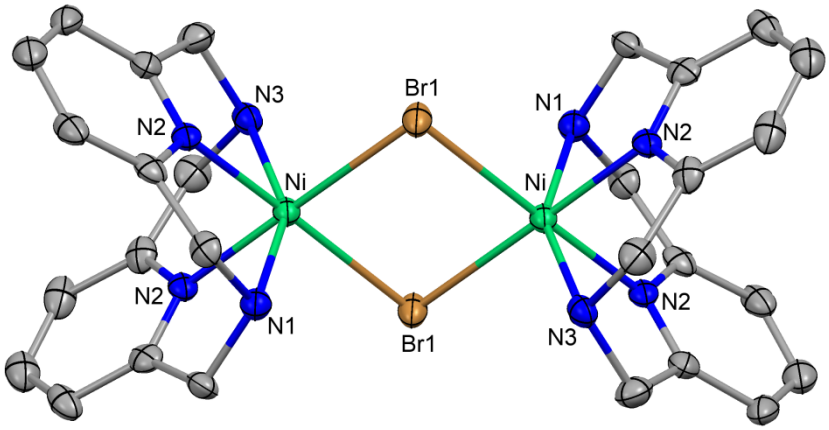

ORTEP of $[(L^{H})Ni(\mu\text{-}Br)]_2^{2+}$ dication at 50% probability level. Hydrogen atoms and bromide anions are omitted for clarity. Selected bond distances [Å] and angles [deg]: Ni-N(2)#1, 2.000(4); Ni-N(2), 2.000(4); Ni-N(1), 2.139(6); Ni-N(3), 2.156(6); Ni-Br(1)#2, 2.5269(8); Ni-Br(1), 2.5270(8); Br(1)-Ni#2, 2.5270(8); N(2)#1-Ni-N(2), 87.1(2); N(2)#1-Ni-N(1), 80.55(16); N(2)-Ni-N(1), 80.55(16); N(2)#1-Ni-N(3), 80.17(16); N(2)-Ni-N(3), 80.16(16); N(1)-Ni-N(3), 153.3(2); N(2)#1-Ni-Br(1)#2, 178.26(12); N(2)-Ni-Br(1)#2, 92.66(11); N(1)-Ni-Br(1)#2, 97.71(11); N(3)-Ni-Br(1)#2, 101.49(11); N(2)#1-Ni-Br(1), 92.66(11); N(2)-Ni-Br(1), 178.26(12); N(1)-Ni-Br(1), 97.71(11); N(3)-Ni-Br(1), 101.49(11); Br(1)#2-Ni-Br(1), 87.55(4); Ni-Br(1)-Ni#2, 92.45(4).

Table S 2. Crystallographic data for $[(L^H)Ni(\mu\text{-}Br)]_2(Br)_2$.

Identification code	CCDC-1878191	
Empirical formula	C28 H32 Br4 N8 Ni2	
Formula weight	917.67	
Temperature	100(2) K	
Wavelength	0.71073 Å	
Crystal system	Monoclinic	
Space group	C 2/m	
Unit cell dimensions	a = 15.109(3) Å	α = 90°
	b = 15.035(3) Å	β = 116.240(6)°
	c = 10.6611(19) Å	γ = 90°
Volume	2172.2(7) $Å^3$	
Z	2	
Density (calculated)	140.3 mg/m^3	
Absorption coefficient	4.570 mm^{-1}	
F(000)	904	
Crystal size	0.30 x 0.21 x 0.16 mm^3	
Theta range for data collection	2.709 to 28.392°	
Index ranges	-20<=h<=20, -20<=k<=20, 14<=l<=14	
Reflections collected	2825	
Independent reflections	2825 [$R_{(int)}$ = 0.0737]	
Completeness to theta = 25.500°	99.6 %	
Absorption correction	Semi-empirical from equivalents	
Max. and min. transmission	0.7457 and 0.5583	
Refinement method	Full-matrix least-squares on F^2	
Data / restraints / parameters	2825 / 0 / 102	
Goodness-of-fit on F^2	1.037	
Final R indices [I>2sigma(I)]	R1 = 0.0576, wR2 = 0.1555	
R indices (all data)	R1 = 0.0833, wR2 = 0.1679	
Largest diff. peak and hole	1.665 and -1.142 e.$Å^{-3}$	

Figure S 30. ORTEP of $[(L^{H})Ni(\mu\text{-}I)]_2(I)_2$.

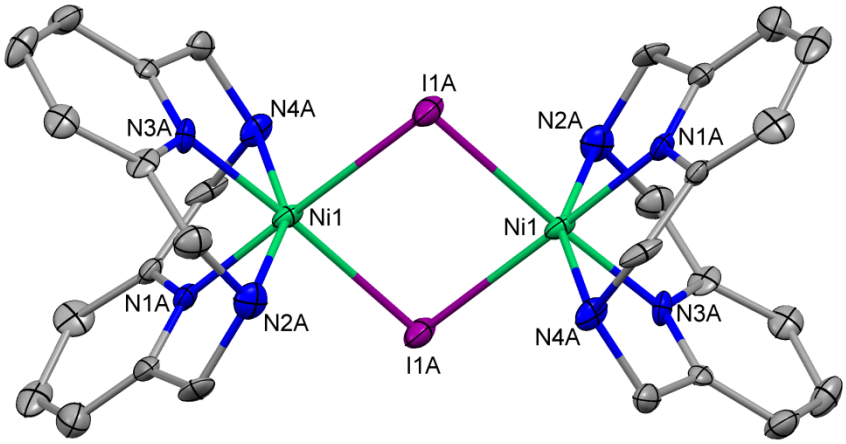

ORTEP of $[(L^{H})Ni(\mu\text{-}I)]_2^{2+}$ dication at 50% probability level. Solvent molecule, hydrogen atoms and iodide anions are omitted for clarity. Selected bond distances [Å] and angles [deg]: Ni(1)-N(3A), 1.981(14); Ni(1)-N(1A), 2.001(15); Ni(1)-N(4A), 2.142(14); Ni(1)-N(2A), 2.148(15); Ni(1)-I(1A)#1, 2.727(2); Ni(1)-I(1A), 2.735(2); I(1A)-Ni(1)#1, 2.727(2); N(3A)-Ni(1)-N(1A), 87.6(6); N(3A)-Ni(1)-N(4A), 80.0(6); N(1A)-Ni(1)-N(4A), 81.4(6); N(3A)-Ni(1)-N(2A), 80.6(6); N(1A)-Ni(1)-N(2A), 80.7(6); N(4A)-Ni(1)-N(2A), 154.0(6); N(3A)-Ni(1)-I(1A)#1, 92.8(4); N(1A)-Ni(1)-I(1A)#1, 178.2(4); N(4A)-Ni(1)-I(1A)#1, 100.4(4); N(2A)-Ni(1)-I(1A)#1, 97.6(4); N(3A)-Ni(1)-I(1A), 175.9(4); N(1A)-Ni(1)-I(1A), 88.6(4); N(4A)-Ni(1)-I(1A), 97.8(4); N(2A)-Ni(1)-I(1A), 100.3(4); I(1A)#1-Ni(1)-I(1A), 91.02(7); Ni(1)#1-I(1A)-Ni(1), 88.98(7).

Table S 3. Crystallographic data for $[(L^{H})Ni(\mu\text{-}I)]_2(I)_2$.

Identification code	CCDC-1878192	
Empirical formula	C30 H40 I4 N8 Ni2 O2	
Formula weight	1169.72	
Temperature	100(2) K	
Wavelength	0.71073 Å	
Crystal system	Monoclinic	
Space group	P 21/n	
Unit cell dimensions	a = 19.061(4) Å	α = 90°
	b = 10.993(2) Å	β = 112.098(5)°
	c = 19.320(4) Å	γ = 90°
Volume	3750.8(12) $Å^3$	
Z	4	
Density (calculated)	207.1 mg/m^3	
Absorption coefficient	4.335 mm^{-1}	
F(000)	2240	
Crystal size	0.32 x 0.23 x 0.16 mm^3	
Theta range for data collection	2.129 to 28.518°.	
Index ranges	-25<=h<=25, -14<=k<=14, -25<=l<=25	
Reflections collected	70239	
Independent reflections	9432 [$R_{(int)}$ = 0.0954]	
Completeness to theta = 25.500°	99.8 %	
Absorption correction	Semi-empirical from equivalents	
Max. and min. transmission	0.7457 and 0.6352	
Refinement method	Full-matrix least-squares on F^2	
Data / restraints / parameters	9432 / 42 / 420	
Goodness-of-fit on F^2	1.501	
Final R indices [I>2sigma(I)]	R1 = 0.1203, wR2 = 0.3393	
R indices (all data)	R1 = 0.1549, wR2 = 0.3795	
Largest diff. peak and hole	7.180 and -7.314 e.$Å^{-3}$	

Figure S 31. ORTEP of $[(L^{H})Ni(CH_3CN)_2](BPh_4)_2$.

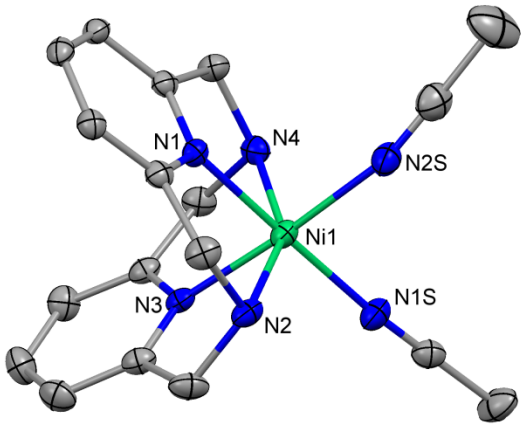

ORTEP of $[(L^{H})Ni(CH_3CN)_2]^{2+}$ dication at 50% probability level. Solvent, hydrogen atoms and BPh_4 anions are omitted for clarity. Selected bond distances [Å] and bond lengths [deg]. Ni(1)-N(1), 1.9973(17); Ni(1)-N(3), 2.0033(17); Ni(1)-N(1S), 2.0479(18); Ni(1)-N(4), 2.1509(17); Ni(1)-N(2S), 2.053(2); Ni(1)-N(2), 2.1667(18); N(1)-Ni(1)-N(3), 86.72(7); N(1)-Ni(1)-N(1S), 177.64(7); N(1)-Ni(1)-N(4), 80.56(7); N(1)-Ni(1)-N(2S), 90.43(7); N(1)-Ni(1)-N(2), 80.10(7); N(3)-Ni(1)-N(1S), 93.19(7); N(3)-Ni(1)-N(4), 80.57(7); N(3)-Ni(1)-N(2S), 176.46(7); N(3)-Ni(1)-N(2), 80.30(7); N(1S)-Ni(1)-N(4), 97.10(7); N(1S)-Ni1-N(2S), 89.57(7); N(1S)-Ni(1)-N(2), 102.21(7); N(4)-Ni(1)-N(2), 153.43(7); N(2S)-Ni(1)-N(4), 96.90(7); N(2S)-Ni(1)-N(2), 101.29(7).

Table S 4. Crystallographic data for $[(L^{H})Ni(CH_3CN)_2](BPh_4)_2$.

Identification code	CCDC-1878193	
Empirical formula	C68 H65 B2 N7 Ni	
Formula weight	1060.60	
Temperature	100(2) K	
Wavelength	0.71073 Å	
Crystal system	Triclinic	
Space group	P-1	
Unit cell dimensions	a = 11.5825(5) Å	α = 98.75(10)°
	b = 13.5215(6) Å	β = 101.46(10)°
	c = 19.6576(8) Å	γ = 103.62(10)°
Volume	2867.7(2) $Å^3$	
Z	2	
Density (calculated)	122.8 mg/m^3	
Absorption coefficient	0.387 mm^{-1}	
F(000)	1120.0	
Crystal size	0.22 x 0.2 x 0.18 mm^3	
Theta range for data collection	2.09 to 25.119°	
Index ranges	-17<=h<=17, -13<=k<=13, -19<=l<=19	
Reflections collected	35330	
Independent reflections	10208 [R_{int} = 0.0398, R_{sigma} = 0.0441]	
Completeness to theta = 25.091°	99.7 %	
Absorption correction	multi-scan	
Max. and min. transmission	0.745 and 0.635	
Refinement method	Full-matrix least-squares on F^2	
Data / restraints / parameters	10208 /0 / 706	
Goodness-of-fit on F^2	0.964	
Final R indices [I>2sigma(I)]	R1 = 0.0419, wR2 = 0.1188	
R indices (all data)	R1 = 0.0588, wR2 = 0.1326	
Largest diff. peak and hole	0.39/-0.35 e.$Å^{-3}$	

Figure S 32. ORTEP of [(L^H)Ni(η^2-BH_4)](BPh_4).

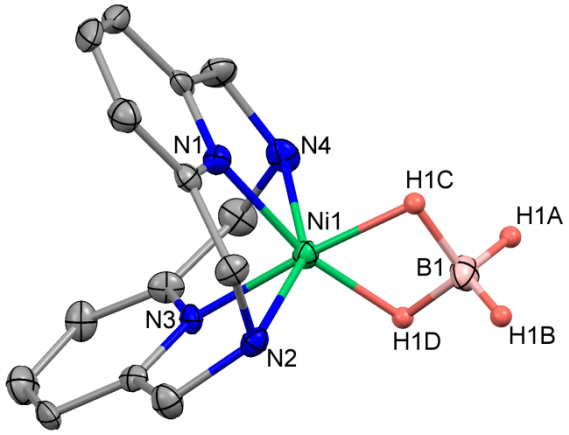

ORTEP of [(L^H)Ni(η^2-BH_4)]$^+$ cation at 50% probability level. Hydrogen atoms and BPh_4 anions are omitted for clarity. Selected bond distances [Å] and bond lengths [deg]. Ni(1)-N(2), 2.150(4); Ni(1)-N(4), 2.155(4); Ni(1)-N(1), 1.970(4); Ni(1)-N(3), 1.983(4), Ni(1)-H(1C), 1.73(5); Ni(1)-H(1D), 1.68(3), B(1)-H(1B), 1.03(8), B(1)-H(1A), 1.06(6), Ni(1)···B(1), 2.176(7); N(2)-Ni(1)-N(4), 152.66(16); N(3)-Ni(1)-N(2), 80.50(17); N(3)-Ni(1)-N(4), 80.29(17); N(1)-Ni(1)-N(2), 79.97(18); N(1)-Ni(1)-N(3), 90.21(16); N(1)-Ni(1)-N(4), 80.83(18); N(4)-Ni(1)-H(1D), 99.21(5); N(3)-Ni(1)-H(1D), 103.80(16); N(1)-Ni(1)-H(1D), 166.0(1); N(2)-Ni(1)-H(1D), 104.16(8); H(1C)-Ni(1)-H(1D), 69.80(1); N(4)-Ni(1)-H(1C), 97.22(5); N(3)-Ni(1)-H(1C), 172.70(7); N(1)-Ni(1)-H(1C), 96.32(6); N(2)-Ni(1)-H(1C), 104.14(7); H(1C)-B(1)-H(1A), 103.80(5); H(1D)-B(1)-H(1B), 114.03(7); H(1D)-B(1)-H(1A), 106.10(11); H(1C)-B(1)-H(1B), 113.29(3); H(1A)-B(1)-H(1B), 115.58(4); H(1C)-B(1)-H(1D), 102.68(4).

Table S 5. Crystallographic data for $[(L^H)Ni(\eta^2\text{-}BH_4)](BPh_4)$.

Identification code	CCDC-1878194	
Empirical formula	C38 H40 B2 N4 Ni	
Formula weight	633.07	
Temperature	100(2) K	
Wavelength	0.7100 Å	
Crystal system	orthorhombic	
Space group	$P2_12_12_1$	
Unit cell dimensions	a = 11.1094(7) Å	α = 90°
	b = 15.0969(9) Å	β = 90°
	c = 18.9302(12) Å	γ = 90°
Volume	3174.9(3) $Å^3$	
Z	4	
Density (calculated)	132.4 mg/m^3	
Absorption coefficient	0.568 mm-1	
F(000)	1336.0	
Crystal size	0.22 x 0.2 x 0.18 mm^3	
Theta range for data collection	2.123 to 25.06°	
Index ranges	-13<=h<=13, -17<=k<=17, 22<=l<=22	
Reflections collected	25414	
Independent reflections	5621 [R_{int} = 0.0967, R_{sigma} = 0.0914]	
Completeness to theta = 25.500°	98.2%	
Absorption correction	None	
Refinement method	Full-matrix least-squares on F^2	
Data / restraints / parameters	5621 / 45 / 422	
Goodness-of-fit on F^2	1.028	
Final R indices [I>2sigma(I)]	R1 = 0.0508, wR2 = 0.0919	
R indices (all data)	R1 = 0.0762, wR2 = 0.1006	
Absolute structure parameter	0.020(11)	
Largest diff. peak and hole	0.65/-0.35 e. $Å^{-3}$	

Figure S 33. ORTEP of $[(L^{H})Ni(\mu\text{-}H)]_2(I)_2$.

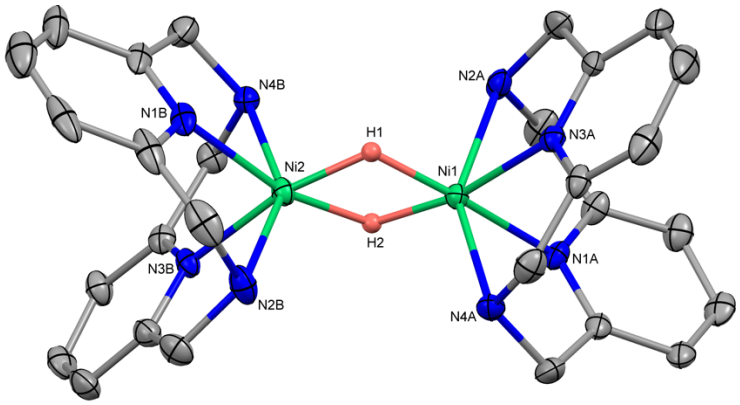

ORTEP of $[(L^{H})Ni(\mu\text{-}H)]_2^{2+}$ dication at 25% probability level. Hydrogen atoms and iodide anions are omitted for clarity. Selected bond distances [Å] and angles [deg]: Ni(1)···Ni(2), 2.5784(13); Ni(1)-N(3A), 2.010(6); Ni(1)-N(1A), 2.014(6); Ni(1)-N(4A), 2.189(6); Ni(1)-N(2A), 2.202(6); Ni(1)-H(1), 1.53(8); Ni(1)-H(2), 1.51(6); Ni(2)-N(3B), 1.999(6); Ni(2)-N(1B), 2.030(6); Ni(2)-N(2B), 2.201(7); Ni(2)-N(4B), 2.204(6); Ni(2)-H(1), 1.53(8); Ni(2)-H(2), 1.60(6); N(3A)-Ni(1)-N(1A), 87.5(2); N(3A)-Ni(1)-N(4A), 79.0(2); N(1A)-Ni(1)-N(4A), 79.8(3); N(3A)-Ni(1)-N(2A), 79.2(3); N(1A)-Ni(1)-N(2A), 79.2(2); N(4A)-Ni(1)-N(2A), 150.2(2); N(3A)-Ni(1)-Ni(2), 133.52(17); N(1A)-Ni(1)-Ni(2), 138.99(18); N(4A)-Ni(1)-Ni(2), 104.21(18); N(2A)-Ni(1)-Ni(2), 105.57(17); N(3A)-Ni(1)-H(1), 101(3); N(1A)-Ni(1)-H(1), 170(3); N(4A)-Ni(1)-H(1), 107(3); N(2A)-Ni(1)-H(1), 97(3); Ni(2)-Ni(1)-H(1), 33(3); N(3A)-Ni(1)-H(2), 167(2); N(1A)-Ni(1)-H(2), 104(2); N(4A)-Ni(1)-H(2), 107(2); N(2A)-Ni(1)-H(2), 98(2); Ni(2)-Ni(1)-H(2), 35(2); H(1)-Ni(1)-H(2), 67(4).

Table S 6. Crystallographic data for $[(L^{H})Ni(\mu\text{-}H)]_2(I)_2$.

Identification code	CCDC-1878195	
Empirical formula	C28 H34 I2 N8 Ni2	
Formula weight	853.85	
Temperature	100(2) K	
Wavelength	0.71073 Å	
Crystal system	Orthorhombic	
Space group	P b c a	
Unit cell dimensions	a = 15.1186(6) Å	α = 90°
	b = 18.4249(7) Å	β = 90°
	c = 23.5902(10) Å	γ = 90°
Volume	6571.3(5) $Å^3$	
Z	8	
Density (calculated)	172.6 mg/m^3	
Absorption coefficient	3.056 mm^{-1}	
F(000)	3360	
Crystal size	0.33 x 0.25 x 0.17 mm^3	
Theta range for data collection	2.373 to 25.091°	
Index ranges	-18=h<=18, -21<=k<=21, -28<=l<=28	
Reflections collected	5808	
Independent reflections	5808 [$R_{(int)}$ = 0.0512]	
Completeness to theta = 25.091°	99.5 %	
Absorption correction	Semi-empirical from equivalents	
Max. and min. transmission	0.7452 and 0.5754	
Refinement method	Full-matrix least-squares on F^2	
Data / restraints / parameters	5808 / 25 / 400	
Goodness-of-fit on F^2	1.062	
Final R indices [I>2sigma(I)]	R1 = 0.0601, wR2 = 0.1353	
R indices (all data)	R1 = 0.0979, wR2 = 0.1510	
Largest diff. peak and hole	2.289 and -0.974 e.$Å^{-3}$	

Figure S 34. ORTEP of $[(L^H)Ni(\mu\text{-}OCH_3)]_2(BPh_4)_2$.

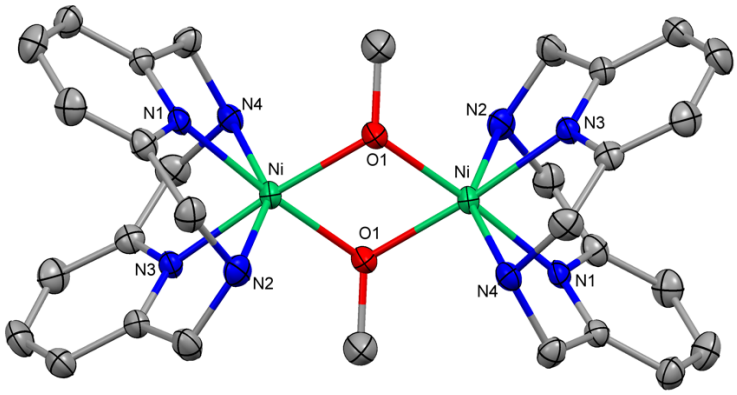

ORTEP of $[(L^H)Ni(\mu\text{-}OCH_3)]_2^{2+}$ dication at 50% probability level. Solvent and hydrogen atoms are omitted for clarity. Selected bond distances [Å] and angles [deg]: Ni-O(1) 2.023(2), Ni-N(1) 2.033(3), Ni-N(3) 2.034(3), Ni-N(4) 2.209(3), Ni-N(2) 2.222(3), O(1)-Ni#1 2.034(2). O(1)-Ni-N(1).175.05(10), O(1)-Ni-O(1)# 178.90(10), N(1)-Ni-O(1)#1 98.88(10), O(1)-Ni-N(3) 98.00(10), N(1)-Ni-N(3) 84.52(10), O(1)#1-Ni-N(3) 174.96(10), O(1)-Ni-N(4) 97.14(10), N(1)-Ni-N(4) 79.12(10), O(1)#1-Ni-N(4) 105.30(10), N(3)-Ni-N(4) 78.94(10), O(1)-Ni-N(2) 105.69(10), N(1)-Ni-N(2) 78.94(10), O(1)#1-Ni-N(2) 98.33(10), N(3)-Ni-N(2) 78.59(10), N(4)-Ni-N(2) 149.83(10), Ni-O(1)-Ni#1 101.10(10).

Table S 7. Crystallographic data for $[(L^{H})Ni(\mu\text{-}OCH_3)]_2(BPh_4)_2$.

Identification code	CCDC-1878196	
Empirical formula	C88 H92 B2 N12 Ni2 O4	
Formula weight	1520.77	
Temperature	100(2) K	
Wavelength	0.71073 Å	
Crystal system	Monoclinic	
Space group	P 21/n	
Unit cell dimensions	a = 16.7786(13) Å	α = 90°
	b = 11.9023(9) Å	β = 105.676(2)°
	c = 21.2510(19) Å	γ = 90°
Volume	4086.1(6) $Å^3$	
Z	2	
Density (calculated)	123.6 mg/m^3	
Absorption coefficient	0.518 mm^{-1}	
F(000)	1604	
Crystal size	0.26 x 0.21 x 0.13 mm^3	
Theta range for data collection	2.198 to 25.249°	
Index ranges	-20<=h<=20, -13<=k<=14, -25<=l<=25	
Reflections collected	32612	
Independent reflections	7398 [R(int) = 0.0744]	
Completeness to theta = 25.500°	99.8 %	
Absorption correction	Semi-empirical from equivalents	
Max. and min. transmission	0.7457 and 0.5573	
Refinement method	Full-matrix least-squares on F^2	
Data / restraints / parameters	7398 / 0 / 490	
Goodness-of-fit on F^2	1.037	
Final R indices [I>2sigma(I)]	R1 = 0.0564, wR2 = 0.1350	
R indices (all data)	R1 = 0.0850, wR2 = 0.1483	
Largest diff. peak and hole	1.196 and -0.318 e.$Å^{-3}$	

Figure S 35. ORTEP of [(L^H)Ni(dbm)](BPh_4).

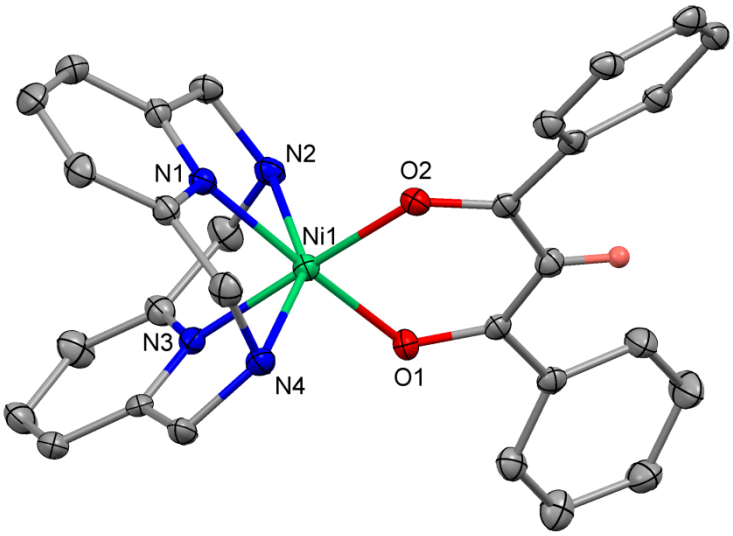

ORTEP of [(L^H)Ni(dbm)]$^+$ cation at 30% probability level. Hydrogen atoms, BPh_4 anions and solvents are omitted for clarity. Selected bond distances [Å] and angles [deg]: Ni(1)-O(2), 2.005(4); Ni(1)-O(1), 2.012(4); Ni(1)-N(3), 2.018(5); Ni(1)-N(4), 2.192(5); Ni(1)-N(1), 2.013(5); Ni(1)-N(2), 2.176(5); O(2)-Ni(1)-O(1), 90.21(16); O(2)-Ni(1)-N(3), 173.89(18); O(2)-Ni(1)-N(4), 94.74(18); O(2)-Ni(1)-N(1), 92.35(18); O(2)-Ni(1)-N(2), 106.80(18); O(1)-Ni(1)-N(3), 92.30(18); O(1)-Ni(1)-N(4), 106.90(19); O(1)-Ni(1)-N(4), 106.90(19); O(1)-Ni(1)-N(1), 172.82(18); O(1)-Ni(1)-N(2), 93.20(18); N(3)-Ni(1)-N(4), 79.20(19); N(3)-Ni(1)-N(2), 78.63(19); N(1)-Ni(1)-N(3), 85.82(19); N(1)-Ni(1)-N(4), 79.6(2); N(1)-Ni(1)-N(2), 79.64(19); N(2)-Ni(1)-N(4), 150.5(2).

Table S 8. Crystallographic data for [(L^H)Ni(dbm)](BPh_4).

Identification code	CCDC-1878197	
Empirical formula	C163 H151 B3 N12 Ni3 O7	
Formula weight	2598.51	
Temperature	100(2) K	
Wavelength	0.710 Å	
Crystal system	monoclinic	
Space group	P-1	
Unit cell dimensions	a = 42.319(3) Å	α = 90°
	b = 22.6000(14) Å	β = 93.976(3)°
	c = 15.7228(9) Å	γ = 90°
Volume	15001.4(17) $Å^3$	
Z	4	
Density (calculated)	115.1 mg/m^3	
Absorption coefficient	0.431 mm^{-1}	
F(000)	5472.0	
Crystal size	0.06 x 0.05 x 0.02 mm^3	
Theta range for data collection	2.757 to 25°	
Index ranges	-50<=h<=50, -26<=k<=26, -18<=l<=18	
Reflections collected	90580	
Independent reflections	26417 [$R_{(int)}$ = 0.0499, Rsigma = 0.0520]	
Completeness to theta = 25.242°	99.6 %	
Absorption correction	Semi-empirical from equivalents	
Max. and min. transmission	0.746 and 0.678	
Refinement method	Full-matrix least-squares on F^2	
Data / restraints / parameters	26417 /121 / 1686	
Goodness-of-fit on F^2	1.021	
Final R indices [I>2sigma(I)]	R1 = 0.0531, wR2 = 0.1309	
R indices (all data)	R1 = 0.0649, wR2 = 0.1403	
Largest diff. peak and hole	2.12/-1.23 e.$Å^{-3}$	
Flack parameter	0.551(13)	

Figure S 36. ORTEP of $[(L^H)Ni(\mu\text{-}SPh)]_2(BPh_4)_2$.

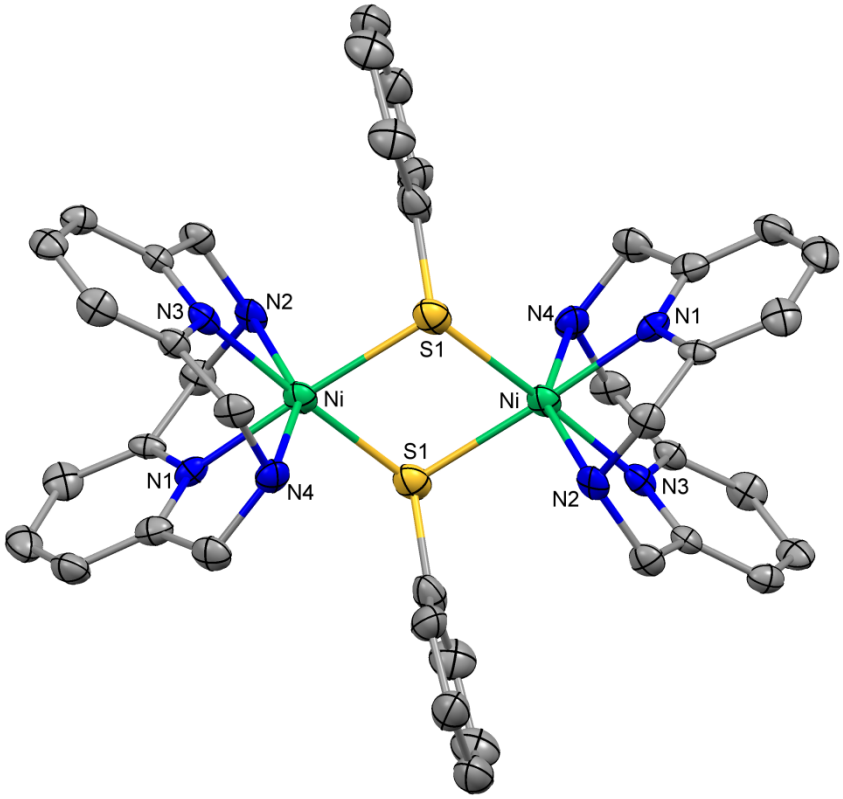

ORTEP of $[(L^H)Ni(\mu\text{-}SPh)]_2^{2+}$ dication at 50% probability level. Hydrogen atoms, BPh_4 anions and solvents are omitted for clarity. Selected bond distances [Å] and angles [deg]: Ni-N(1) 2.036(5), Ni-N(3) 2.043(5), Ni-N(4) 2.188(5), Ni-N(2) 2.205(5), Ni-S(1) 2.4193(18), Ni-S(1)#1 2.4342(19. N(1)-Ni-N(3) 83.74(18), N(1)-Ni-N(4) 79.38(19), N(3)-Ni-N(4) 78.89(18), N(1)-Ni-N(2) 78.75(18), N(3)-Ni-N(2) 78.37(18), N(4)-Ni-N(2) 149.9(2), N(1)-Ni-S(1) 176.76(13), N(3)-Ni-S(1) 97.36(13), N(4)-Ni-S(1) 97.81(15), N(2)-Ni-S(1) 104.45(14), N(1)-Ni-S(1)#1 95.88(13), N(3)-Ni-S(1)#1 173.77(13), N(4)-Ni-S(1)#1 107.18(14), N(2)-Ni-S(1)#1 95.45(14), S(1)-Ni-S(1)#1 83.36(6), Ni-S(1)-Ni#1 96.63(6).

Table S 9. Crystallographic data for $[(L^{H})Ni(\mu\text{-}SPh)]_2(BPh_4)_2$.

Identification code	CCDC-1878198	
Empirical formula	C96 H94 B2 N12 Ni2 S2	
Formula weight	1618.99	
Temperature	100(2) K	
Wavelength	0.71073 Å	
Crystal system	Triclinic	
Space group	P-1	
Unit cell dimensions	a = 10.8252(14) Å	α = 70.982(4)°
	b = 11.8798(16) Å	β = 72.243(3)°
	c = 17.529(3) Å	γ = 78.092(3)°
Volume	2015.3(5) $Å^3$	
Z	1	
Density (calculated)	133.4 mg/m^3	
Absorption coefficient	0.576 mm^{-1}	
F(000)	852	
Crystal size	0.25 x 0.16 x 0.12 mm^3	
Theta range for data collection	2.680 to 25.252°	
Index ranges	-12<=h<=12, -14<=k<=14, -21<=l<=21	
Reflections collected	19037	
Independent reflections	7257 [$R_{(int)}$ = 0.1178]	
Completeness to theta = 25.242°	99.7 %	
Absorption correction	Semi-empirical from equivalents	
Max. and min. transmission	0.7457 and 0.6136	
Refinement method	Full-matrix least-squares on F^2	
Data / restraints / parameters	7257 / 0 / 524	
Goodness-of-fit on F^2	1.004	
Final R indices [I>2sigma(I)]	R1 = 0.0791, wR2 = 0.1532	
R indices (all data)	R1 = 0.1780, wR2 = 0.1849	
Largest diff. peak and hole	0.673 and -0.546 $e.Å^{-3}$	

Figure S 37. ORTEP of [(L^H)Ni(CO_3)].

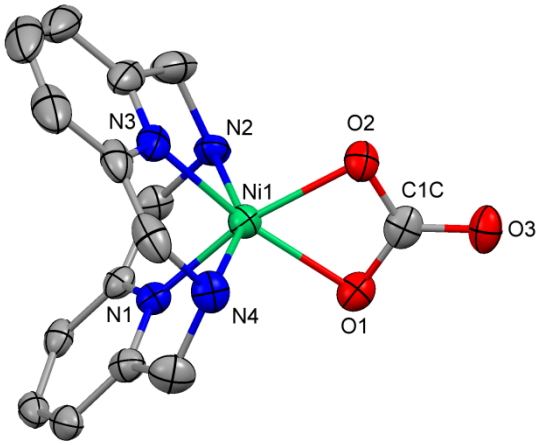

ORTEP of [(L^H)Ni(CO_3)] at 50% probability level. Hydrogen atoms are omitted for clarity. Selected bond distances [Å] and bond lengths [deg]. Ni(1)-O(1), 2.087(2); Ni(1)-O(2), 2.070(2); Ni(1)-N(4), 2.175(3); Ni(1)-N(1), 1.979(2); Ni(1)-N(3), 1.990(3); Ni(1)-N(2), 2.170(3); Ni(1)-C(1C), 2.451(3); O(1)-C(1C), 1.304(4); O(2)-C(1C), 1.293(4); O(3)-C(1C), 1.268(4). O(1)-Ni(1)-N4, 97.45(10); O(1)-Ni(1)-N(2), 105.36(9); O(1)-Ni(1)-C(1C), 32.15(10); O(2)-Ni(1)-O(1), 63.98(8); O(2)-Ni(1)-N(4), 105.66(10); O(2)-Ni(1)-N(2), 98.07(9); O(2)-Ni(1)-C(1C), 31.84(10); N(4)-Ni(1)-C(1C), 103.97(10); N(1)-Ni(1)-O(1), 101.01(9); N(1)-Ni(1)-O(2), 164.22(9); N(1)-Ni(1)-N(4), 80.10(10); N(1)-Ni(1)-N(3), 89.57(10); N(1)-Ni(1)-N(2), 80.71(10); N(3)-Ni(1)-O(1), 168.72(10); N(3)-Ni(1)-O(2), 105.78(9); N(3)-Ni(1)-N(4), 80.36(11); N(3)-Ni(1)-N(2), 80.04(11); N(2)-Ni(1)-N(4), 152.54(11).

Table S 10. Crystallographic data for [(L^H)Ni(CO_3)].

Identification code	CCDC-1878199	
Empirical formula	C14H15N5NiO3	
Formula weight	360.02	
Temperature	100(2) K	
Wavelength	0.71073 Å	
Crystal system	trigonal	
Space group	R-3	
Unit cell dimensions	a = 30.9603(10) Å	α = 90°
	b = 30.9603(10) Å	β = 90°
	c = 11.4869(5) Å	γ = 120°
Volume	9535.5(7) $Å^3$	
Z	18	
Density (calculated)	112.9 mg/m^3	
Absorption coefficient	0.932 mm^{-1}	
F(000)	3348.0	
Crystal size	0.08 x 0.05 x 0.02 mm^3	
Theta range for data collection	2.276 to 24.999°	
Index ranges	-36<=h<=36, -36<=k<=36, -13<=l<=13	
Reflections collected	38791	
Independent reflections	3737 [R_{int} = 0.0493, R_{sigma} = 0.0266]	
Completeness to theta = 25.242°	99.7 %	
Absorption correction	Semi-empirical from equivalents	
Max. and min. transmission	0.7457 and 0.6136	
Refinement method	Full-matrix least-squares on F^2	
Data / restraints / parameters	3737 / 0 / 208	
Goodness-of-fit on F^2	1.139	
Final R indices [I>2sigma(I)]	R1 = 0.0429, wR2 = 0.1146	
R indices (all data)	R1 = 0.0568, wR2 = 0.1285	
Largest diff. peak and hole	0.45/-0.40 e.$Å^{-3}$	

Figure S 38. ORTEP of $[(L^{H})Ni(H_2O)_2](HSO_4)0.5(SO_4)$.

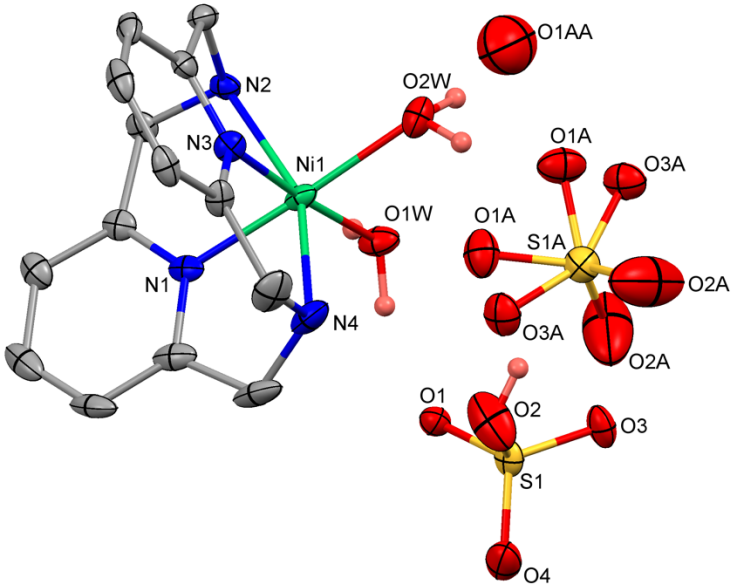

ORTEP of $[(L^{H})Ni(H_2O)_2](HSO_4)0.5(SO_4)$ at 50% probability level. Hydrogen atoms are omitted for clarity. Selected bond distances [Å] and bond lengths [deg]. Ni(1)-O(1W), 2.041(4); Ni(1)-N(2), 2.148(4); Ni(1)-N(3), 1.986(4); Ni(1)-N(1), 1.998(5), Ni(1)-N(4), 2.164(5), Ni(1)-O(2W), 2.086(4), S(1)-O(1), 1.453(4); S(1)-O(3), 1.451(4); S(1)-O(4), 1.463(4); S(1)-O(2), 1.512(4); S(1A)-O(3A) 1.414(8); S(1A)-O(3A#), 1.414(8); S(1)A-O(1A), 1.444(9); S(1A)-O(1A#), 1.444(9); S(1A)-O(2A), 1.459(6); S(1A)-O(2A#), 1.459(6). O(1W)-Ni(1)-N(2), 97.99(16); O(1W)-Ni(1)-N(4), 101.83(17); O(1W)-Ni(1)-O(2W), 85.85(16); N(2)-Ni(1)-N4, 152.85(18); N(3)-Ni(1)-O(1W), 176.06(17); N(3)-Ni(1)-N(2), 80.68(17), N(3)-Ni(1)-N(1), 89.43(17); N(3)-Ni(1)-N(4), 80.66(18); N(3)-Ni(1)-O(2W), 90.61(17); N(1)-Ni(1)-O(1W), 94.02(16); N(1)-Ni(1)-N(2), 80.68(17); N(1)-Ni(1)-N(4), 79.59(19); N(1)-Ni(1)-O(2W), 177.20(17); O(2W)-Ni(1)-N(2), 96.57(16); O(2W)-Ni(1)-N(4), 103.17(18); O(1)-S(1)-O(4), 110.3(2); O(1)-S(10-O(2), 107.7(3); O(3)-S(1)-O(1), 111.9(2); O(3)-S(1)-O(4), 111.8(2); O(3)-S(1)-O(20, 108.1(2); O(4)-S(1)-O(2), 106.7(3); O(3A#)-S(1A)-O(3A), 151.1(8); O(3A)-S(1A)-O(1A), 111.5(7); O(3A#)-S(1A)-O(1A), 39.9(4); O(3A#)-S(1A)-O(1A#), 111.5(7); O(3A)-S(1A)-O(1A#), 39.9(4); O(3A)-S(1A)-O(2A), 99.6(5); O(3A)-S(1A)-O(2A#), 97.4(5); O(3A#)-S(1A)-O(2A), 97.4(5); O(3A#)-S(1A)-O(2A#), 99.6(5); O(1A#)-S(1A)-O(1A), 72.9(8), O(1A#)-S(1A)-O(2A#), 112.3(4), O(1A#)-S(1A)-O(2A), 124.8(5), O(1A)-S(1A)-O(2A), 112.3(4); O(1A)-S(1A)-O(2A#), 124.8(5); O(2A#)-S(1A)-O(2A), 107.5(6).

Table S 11. Crystallographic data for $[(L^{H})Ni(H_2O)_2](HSO_4)0.5(SO_4)$.

Identification code	CCDC-1878200	
Empirical formula	C14 H21 N4 Ni O9 S1.5	
Formula weight	496.15	
Temperature	100(2) K	
Wavelength	0.710 Å	
Crystal system	monoclinic	
Space group	C2/c	
Unit cell dimensions	a = 21.7139(16) Å	α = 90°
	b = 11.0715(8) Å	β = 100.803(2)°
	c = 16.0808(12) Å	γ = 90°
Volume	3797.4(5) $Å^3$	
Z	8	
Density (calculated)	173.6 mg/m^3	
Absorption coefficient	1.246 mm^{-1}	
F(000)	2056.0	
Crystal size	0.05 x 0.05 x 0.02 mm^3	
Theta range for data collection	2.9040 to 25.095°	
Index ranges	-25<=h<=25, -13<=k<=1, -19<=l<=19	
Reflections collected	22394	
Independent reflections	3386 [R_{int} = 0.0955, R_{sigma} = 0.0710]	
Completeness to theta = 25.242°	99.9 %	
Absorption correction	multi-scan	
Max. and min. transmission	0.7456 and 0.6337	
Refinement method	Full-matrix least-squares on F^2	
Data / restraints / parameters	3386 / 22 / 284	
Goodness-of-fit on F^2	1.019	
Final R indices [I>2sigma(I)]	R1 = 0.0592, wR2 = 0.1215	
R indices (all data)	R1 = 0.0965, wR2 = 0.1369	
Largest diff. peak and hole	1.72/-1.23 e.$Å^{-3}$	

References

1. F. Bottino, M. Di Grazia, P. Finocchiaro, F. R. Fronczek, A. Mamo and S. Pappalardo, *J. Org. Chem.*, 1988, **53**, 3521-3529.
2. M. R. Willcott, *J. Am. Chem. Soc.*, 2009, **131**, 13180.
3. M. Strohalm, D. Kavan, P. Novak, M. Volny and V. Havlicek, *Anal. Chem*, 2010, **82**, 4648-4651.